

BEHAVIOUR UNDER SEISMIC LOADING OF
REINFORCED CONCRETE BEAM-COLUMN
JOINTS WITH ANCHORAGE BLOCKS.

A report submitted in partial fulfillment of
the requirements of the degree of Master of
Engineering at the University of Canterbury,
Christchurch, New Zealand.

by
R.N. PATTON

1972.

CONTENTS.

	Page.
ABSTRACT.	iv
ACKNOWLEDGEMENTS.	vi
NOTATION.	vii
1. INTRODUCTION.	
1.1 General Design Philosophy	1
1.2 Review of Previous Work	2
1.3 Scope	3
2. DESIGN OF SPECIMENS.	
2.1 Design Concept	5
2.2 Code Restrictions	5
2.3 Dimensions and Reinforcements	5
2.3.1 Beam	5
2.3.2 Beam Secondary Reinforcement	6
2.3.3 Column	7
2.3.4 Column Secondary Reinforcement	7
2.3.5 Beam Bar Anchorage	9
2.3.6 Joint Reinforcement	9
3. TEST SPECIMENS.	
3.1 Dimensions	11

	Page.
3.2 Reinforcement.	11
3.2.1 Unit 1.	11
3.2.2 Unit 2.	13
3.2.3 Unit 3.	13
3.3 Materials	16
3.4 Fabrication of Units	17
3.5 Instrumentation	18
3.6 Loading Arrangement.	19
3.7 Simulation of Seismic Loading	19
4. TEST RESULTS.	
4.1 General Features of Tests.	22
4.2 Ultimate Strength of Units	24
4.3 Unit 1	26
4.3.1 Load-Deflection.	26
4.3.2 Moment Rotation for Columns.	29
4.3.3 Strains in Main Column Bars.	32
4.3.4 Strains in Main Beam Bars	35
4.3.5 Strains Within the Joint.	38
4.3.6 Crack Development and Mode of Failure	46
4.4 Unit 2	50
4.4.1 Load-Deflection.	50
4.4.2 Moment Rotation for Columns.	53

	Page.
4.4.3 Strains Within the Joint.	57
4.4.4 Crack Development and Mode of Failure . .	63
4.5 Unit 3	69
4.5.1 Load-Deflection.	69
4.5.2 Moment Rotation for Columns.	71
4.5.3 Strains Within the Joint.	74
4.5.4 Crack Development and Mode of Failure . .	81
5. CONCLUSIONS AND SUGGESTED FUTURE RESEARCH.	
5.1 Conclusions	87
5.2 Suggested Future Research.	89
APPENDIX A: REFERENCES.	

ABSTRACT.

This report deals with the behaviour of beam-column joints of reinforced concrete frames with anchorage blocks. The beam entered one face of the column only and the beam flexural reinforcement was anchored in an anchorage block (beam stub) beyond the joint. The frames were subjected to high intensity cyclic loading to simulate earthquake loads.

An experimental program consisting of three full scale tests was conducted to investigate the behaviour of the joints in a lower storey of a multi-storey frame. The beam was designed to have a theoretical ultimate moment of resistance that was about twenty per cent greater than the combined moment of resistance of the columns. This was so the basic ductility requirements for columns could also be studied. The main design parameter was the amount and arrangement of transverse steel reinforcement within the joint. All three units were subjected to the same program of static cyclic loading and the experimental moment-rotation characteristics were compared.

Results from the tests were very encouraging and it should be possible with the information obtained, to postulate a detail which will successfully take the shear forces imposed on the joint during cyclic loading.

Four main factors arise from the tests and these should be considered in detailing reinforced beam-column joints;

- i) Shear crack patterns occur only in the actual joint region and on a diagonal, not a 45 degree, basis.
- ii) The radiused part of the main beam flexural bars should be situated outside the line of the exterior column reinforcing bars.
- iii) The provision of ties around the column bars in the joint region is much more effective than providing ties which also take in the anchorage block region.
- iv) The unsupported length which a column tie spans between two 90 degree bends should be restricted. If the length is too long then special transverse ties should be positioned through the joint.

ACKNOWLEDGEMENTS.

This investigation was carried out in the Civil Engineering Department of the University of Canterbury, of which Professor H.J. Hopkins is Head.

The assistance and encouragement given to me during the course of this project is gratefully acknowledged.

My special thanks go to:-

Professor R. Park and Dr. T. Paulay, supervisors of this project for their guidance on all matters, relating to the tests and to the writing of this report.

G.W. Renton, Graduate Student, without whose assistance, experience in testing procedures, and provision of test rig and mould, this project would not have been completed in the required time.

The technical assistance given me by Messrs. H.T. Watson and P.C. Dawson, Technical Officers; Messrs A.G. Foote and J. Sheard, Senior Technicians; S. Robinson, Technician and other technicians of the Department. My special thanks go to Messrs N.W. Prebble, Senior Technician and G.W. Sim, Technician for the fabrication of the test specimens and for the many frustrating hours they spent in seeing this project through to completion.

Also special thanks are due to Mrs N. Robinson for the typing of this report.

NOTATION.

A_c	Nett spalled area of column.
A_g	Gross concrete area of column.
A_s	Area of tension reinforcement.
A'_s	Area of compression reinforcement.
A_{sh}	Area of one leg of transverse bar.
A''_{sh}	Total area of transverse hoop.
A_{st}	Total area of steel reinforcement in column.
A_v	Total area of web reinforcement for shear purposes.
A'_v	Total area of hoops required in joint region.
a	Centre to centre spacing of special confinement hoops.
a_s	Area of individual bar.
b	Width of compression face of section.
D_b	Diameter of bar.
d	Distance from extreme compression fibre to centroid of tensile reinforcement.
f'_c	Concrete cylinder compressive stress.
f_y	Yield stress of steel.
f''_{yh}	Yield strength of confining reinforcement.
h'	Maximum unsupported length of rectangular hoop measured between perpendicular legs of the hoop.
L_d	Anchorage length of tension bars.
N_u	Design axial load normal to the cross section occurring simultaneously with V_u , to be taken positive for compression and negative for tension.
P	Axial load on column.

P_b	Axial load on column for balance failure.
P_o	Ultimate load capacity of column with axial load only applied.
P'_u	Maximum design axial load.
p	A_s/bd .
p'	A'_s/bd
p'_s	$0.45 (A_g/A_c - 1) f'_c/f_y$
p_t	A_{st}/bd .
s	spacing of stirrups or hoops.
T	$A_s f_y$ total tensile force in beam flexural reinforcement.
T'	$K A_s f_y$ where K is number from 0 to 1.
V'	Horizontal shear on joint shear.
V_c	Total shear carried by concrete section.
V_j	Design joint shear force.
v_c	Shear per unit area carried by concrete.
ϕ	Capacity reduction factor;
	Rotation in column at applied load.
ϕ_y	Rotation in column at first yield.
ϕ_u/ϕ_y	Column Rotational ductility factor.
Δ	Deflection of beam at applied load.
Δ_y	Deflection of beam at first yield.
Δ_u/Δ_y	Deflection ductility factor for whole unit.

CHAPTER 1.

INTRODUCTION.

1.1 GENERAL DESIGN PHILOSOPHY. In a country like New Zealand, with the natural resource of concrete there is a distinct economic advantage to be gained with its use, compared with structural steel, in many multi-storey buildings. As in many seismic prone countries, buildings are generally becoming taller and the use of structural concrete presents major design and detailing problems due to the ever present possibility of earthquakes. Because of the relatively short time that the basic principles of sound seismic design, for reinforced concrete frames have been observed, there exists in the codes of practice of New Zealand and other countries many important design clauses which in reality remain unproved.

The current design philosophy is to proportion the forces in a structure such that even after a severe earthquake it will remain standing. Because of economic considerations it is not possible nor desirable to detail such a structure so that it remains in the elastic range even when subjected to severe seismic action. The benefits of the post-elastic behaviour of a structure are now fairly well documented. A frame can be designed such that there is considerable energy absorption, after yielding has occurred, in various members throughout the structure. The design of such a steel structure is relatively straight forward, but in the case of a concrete frame, because of the brittle nature of the material, the problem is more difficult.

Park¹ has shown that if a structure's ductility factor is to lie between four and six as suggested by Blume Newmark and Corning⁵, then section ductilities of the order of ten to sixteen or greater may be required. The members of a concrete frame must be detailed in such a way as to withstand these rotations imposed upon them, in a ductile fashion. It is therefore essential that brittle failures due to shear, bond or joint deterioration, be guarded against. It is the last one of these types of failures, in conjunction with the first two, that is at present causing a great deal of concern.

1.2 REVIEW OF PREVIOUS WORK. Meggett⁷ gives a report of the small amount of work carried out up to 1970 and suitably criticises their shortcomings. The tests on the type of joint which has a beam framing into one face of a column has been the subject of many sets of tests recently at the University of Canterbury. Although at first sight this type of structure appears to be rather impractical, apart from occurring in composite shear wall-framed buildings, the type of failure observed in the earlier tests at the University of Canterbury indicates that conclusions from these results can be made for beams framing into one, two, or three faces of a column. The reason for this is, that the failure of the joint occurred partly because the beam tensile flexural reinforcement was anchored in the joint region.

Tests carried out by Renton² at the University of Canterbury indicated that present code requirements where they exist for this

type of joint, proved inadequate especially when section ductility requirements as suggested by Park¹ are required. The tests indicated that no really satisfactory steel arrangement could be found which gave adequate resistance to the joint shear even with the beneficial effect of the axial load. It was recognised that as one of the main factors contributing to the degradation of the joint was the anchorage of the beam flexural steel in this area, then one possible improvement would be to anchor the steel outside the joint region.

1.3 SCOPE. The object of this research program was to see if there was any benefit to be gained by providing for the anchorage of the main flexural bars outside the joint region in an anchorage block on the far side of the column beyond the joint. This was not considered to be impracticable as many prestressed concrete buildings exist today with such an anchorage block.

Laboratory testing of model structures or parts of structures is one way of observing behaviour under simulated seismic action. In reinforced concrete frames, modelling of the structural components becomes very difficult especially when investigating elements such as joints where the significance of the cover concrete, spalling, and the ratio of the net spalled concrete area to the gross concrete area is important. Hence it is necessary to resort to full scale testing if reliable results are to be obtained with which to verify or change existing code clauses.

Three full size specimens, representing an element from a lower storey of a building were tested. The specimens were essentially

the same except in the joint region where different steel arrangements were used in each case.

CHAPTER II.

DESIGN OF SPECIMENS.

2.1 DESIGN CONCEPT. A reaction frame already existed from previous tests which placed limitations on the specimen size and loading. A column dimension of 15 inches square was decided upon as it was necessary, with the limiting size of the rig, to have an axial load of reasonable proportions associated with a lower storey column. To ensure a tension failure in the column it was reinforced with 4 No.-9 bars. The chosen applied axial column load was $0.481 P_b$ or $0.159 P_o$. The beam was designed so its ultimate moment of resistance was about 20 per cent greater than the combined ultimate moment of resistance of the column sections. Material properties assumed in the design were

reinforcement $f_y = 45000$ psi

concrete $f'_c = 4000$ psi

2.2 CODE RESTRICTIONS. The specimens were designed according to ACI 318 - 71³. Column ductility and joint shear requirements were also designed using the M.O.W. code⁴; "Design of Public Buildings". The most conservative values obtained were used.

2.3 DIMENSIONS AND REINFORCEMENT.

2.3.1 Beam. The beam section was 25 inches deep and 12 inches wide and contained 4 - No. 10 bars in the top and in the bottom with $1\frac{1}{2}$ inch cover to the main reinforcement. This gave an effective depth of 22.875 inches and a distance between reinforcement centroids of 20.75 inches. Reinforcement ratios were; $p = p' = 0.0183$. The

ultimate capacity of the beam was assumed to be that given by the steel couple made up of the tension and compression reinforcement. Calculations from test results gave a very close correlation with this theoretical value.

The beam's ultimate moment capacity based on the design material strengths was 4,630 kip-ins.

2.3.2 Beam Secondary Reinforcement. Beam stirrups were designed in accordance with the requirements of ACI 318 - 71. Ties were $\frac{3}{8}$ in. diameter plain reinforcing bar. Because the specimen was designed so that the plastic hinges would form in the columns it was deemed unnecessary to provide special stirrups for ductility in the beam. Stirrups were provided only to carry the shear in the beam which was present due to the loading being applied at its end. The area of web reinforcement required was found using

clause A.5.9 of ACI 318 - 71

$$A_v = 0.15 A_s \frac{s}{d} \quad (1)$$

where A_s is the total area of tensile reinforcement in the beam. For $\frac{3}{8}$ dia. ties in which $A_v = 0.22 \text{ in}^2$ and $A_s = 4.92 \text{ in}^2$ the stirrups had a required spacing of 6.85". Minimum requirements were a spacing of $\frac{d}{4} = 5.75 \text{ ins}$ for a length of $4d = 7' - 8"$ from column face. Because these requirements were for the formation of a hinge in the beam, the amount of reinforcement was reduced as hinging was envisaged to occur in the column. This required $\frac{3}{8}$ in. diameter stirrups at 8 in. spacing for $2d = 3' - 10"$ and $\frac{3}{8}$ in. stirrups at 11 in. spacing for the remainder of the beam.

2.3.3 Column. A column 15 ins. square was chosen for reasons discussed in section 2.1. Reinforcement was 4 - No. 9 deformed bars ($A_{st} = 4.00 \text{ in}^2$) giving $P_t = 0.0175$. The cover was $1\frac{1}{2}$ - ins. to the main reinforcement. The design axial load was 148 kips. When the load was acting down this gave an increased axial load to the bottom column of approximately 35 kips to 183 kips. As the column was designed to have a tension failure, an increase in axial load increased the ultimate moment of resistance. This gave a ultimate moment capacity based on design material strengths of 1,869 kip ins. for axial load of 148 kips and 2,020 kip ins. for axial load of 183 kips. Because the specimen within the reaction frame is statically determinate then it is only possible to obtain equal and opposite horizontal shears at the top and bottom. This meant that the moment applied to the column could not exceed the ultimate moment of resistance of the weakest section which was where the lower axial load was applied. Hence the combined moment of resistance of the columns was taken as 3,738 kip ins. Therefore at the joint the ratio of the beam's ultimate capacity to the total column ultimate capacity was 1.23.

2.3.4 Column Secondary Reinforcement. Lateral steel requirements for the column were designed from ACI 318 - 71 or M.O.W. codes, the most conservative value of the two being taken. As a hinge was expected to form in the column, full design requirements were used. To carry the shear in the column, due to the horizontal reactions, it was found that the concrete was adequate and hence only nominal ties were required. These were $\frac{3}{8}$ in. diameter ties at 10" c/s.

Conforming to ACI 318 - 71 requirements $P'_u > 0.4P_b$

where P'_u = maximum design axial load

and P_b = balanced axial load capacity

hence special confinement reinforcement was required. For the section $A_g/A_c = 1.28$, where A_c = spalled concrete area.

Using the following equations;

$$p_s = 0.45 \left(\frac{A_g}{A_c} - 1 \right) \frac{f'_c}{f_y} \quad \text{--- (2)}$$

$$\text{and } A_{sh} = h' p'_s \frac{a}{2} \quad \text{--- (3)}$$

where h' = max. unsupported length of rectangular hoop

A_{sh} = area of tranverse bar (1 leg)

a = centre to centre spacing of hoops

it was found that $A_{sh} = 0.282 \text{ in}^2$, requiring $5/8$ in. diam. bars at $4\frac{1}{4}$ -ins. over a distance of 18 ins.

Conforming to M.O.W. Code requirements $P'/A_g = 0.66 \text{ k.s.i.}$ was greater than $0.12 f'_c = 0.48 \text{ k.s.i.}$ hence special transverse reinforcement required. The equation appearing in the Code of May 1970 has since been modified to

$$A_{sh}'' = 0.15 a h'' \frac{f'_c}{f_y h} \quad \text{--- (4)}$$

for columns of small area

where A_{sh}'' = total area of transverse hoop

a = centre to centre spacing of hoops in inches with
max. of 4 ins.

h'' = max. unsupported length of rectangular hoop measured
between perpendicular legs of the hoop

$f_y h$ = yield strength of confining reinforcement.

From the above equations it was found that $5/8$ -in. diam. bars at $3\frac{1}{2}$ -ins. were required. The M.O.W. requirements were used as they were the more conservative.

2.3.5 Beam Bar Anchorage. The anchorage length required for the beam bars, within the joint and anchorage block region were found from the Development Length equations in Chapter 12 of ACI 318-71. The anchorage or development length, in inches, required for No. 11 or smaller bars is;

$$L_d = \frac{0.04 a_s f_y}{f_c} \quad \text{--- (5)}$$

where a_s = area of individual bar.

The minimum development length is given by

$$L_d = 0.0004 D_b f_y \text{ or } 12 \text{ ins.}$$

where D_b = diameter of bar.

This gave a required anchorage length of 32 ins for the No. 10 bars.

The length of the anchorage block was determined by providing the required anchorage length between the front of the column face and a point halfway around the 'hairpin'. This required an anchorage block of 10 inches long.

2.3.6 Joint Reinforcement. This was the only parameter to be varied in the three tests. All requirements mentioned in sections 2.3.1 to 2.3.5 were common to all three specimens (see fig. 2.1). The three joints were designed assuming a 45 degree diagonal tension crack pattern. The actual design of each joint unit is described in the following chapter.

CHAPTER III.

TEST SPECIMENS.

3.1 DIMENSIONS. The dimensions of the specimen were governed largely by the size of the test rig available. Assuming that the points of contraflexure (ends of the specimen members) were at the mid-height and mid-span of the columns respectively, this would mean that the specimens were from a frame with 10' - 8" interstorey height and 21' - 7" span Fig. 2.1 illustrates the size of the specimen. Dimensions of joint reinforcement are shown in Figs. 3.1, 3.2, 3.3.

3.2 REINFORCEMENT. All three units had reinforcement as designed for in the previous chapter (see fig. 2.1). The joint details for each specimen were different (see Figs. 3.1, 3.2, 3.3).

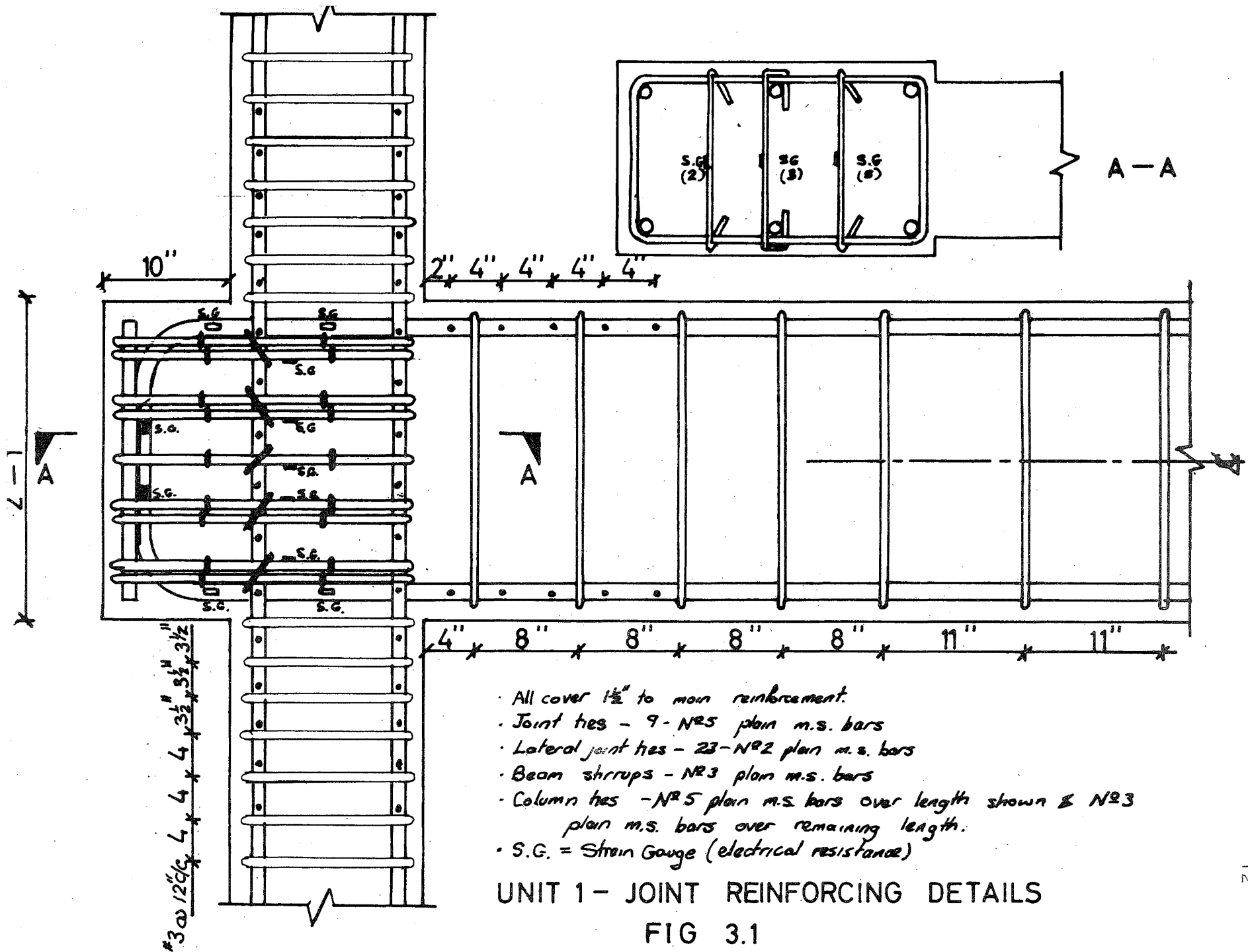
3.2.1 Unit 1. The joint was designed so that the steel ties would take all the shear. In other words it was assumed that the concrete took no shear at all. A 45 degree crack pattern was assumed to occur in the joint and an analysis was carried out according to Paulay¹. On the assumption that yielding would occur in the column bars the shear across the joint from the beam flexural steel was taken as $0.8 A_s f_y$ instead of $A_s f_y$. A value equal to the horizontal reaction in the column was then deducted from this value and joint designed to that shear force

$$\text{i.e. } V_j = T' - V' \quad \text{--- (6) where } T' = 0.8 f_y A_s$$

$V' =$ horizontal shear

$$A_v = \frac{a V_j}{\phi f_{yd}} \quad \text{--- (7) where } \phi = 1$$

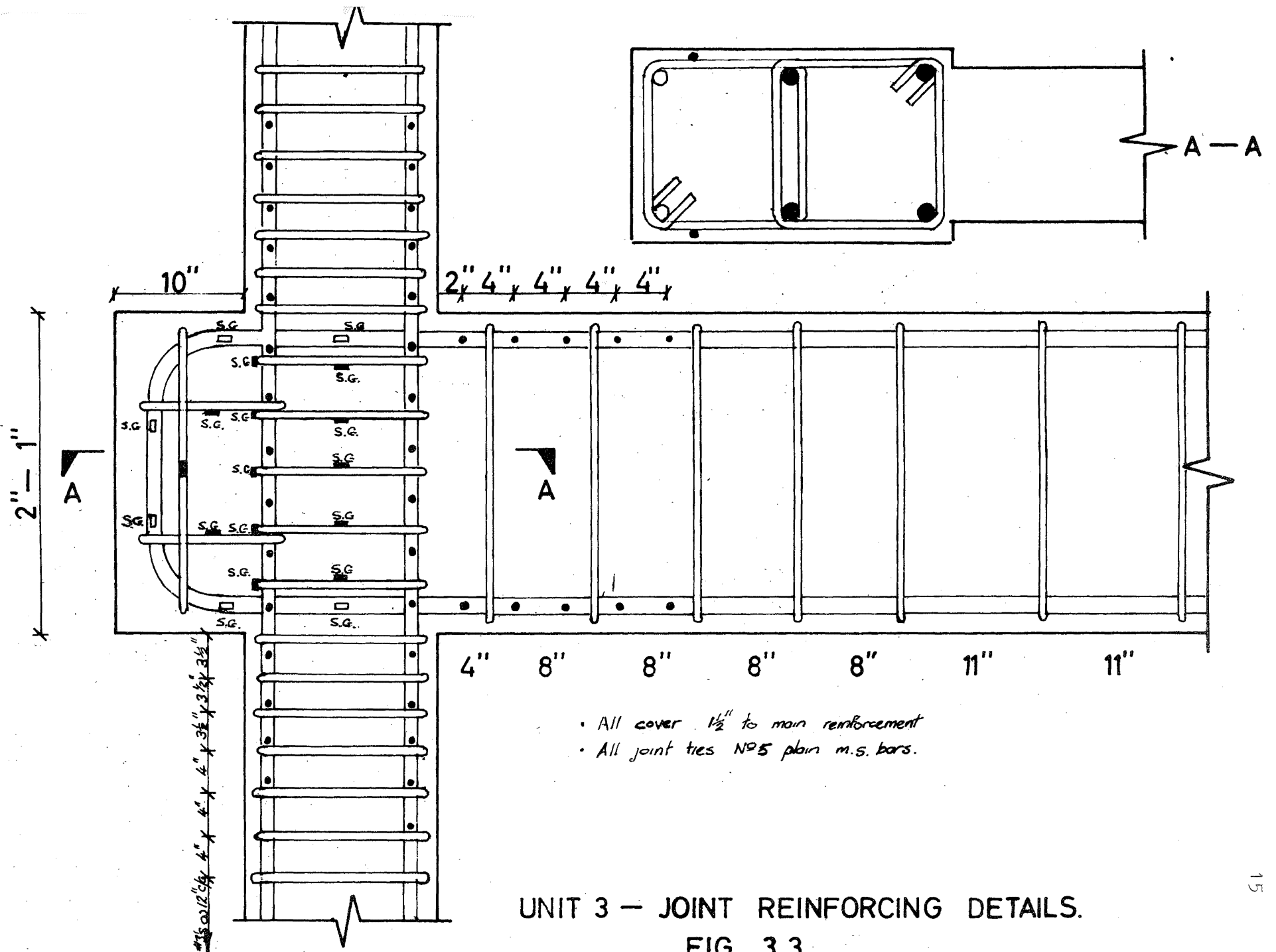
$a =$ spacing of ties.



As the joint had an anchorage block attached, it was difficult to give a value for 'd'. This was taken to be the value Paulay¹ gives assuming no anchorage block (i.e. the distance from the centroid of the tension steel to the extreme concrete compression fibre). This led to 9 - $\frac{5}{8}$ in. diameter ties being required in the joint. The same number were also used in the final specimen tested by Renton² and resulted in the best performance of his series. The number of ties required were more than the M.O.W. code minimum requirements ($\frac{5}{8}$ " ϕ bars at $3\frac{1}{2}$ " crs). For construction purposes ties were placed in pairs (see fig. 3.1) and 2 - No. 9 bars were placed against the end of the hairpin, again to facilitate ease of construction. Also, it was envisaged that these No. 9 bars would help the anchorage of the beam compression steel if required. A number of No. 2 lateral ties were passed through the joint, (23 in all) as shown in fig. 3.1, and several were strain-gauged in an effort to ascertain the perpendicular joint forces on the main hoop ties.

3.2.2 Unit 2. Unit 2 was designed on the same basis as Unit 1 i.e. no shear carried by concrete and the 45 degree crack assumption. This led to the same reinforcement as for Unit 1, the only difference was that the 23 - No. 2 ties through the joint were replaced by 5 - No. 5's placed at the position of the outer column bars. The areas of the ties in each case are the same. (see fig. 3.2).

3.2.3 Unit 3. Design requirements here were that the concrete be proportioned to take some of the shear. As before a 45 degree crack formation was proposed and the area of concrete considered



was that within the column region. Using ACI 318 - 71 Clause 11.4.4 the shear stress carried by the concrete is

$$v_c = 3.5 \sqrt{f'_c} \sqrt{1 + 0.002 \frac{N_u}{A_g}} \quad (8)$$

where N_u = design axial load normal to the cross section occurring simultaneously with V_u , to be taken as positive for compression and negative for tension.

This gives $v_c = 286$ psi and $V_c = 55.5$ kips using the actual concrete strength

$$\text{Now } V'_j = T' - V_c - V' \quad (9)$$

giving $V'_j = 79.5$ kips to be taken by the ties.

Using equation;

$$A'_v = \frac{aV'_j}{f_y d} \quad (10)$$

resulted in 5 - No. 5 ties being required in the joint. The ties in this case were only around the column bars with 2 No. 5 ties in the anchorage block. Also, an additional vertical tie was provided in the anchorage block in an effort to help in confinement of the beam compression steel. Fig. 3.3 shows the joint steel arrangement.

3.3 MATERIALS. All concrete used was premix and it was brought from the plant by agitator truck. The concrete was required to have a 28 day crushing strength of 4000 psi. with a 3 - in. slump. Actual concrete strengths were ascertained by testing of 6 - in. diam. by 12 - ins. high cylinders after 28 days. The average of three tests per unit is given in Table 3.1.1. Deformed bars were used for the flexural steel in the beam and columns and plain bars were used for all ties, stirrups and special reinforcement required in the joint and columns. Steel for all three specimens was obtained in one

batch and tensile tests were carried out for each different types of bar. The average results are presented in Table 3.1.2.

TABLE 3.1 MATERIAL PROPERTIES OF UNITS.

3.1.1 CONCRETE.

Unit No	Concrete Cylinder Strength f_c psi.	Concrete Tensile Strength psi.
1	4820	664
2	3830	532
3	4510	732

3.1.2 STEEL TENSILE STRESSES k.s.i.

Unit No.	Beam Yield Ult.		Column Yield Ult.		5/8" ties Yield Ult.		1/4" ties Yield Ult.	
1								
2	41.4	66.8	42.1	67.5	46.2	71.8	46.5	71.0
3								

3.4 FABRICATION OF UNITS. The larger bars were gas cut and the smaller ones guillotined to length. The reinforcing cage was constructed flat on the ground and all bars were wire tied together. Small spacers and a few tack welds were used to facilitate easier positioning of the reinforcement.

The mould used, had steel sides and a core board bottom. All areas of the mould exposed to the concrete were vanished and a coat of mould oil was applied just prior to the casting of a specimen. For ease of handling and preparation the mould was placed on its side (column and beam horizontal) rather than with the column vertical.

Concrete was poured directly from the truck and compaction was achieved with the aid of a spud vibrator. After screeding and hand trowelling the specimen was moist cured for a period of one week by covering it with layers of damp sacking. Test cylinders and prisms were cured in a similar manner along side the specimen. Upon removal of the formwork after a period of about ten days the specimen was painted with a white oil based paint to aid crack detection during testing.

3.5 INSTRUMENTATION. Measurements taken were: the load applied to the end of the beam, the beam and column deflections, the column rotations, and strains in the column, beam and joint reinforcement. Also a number of Linear Variable Displacement Transformers' (L.V.D.T.'S) were attached to the columns (two above and two below the beam, one on each face of column). These gave a measure of column rotation and the values were fed into one axis of a X - Y plotter. Measurement of load applied was fed into the other axis and this then gave a continuous plot applied load versus column rotation for the top and bottom columns. The plot could be used observe section ductility as the test progressed.

Strains in the flexural reinforcement of the columns and beam were measured with Demountable Mechanical (Demec) gauges with a 4 - in. gauge length. This was achieved by welding $\frac{1}{4}$ - in. diameter studs to the reinforcement so that they appeared flush with the exterior face of the beam or column. A plastic tube was put over the stud during the casting of the concrete and removed after curing to keep the stud from contact with the concrete. Demec points were

waxed onto the ends of the studs.

'Kyowa' type KF - 15 - C8 -11 electric resistant strain gauges were used on the hoop ties in the joint region and on the beam flexural reinforcement in the anchorage region (i.e. in the region of the joint and anchorage block).

3.6 LOADING ARRANGEMENT. The axial load was applied at the top of the column by means of a 100 ton hydraulic jack worked by a handpump system. A calibrated load cell was then used to give the load values applied. The cyclic loading was applied by means of a mechanical screw arrangement at the extreme end of the beam. The advantage of this system is that the loads can be applied with a good degree of accuracy and when the specimen is yielding it is possible to apply the load and hold the system at a constant deflection.

3.7 SIMULATION OF SEISMIC LOADING. Earthquakes apply a complex pattern of dynamic loading to a building in a relatively short period of time. It would be very difficult to reproduce this loading pattern on a full scale model and only a small amount of information would be collected during the duration of the test. The loading actually applied in the tests was a slow cyclic loading patterned to represent earthquake loading. Use of this slow cyclic loading pattern is probably conservative as Blume et al⁹ indicate that a more rapid loading of a structure leads to greater strength and energy absorption characteristics.

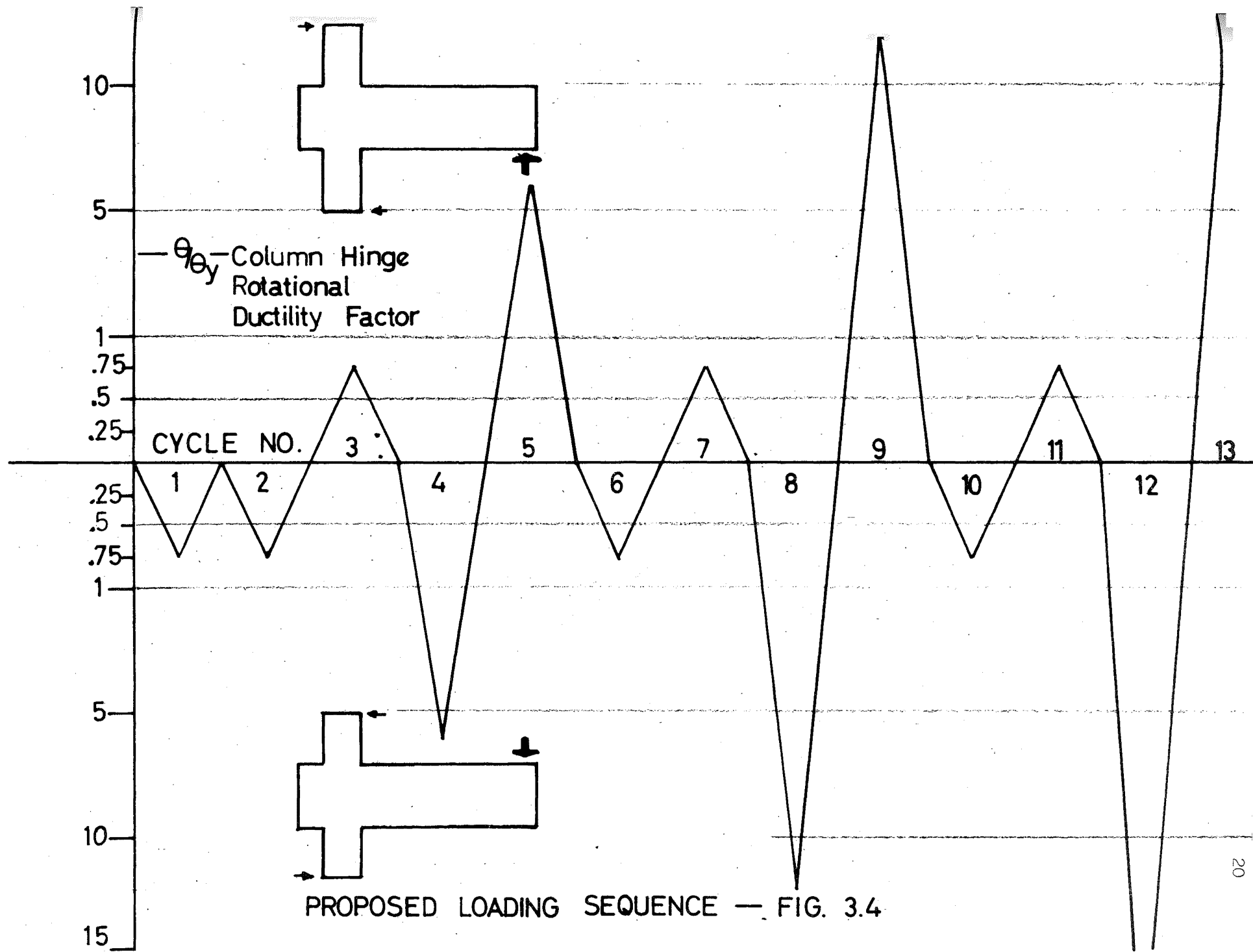


Fig. 3.4 shows the loading sequence adopted in these tests. Cycles 1,2,3,6,7,10,11 are elastic cycles to 75 per cent of the theoretical first yield load. The later elastic cycles shown in Fig. 3.4 are slightly misleading as it was endeavoured to obtain the same load intensity as in the first elastic cycles. This meant much larger ductilities required than those shown on the diagram. Cycle 2 was in the same direction as the first cycle to give a more accurate value for the initial stiffness of the cracked section. The other cycles into the post-elastic range require greater ductility with each cycle increment. One of the reasons for this is that with each successive loading cycle the stiffness of the specimen reduces and a greater plastic rotation is required to give an adequate moment of resistance. The loading pattern is such that equal plastic deformation is enforced in each direction. This may be imposing rather harsh conditions on the structure as it is possible that when the structure has its first excursion into the plastic range the deformation cycle does not oscillate about the original zero position but has a bias in one direction, as has been shown in some dynamic response analyses. In other words the structure leans progressively further in one direction during successive loading cycles.

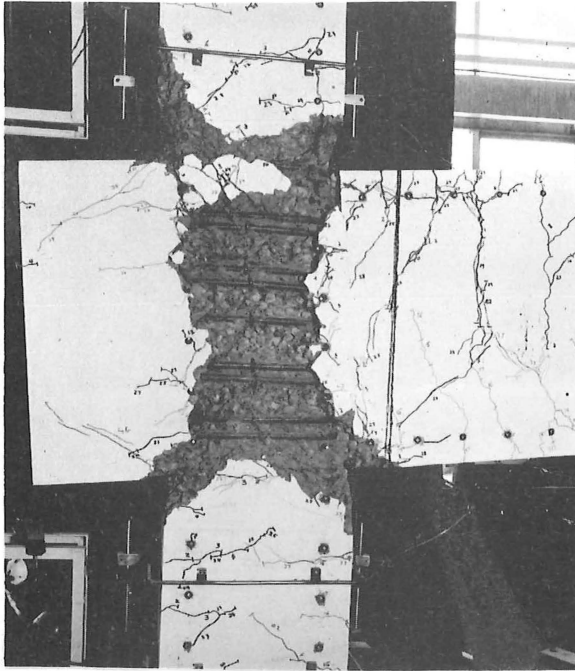
The intended loading sequence shown in Fig. 3.4. was not necessarily attained in the tests, In particular the later elastic cycles attaining the required 75 per cent first yield load of the elastic cycles.

CHAPTER IV.

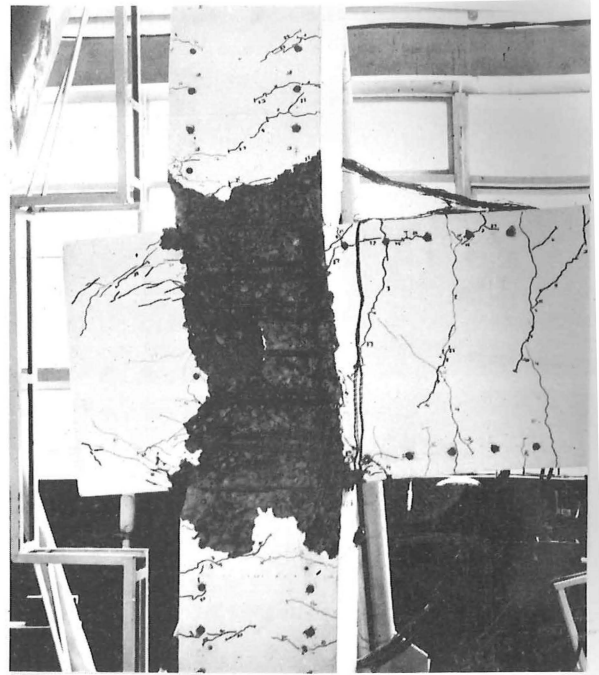
TEST RESULTS.

4.1 GENERAL FEATURES OF TESTS. Results from the three tests revealed some interesting information. The diagonal crack pattern, which is characteristic of the tensile shear stresses within the joint, was not made up of 45 degree cracks. Rather the cracks formed on a diagonal basis which ran approximately from corner to corner in the joint. A corollary of this is that even though a substantial amount of the beam flexural reinforcement is anchored outside the joint region the diagonal cracks occurred only within joint, i.e. in the area bounded by the main column bars and the beam bars. In all cases the anchorage block remained intact with very little cracking except for slight bond cracking along the line of the beam reinforcement and the spalling of some of the cover concrete adjacent to the joint in UNIT 1 and UNIT 3. Figs. 4.1.1, 4.1.2 and 4.1.3 show the three test specimens at the end of their respective loading sequences. UNIT 1 showed plastic rotation in the column above and below the joint whilst UNIT 2 and UNIT 3 were considered to have failed in the joint.

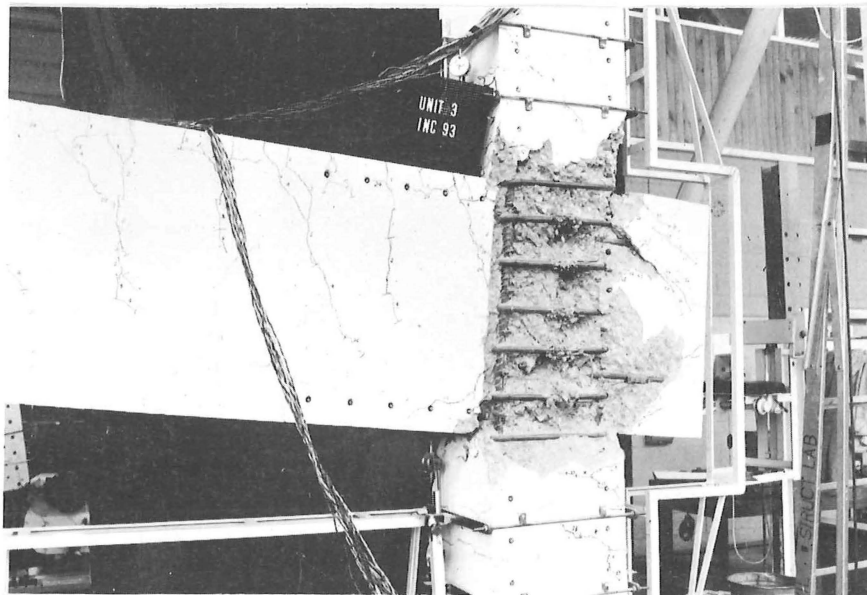
The rate of stiffness degradation, with successive loading cycles, of sections is an important factor which affects the overall ductility requirements for the whole structure. The tests show that the various joint steel arrangements lead to different degrees of disintegration of concrete in the joint region with a corresponding reduction of section stiffness for ductility purposes. It is necessary to ensure that the joint is kept intact as long as possible



UNIT 1.
Fig. 4.1.1.



UNIT 2.
Fig. 4.1.2.



UNIT 3.
Fig. 4.1.3.

to ensure a minimum loss of stiffness in the structure.

4.2 ULTIMATE STRENGTH OF UNITS. Table 4.1 shows the theoretical ultimate capacities for the columns calculated from the actual material properties given in Table 3.1. These are compared with maximum experimental values obtained from the first plastic cycle i.e. cycle 4.

In Table 4.2 the ratio of the theoretical ultimate moments to the experimental moments, for each cycle, is given.

THEORETICAL AND EXPERIMENTAL MOMENTS FOR UPPER COLUMN.

TABLE 4.1.

Unit No.	Ultimate	Mom. Kip.in.	$\frac{M_{\text{expt}}}{M_{\text{ult}}}$
	Theory	Expt	
1	1,872	2,060	1.08
2	1,845	1,945	1.06
3	1,846	1,930	1.05

MOMENT DEGRADATION WITH REPEATED LOAD CYCLES.

TABLE 4.2.

Unit No.	$\frac{M_{\text{expt}}}{M_{\text{ult}}}$							
	Cycle 1	2	3	4	5	6	7	8
1	0.81	0.81	0.81	1.08	1.00	0.70	0.60	1.03
2	0.82	0.82	0.82	1.06	1.03	0.74	0.64	0.94
3	0.82	0.82	0.82	1.05	1.01	0.82	0.73	0.92

9	10	11	12	13
1.01	0.70	0.60	0.94	0.84
0.89	0.67	0.57	0.70	0.57
0.84	0.67	0.62	-	-

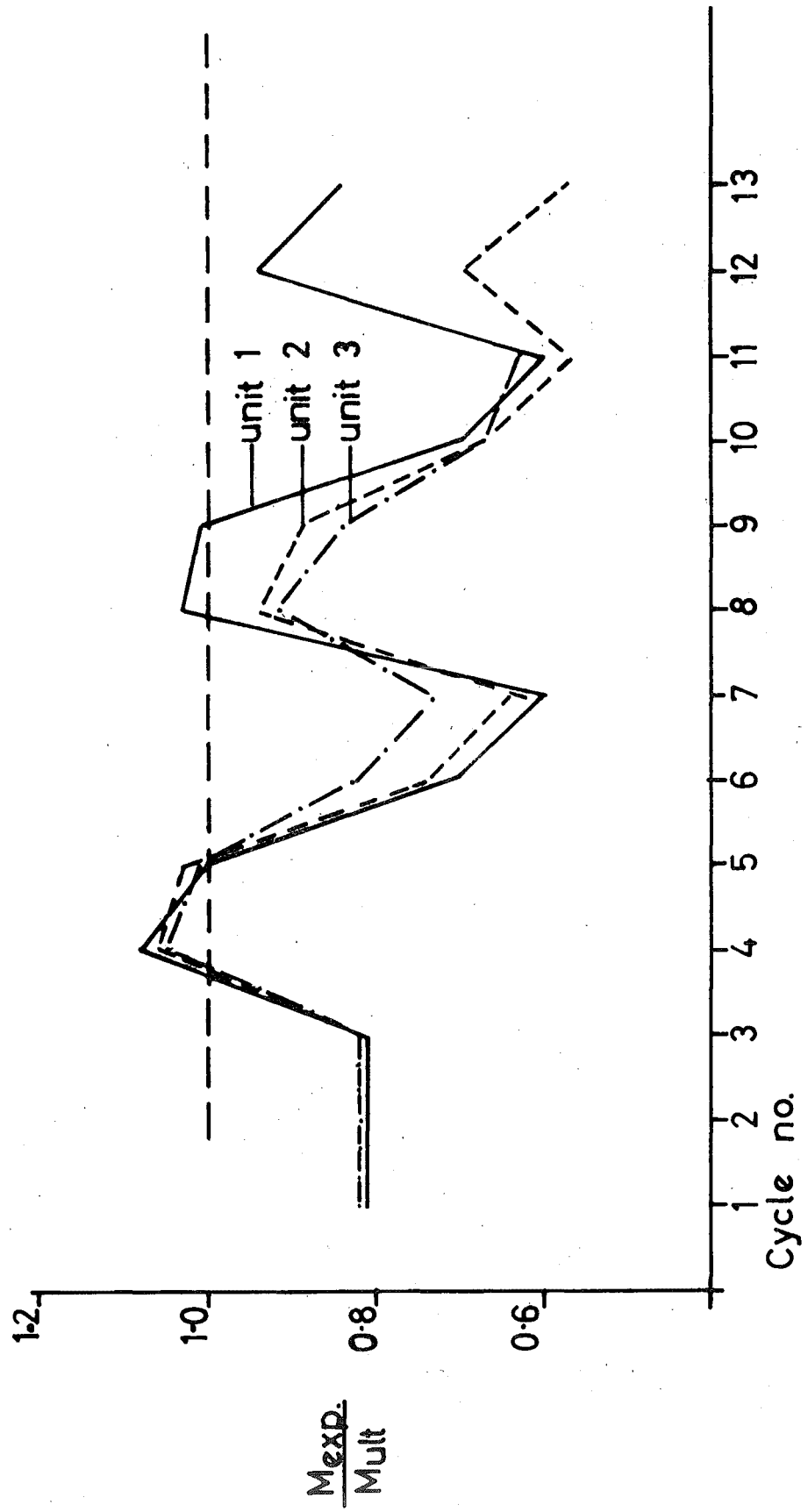
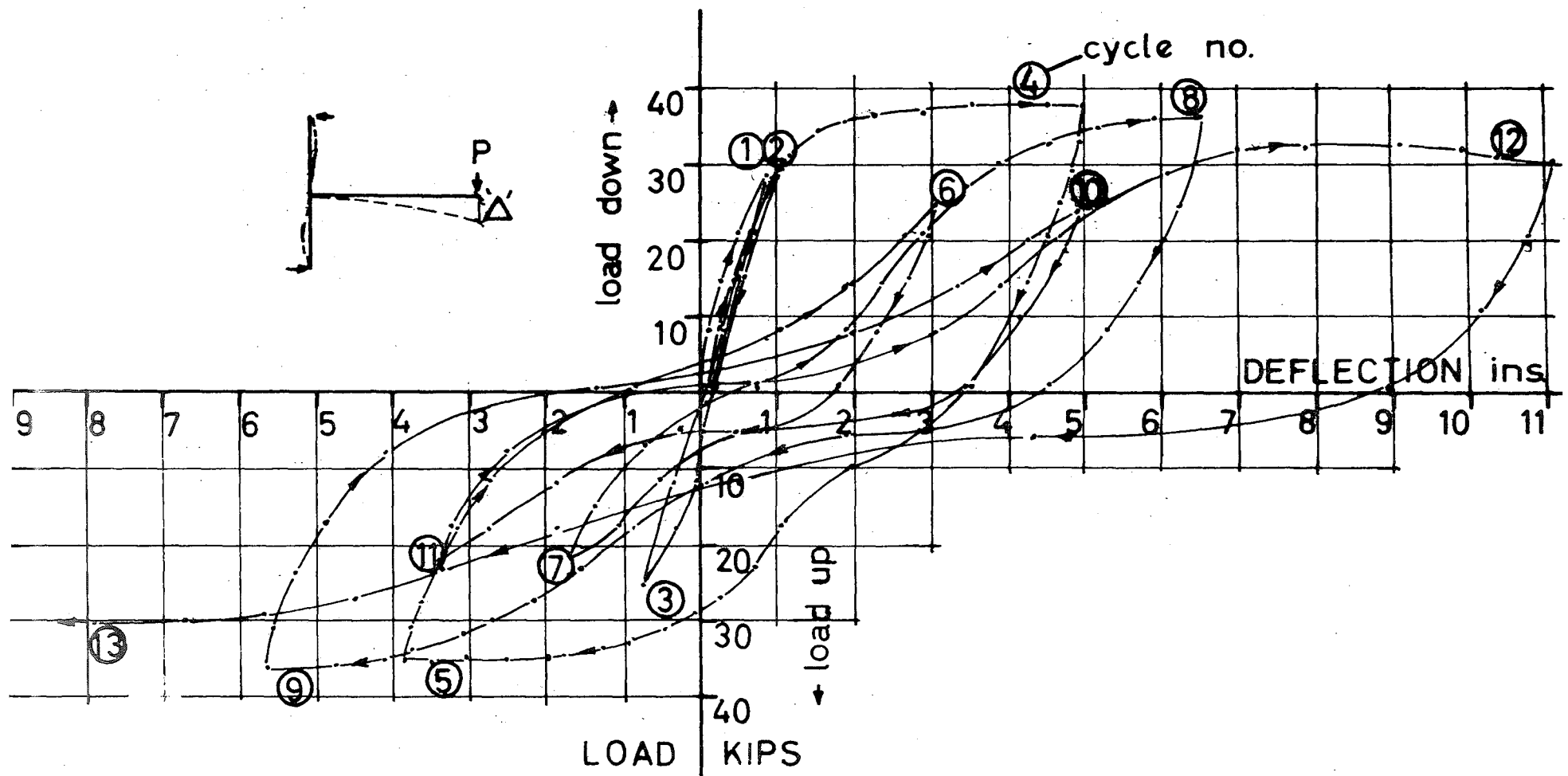
FIG 4.1.4

Fig. 4.1.4 shows a plot of Table 4.2.

4.3 UNIT 1.

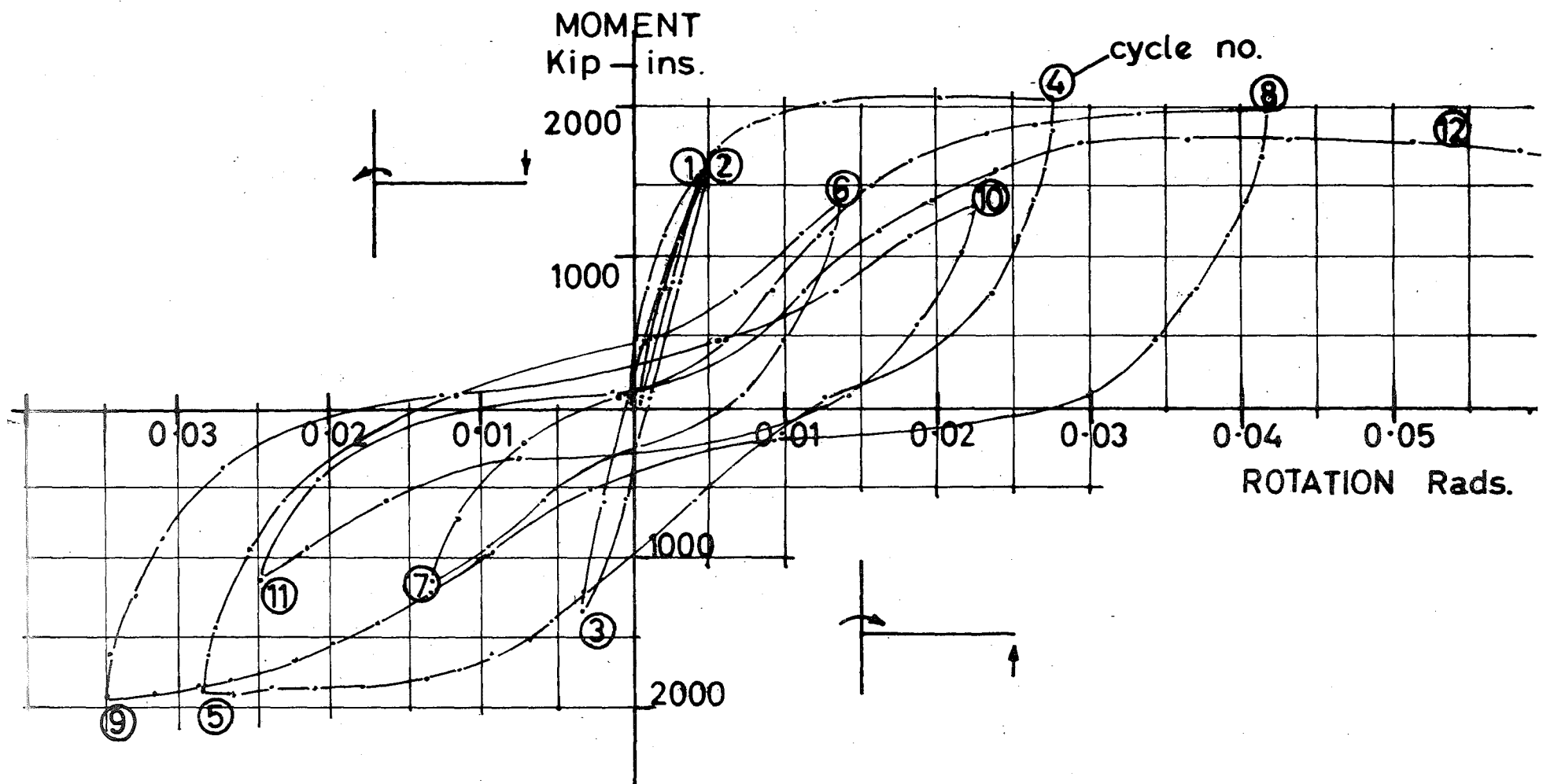
4.3.1 Load-Deflection. Because there was yielding of the beam steel, which was not expected, deflections at the beam end were used to give a load-deflection curve which in turn gives an indication of the ductility available from the whole unit. The load-deflection curve for UNIT 1 (see fig. 4.2) indicates a favourable moment of resistance at fairly large ductility factors. In the diagram the displacement ductility factor $\left(\frac{\Delta}{\Delta_y}\right)$ corresponds closely to the deflection in inches.

Cycles 1 and 2 are the so called linear-elastic cycles. The non-linearity especially in cycle 1 is due to the formation of cracks as the load was increased. The second cycle exhibits a much more linear nature as the majority of cracking has occurred although more cracks were observed in the last load increment of cycle 2. Cycle 3 in the other direction ensured that cracking had occurred in both directions. The 'kink' in the curve in cycle 3 which also shows up more distinctly in following cycles indicates increasing stiffness of the section due to the closing of cracks from the previous cycle. The rounding off of the top of graph suggests a loss of stiffness. This is due to the non linear stress-strain relationship of the flexural steel in the column and beam after it has yielded in the first plastic cycle. This phenomenon is known as the Bauschinger effect.



UNIT 1 — LOAD DEFLECTION CURVE

FIG 4.2



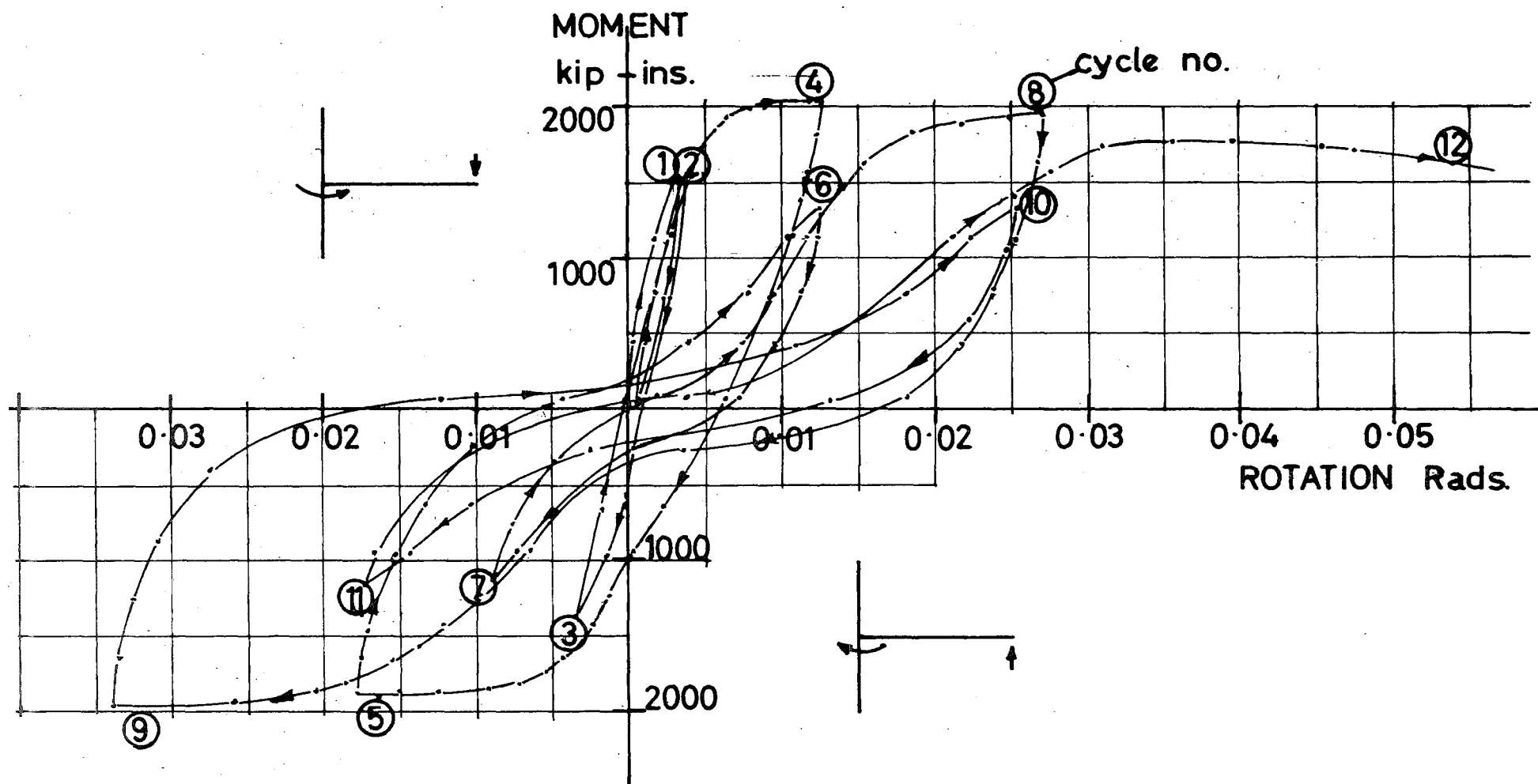
MOMENT - ROTATION CURVE
UPPER COLUMN - UNIT 1

FIG 4.3

The increase on the theoretical ultimate moment which occurred in cycles 4,8,9 was due mainly to the strain hardening of the column bars. For example in cycle 4 the strain in the bars at the level of the beam face was 15 ey which was approximately the start of the strain hardening range. Cycles 6,7,10,11 were taken only to 89 per cent of the initial elastic cycles 1,2,3. Cycle 12 had a moment of resistance of 94 per cent of the theoretical ultimate strength at a ductility of 9. At a ductility of 11, 90 per cent of the theoretical value was obtained. These results were fairly satisfactory from the point of view of the maximum moment of resistance attained. The disturbing feature is the large deflection required before this strength was realized in the later cycles.

4.3.2 Moment Rotation for Columns. A plastic hinge was observed to form in the column above and below the joint (see Fig. 4.1.1) and the extent of the rotation may be seen in the moment-rotation curves shown in Figs. 4.3 and 4.4. Although there was yielding of the beam steel and the formation of a crack where the beam joins the column, it is evident that substantial plastic rotation occurred in the column.

For the upper column (Fig. 4.3) the results show good load carrying ability. Elastic cycle 1 exhibits non linearity due to cracking occurring and cycle 2 shows a more linear nature. Cycle 3 does not show the effect of the cracks closing as distinctly as in the load-deflection plot but this phenomenon is more obvious in the later cycles. Cycles 8 and 9, even though they were the second



MOMENT — ROTATION CURVE
LOWER COLUMN — UNIT 1

FIG 4.4

such plastic cycles, attained the full theoretical ultimate moment of resistance at a maximum section ductility of 8.5 for cycle 8 and - 7 for cycle 9. Cycle 12 had an ultimate moment of resistance of something like 90 per cent of the theoretical value of a rotational ductility factor $\left(\frac{\phi}{\phi_y}\right)$ of 12.

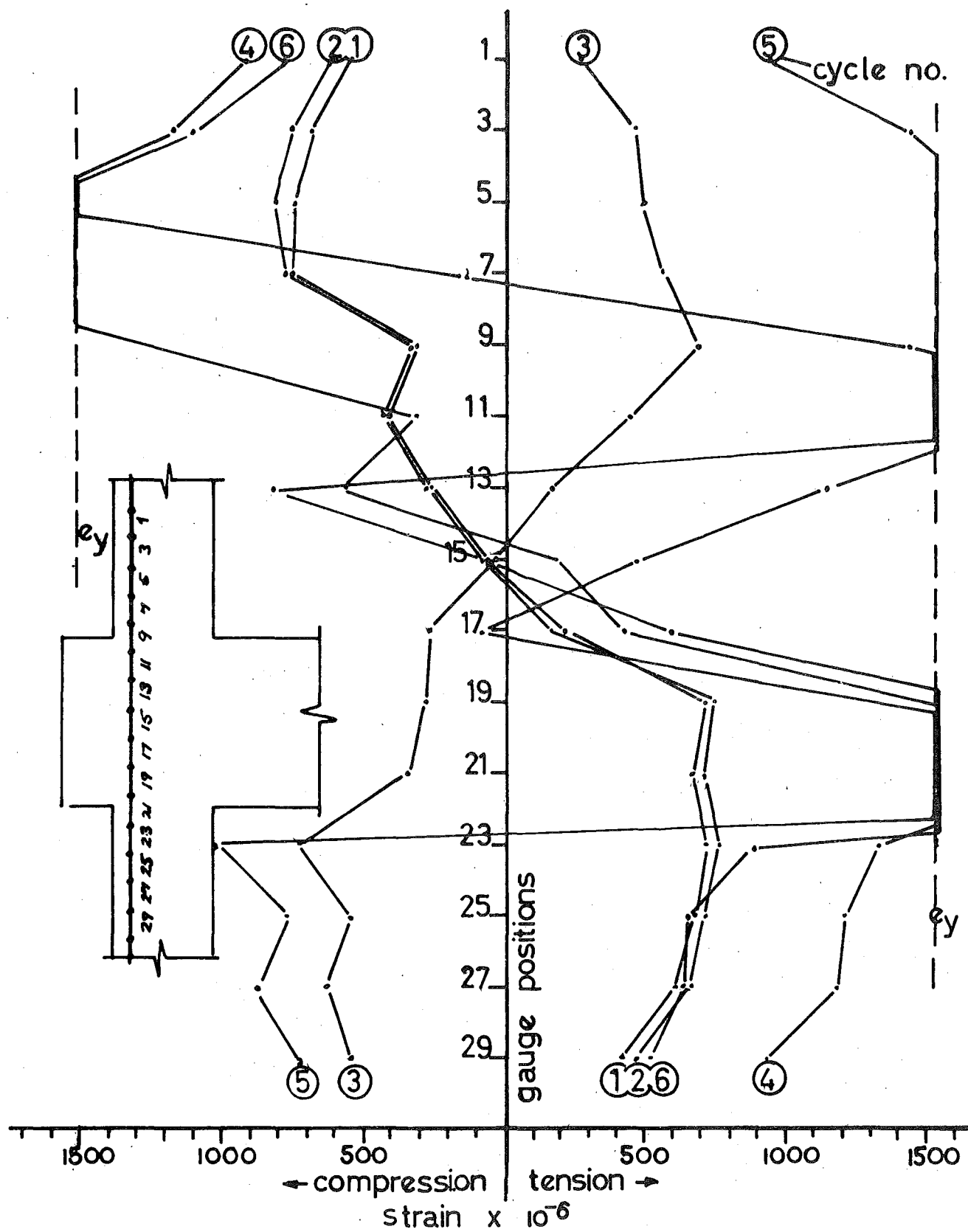
The stiffness degradation of the column with each successive load cycle appeared to be less than that of the load-deflection plot of the whole unit. This indicated that excessive cracking in the joint led to a loss of stiffness of the whole system even though the sections were still relatively intact. This shows the importance of keeping the joint region from breaking down through a successive number of plastic load cycles.

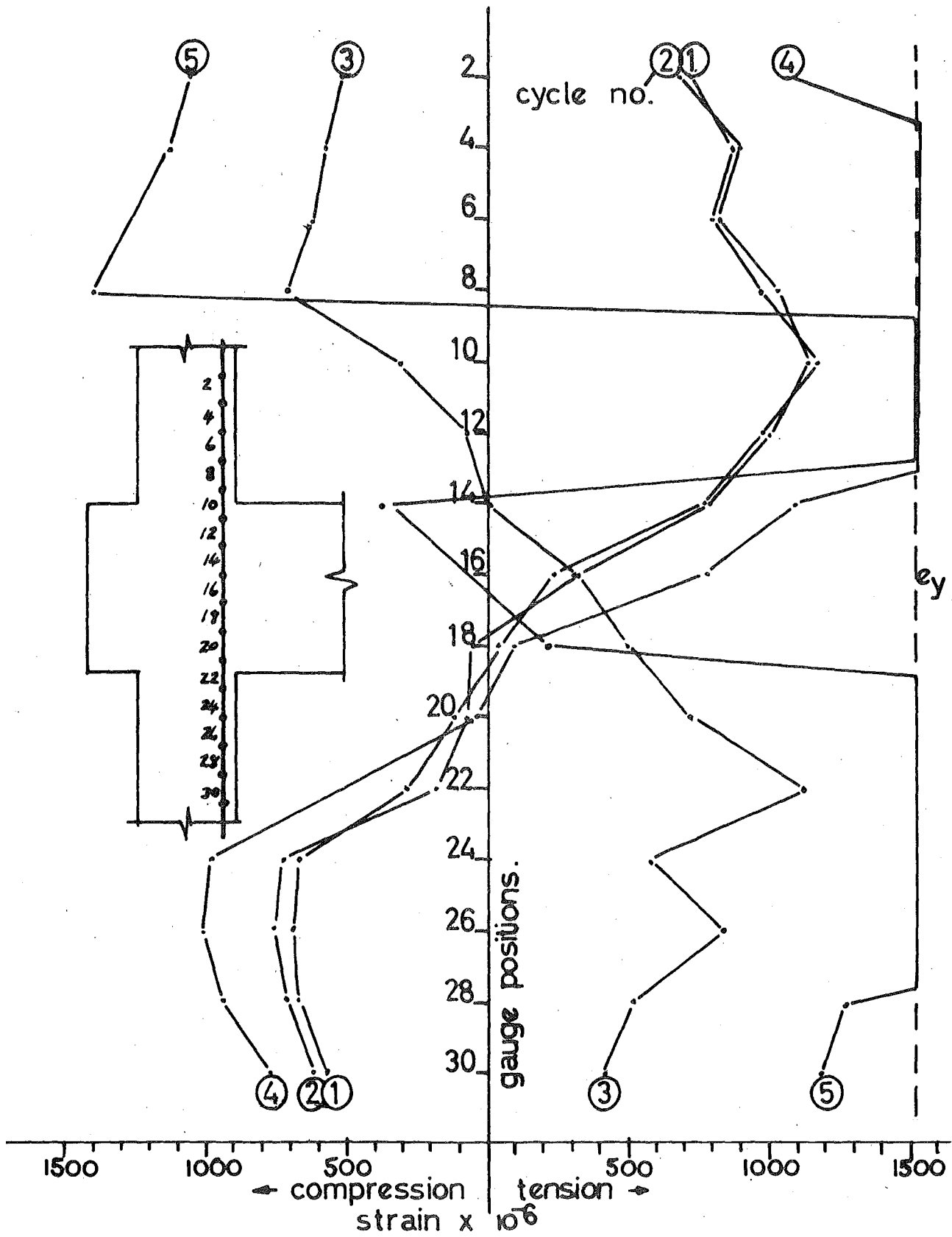
The column rotations below the joint show a different pattern. The elastic cycles are similar to the upper column but very little rotation was observed in the first plastic cycle. (i.e. cycle 4). A rotational ductility factor of about 3 was observed while the top column had a value of about 6. This is because of the loading arrangement. The upper column had a axial load of 148 kips whereas the lower column had an axial load of 148 kips plus the load applied at the end of the beam. Because the columns were designed to ensure a tension failure this meant that an increase in axial load led to an increase in the ultimate moment of resistance. Hence in the first cycle most of rotation occurred in the upper column and the bottom column steel only just yielded. In cycle 5 the column axial loads were effectively reversed and there was a greater rotation

in the lower column. The Bauschinger effect and the late closing of crack contributed to a greater rotational ductility in lower column in cycle 8 but, as in cycle 4, the rotation was limited for similar reasons. This phenomenon was not observable in the upper column rotations because when the load was acting up in the odd numbered cycles the full increase in axial load did not occur. The smaller increase was compensated by a reduction in the lower column vertical reaction.

From observation of the failed specimen (fig. 4.1.1) and from an inspection of the moment curvature curves for the columns of UNIT 1 it appears that the requirements for ductility are adequate as the column still had an ultimate moment of resistance of 90 per cent of the theoretical value, at a rotational ductility factor of 12. The degradation of the load carrying ability of the specimen appeared to be due more to the breaking down of the joint rather than distress in the column.

4.3.3 Strains in Main Column Bars. Fig. 4.5 shows the distribution of strains in the outer column bars, for the first six cycles. Because UNIT 1 was the only Unit to have hinges form in the column the strains were plotted only for this specimen. The elastic cycles showed a strain plot in accordance with what was expected. The interesting point here was that the compressive strains were of the same order as the tensile strains which would not be expected after cracking had occurred. Cycle 4 showed that the outer column bars yielded in compression as well as tension which verified the theoretical assumption. There was not much point in plotting strains





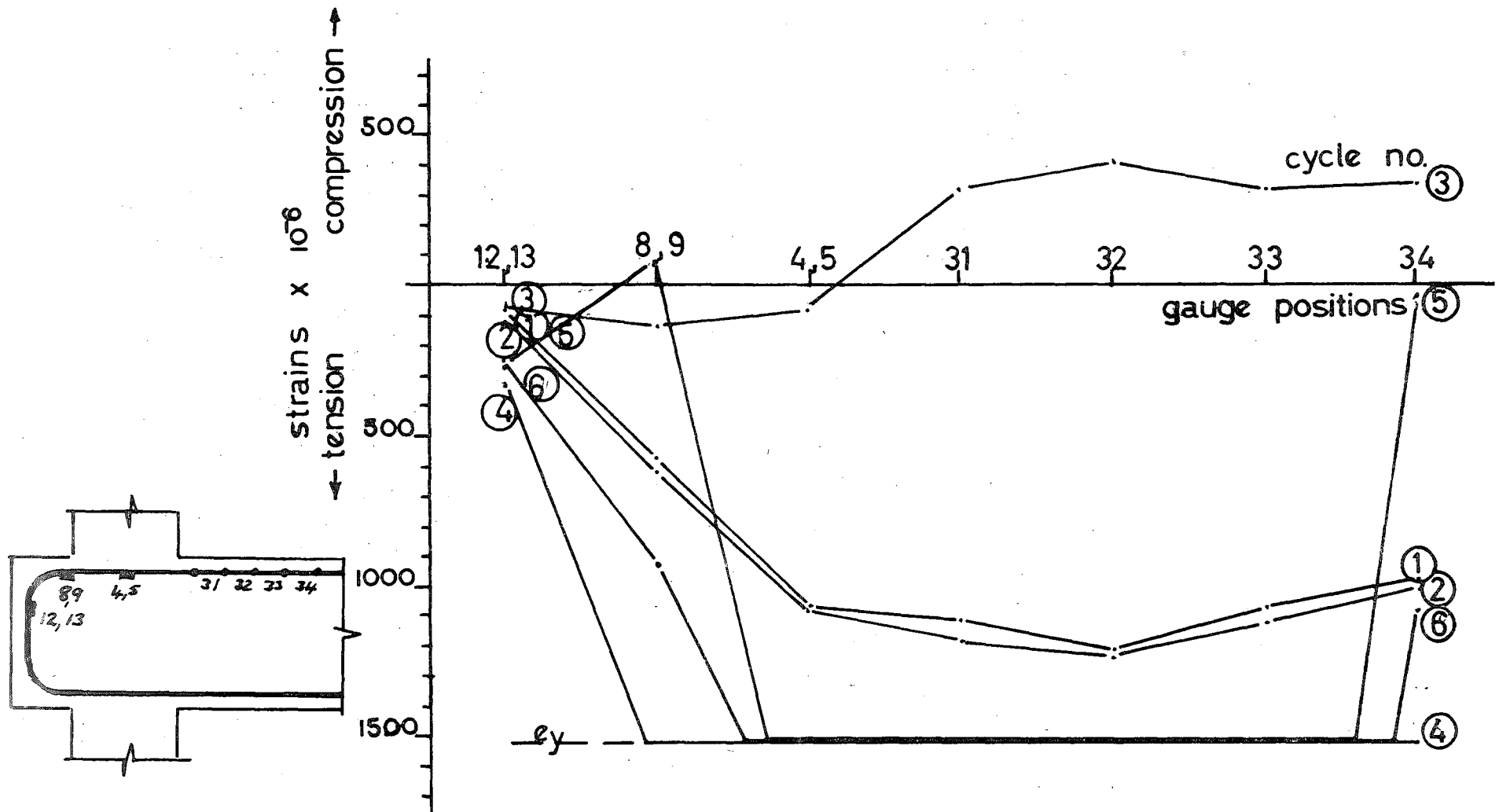
Strains in Inner Column Bars

FIG 4.6

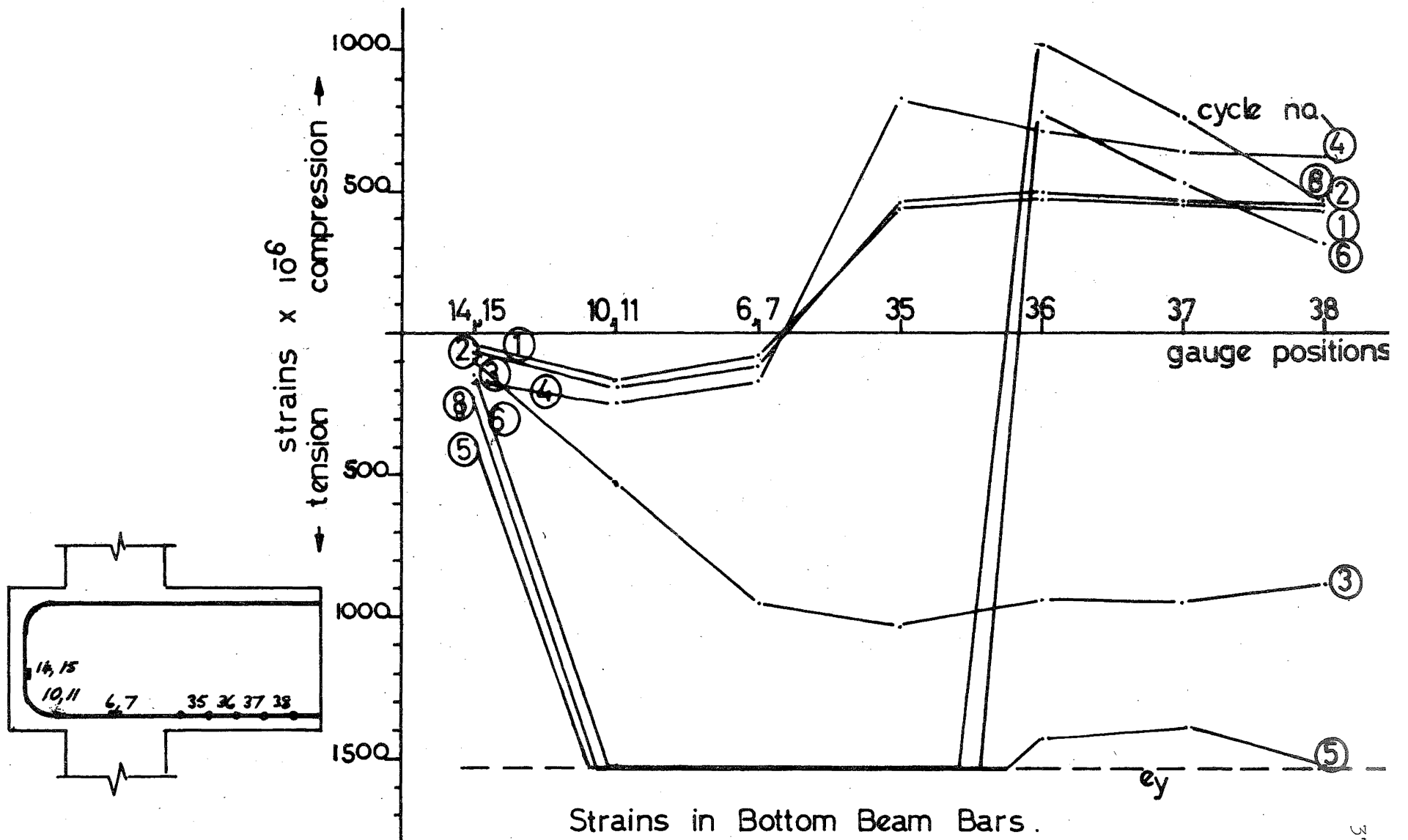
beyond cycle 5 because yield tensile strains were observed in this cycle where compressive strains should occur. This was because once the steel had yielded the Bauschinger effect needs to be considered. Hence from this point onwards it is necessary to work in stresses rather than strains.

Fig. 4.6 shows the strains in the inner column bars. The elastic cycle plots were much as expected. The significant point was that the tensile strains were greater than the compressive ones which would be expected. Cycle 4 shows that the lower column bar did not yield in compression as did the upper one. This was because the axial load was higher in the bottom column, hence its moment of resistance was higher and consequently the steel strains were lower, for this cycle.

4.3.4 Strains in Main Beam Bars. Fig. 4.7 shows the distribution of strains in the upper beam bars. The elastic cycles are as expected, with tensile strains greater than compressive strains. Even in the elastic cycle strains are present beyond the bend in the reinforcement. The first elastic cycle led to substantial yielding in the beam steel. One of the reasons for this is probably that the moment of resistance at first yield is less than the ultimate moment of resistance. Cycle 5 shows the Bauschinger effect with tensile yield strains instead of compressive strains. Fig. 4.8 shows strains in bottom beam reinforcement. Tensile strains and Bauschinger effect again dominate. The interesting point is the tension values in the anchorage region when the bars in the beam itself were in compression.



Strains in Upper Beam Bars.
FIG 4.7



Strains in Bottom Beam Bars.

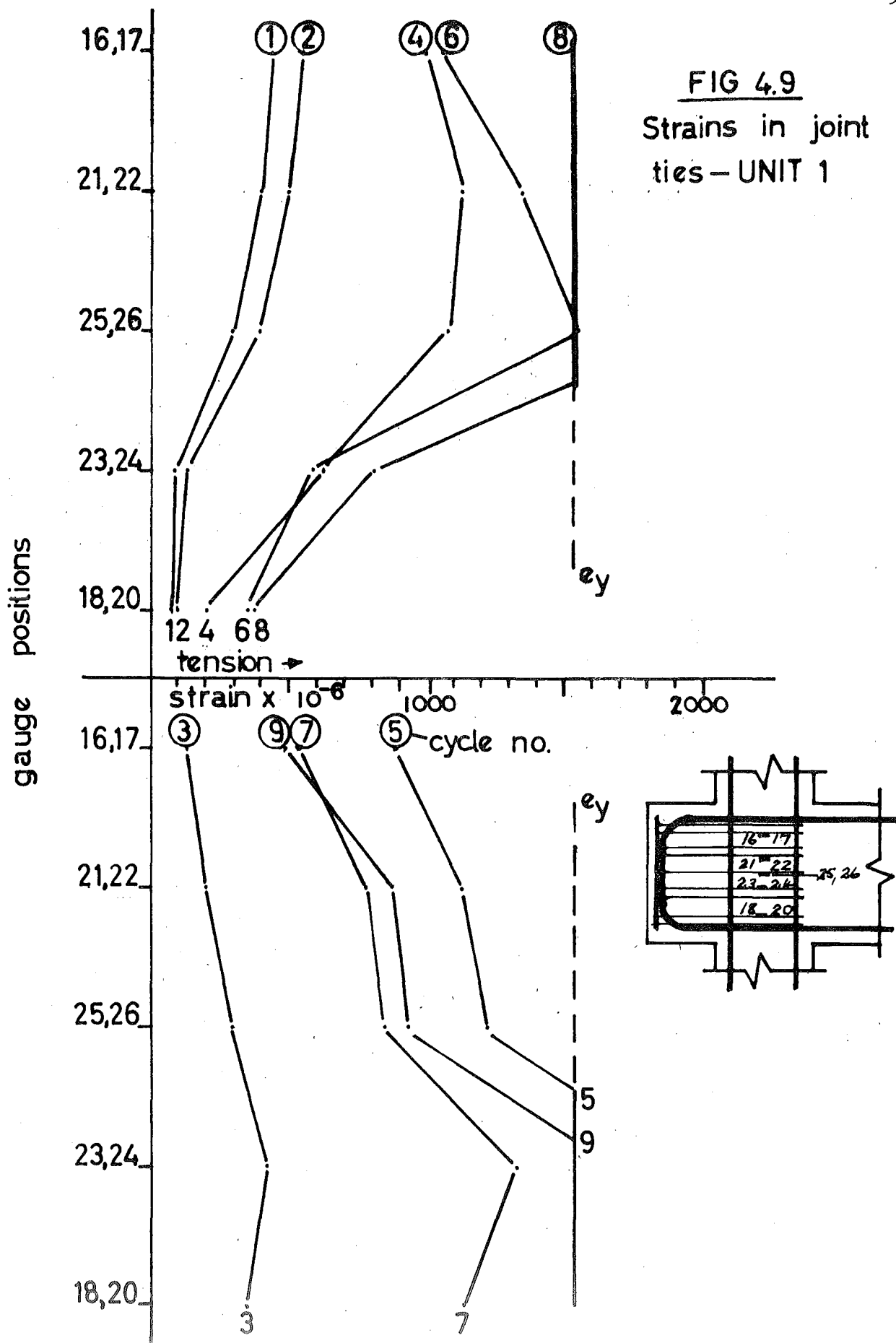
FIG 4.8

4.3.5 Strains Within the Joint. Lateral ties passing through the joint were strain gauged to give some indication of the normal forces present in the main ties. The appearance of diagonal cracks in the joint region showed that the shear forces were confined to this area and cracks generally formed on a corner to corner basis rather than at 45 degrees. This meant that the 45 degree assumption was invalid.

Fig. 4.9 shows the distribution of strains, for the peaks of various load cycles, in the joint ties at a position in the middle of the joint. The ties were placed in groups of two with a $\frac{1}{2}$ inch spacing between them. This was necessary to allow the DEMEC studs to be placed on the column bars. In practice placing the ties in pairs is an undesirable procedure as it leads to greater spacing and hence spalling between the ties. From Fig. 4.9 it can be seen that all ties have yielded by the end of cycle 9. This in itself is of great significance and it is desirable for the ties not to yield. Once the ties yield they are able to bow outwards very easily and cannot satisfactorily confine the concrete within the joint. It was realized here that since the shear forces were confined to the joint region the tie detail used could be improved by placing the ties only around the column bars, without extending them into the anchorage block. Ties were placed around the column bars in UNIT 3 and even though there were only five ties instead of nine, the performance of the unit was almost identical with that of the first two units (see Table 4.2) especially in the earlier cycles.

Strain plots show in this case that the assumption that the ties take equal amounts of shear is invalid. For the load applied

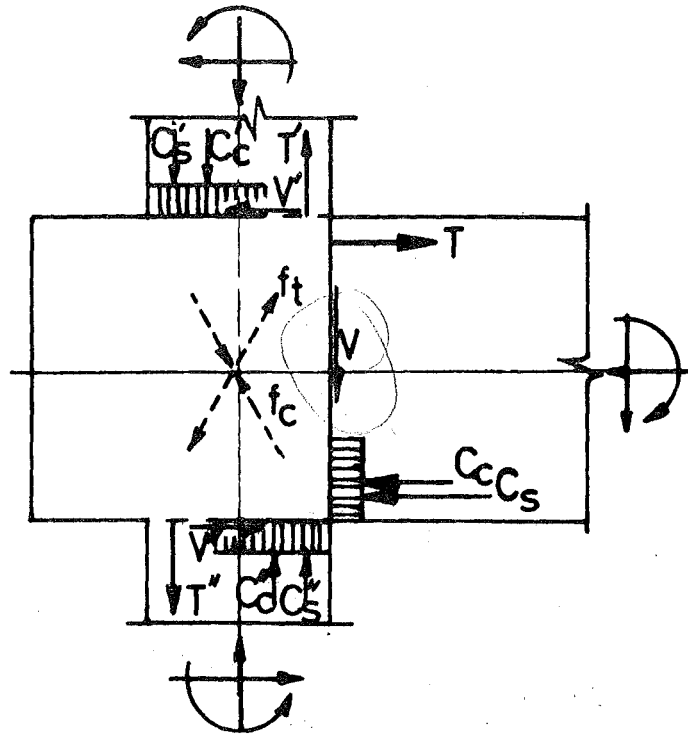
FIG 4.9
Strains in joint
ties – UNIT 1



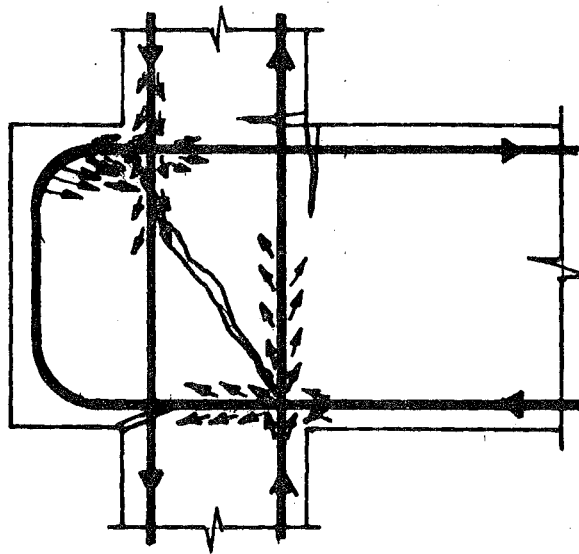
down at the end of the beam the top ties are more highly strained and for the opposite loading direction the bottom ties are more highly strained. The reason for this is that these ties cross a major diagonal crack. As the cracks do not pass exactly from corner to corner major cracks do not pass through the extreme top and bottom ties with each load reversal. Fig. 4.10 shows the mechanism of the joint failure as described above.

Fig. 4.11, showing a plot of the strains within the lateral ties through the middle of the joint, indicates the presence of significant normal forces on the main joint ties. These ties helped to slow down the joint degradation and ensured that the main ties exerted an effective confining force for a greater number of load cycles. However, from the plot of strains it is obvious that these ties were not sufficient to restrain the main ties in the later cycles. The lateral tie second from the top was the first to yield in cycle 5. There appears to be an anomaly here in that in cycle 5 (see Fig. 4.9) it is the lower main ties which yield. This can be explained by the accuracy in the construction of the specimen. The lateral ties will efficiently restrain the main ties only if there is a metal to metal contact between the bars. This means that if there is a gap initially present then considerable yielding can take place before the effect of the lateral ties is fully realized. Hence from a practical point of view this method of confining is unsatisfactory.

Fig. 4.12 gives an indication of the lateral forces present at the level of the exterior column bars. The lateral forces present are much less than at the centre further showing that the shear forces

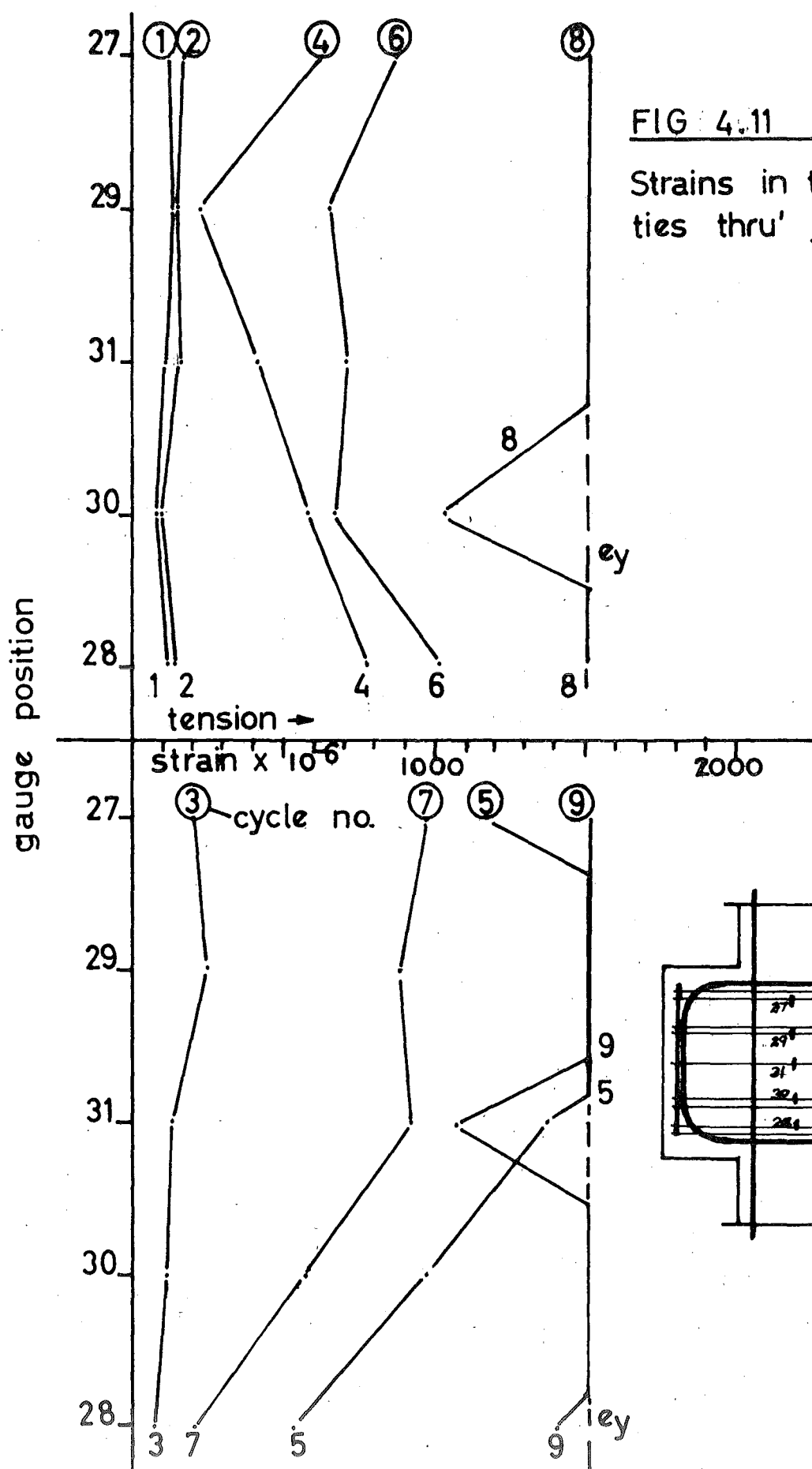


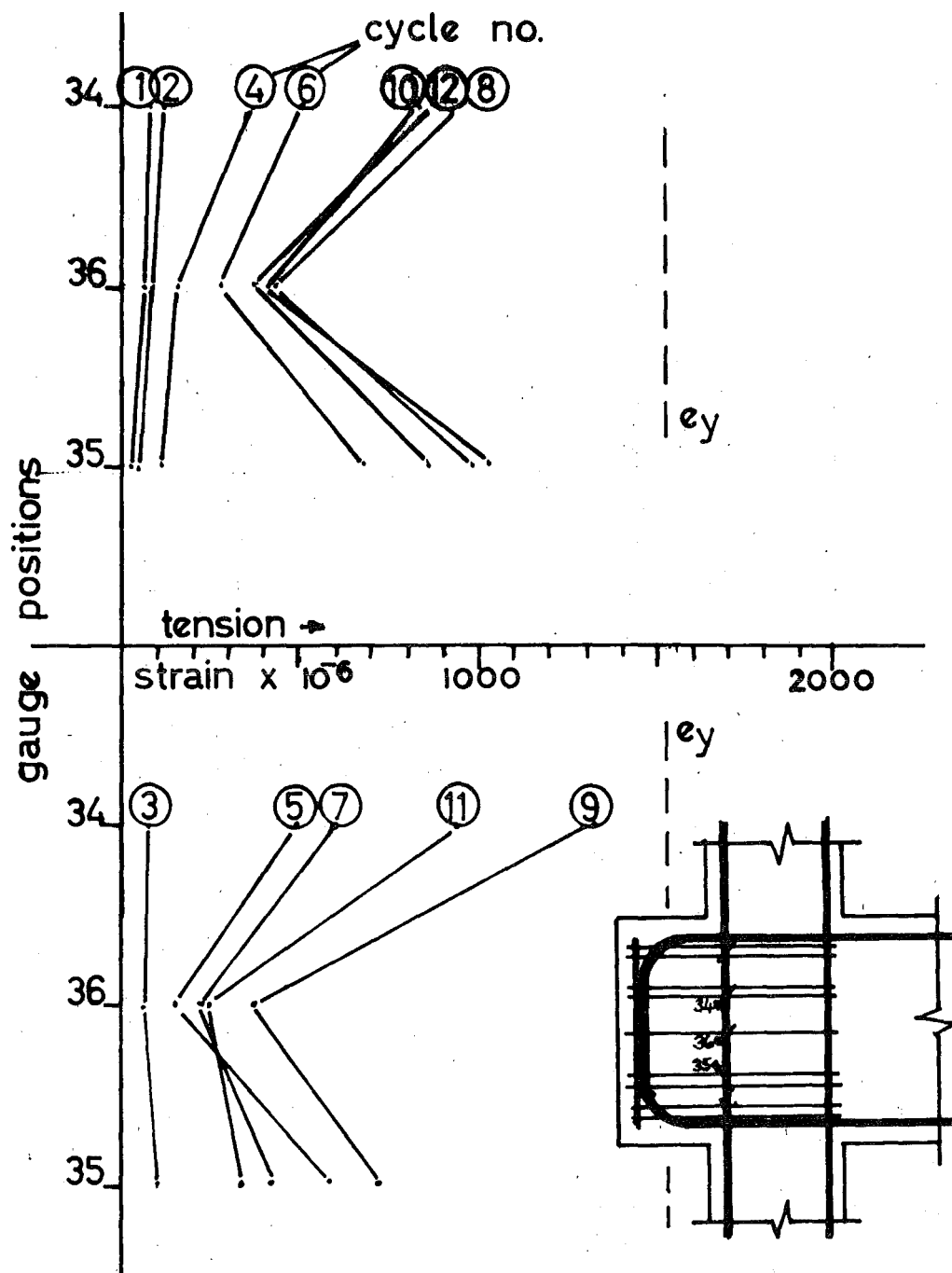
Forces acting on the joint



Distribution of forces within the joint
& formation of diagonal tension crack.

FIG 4 10



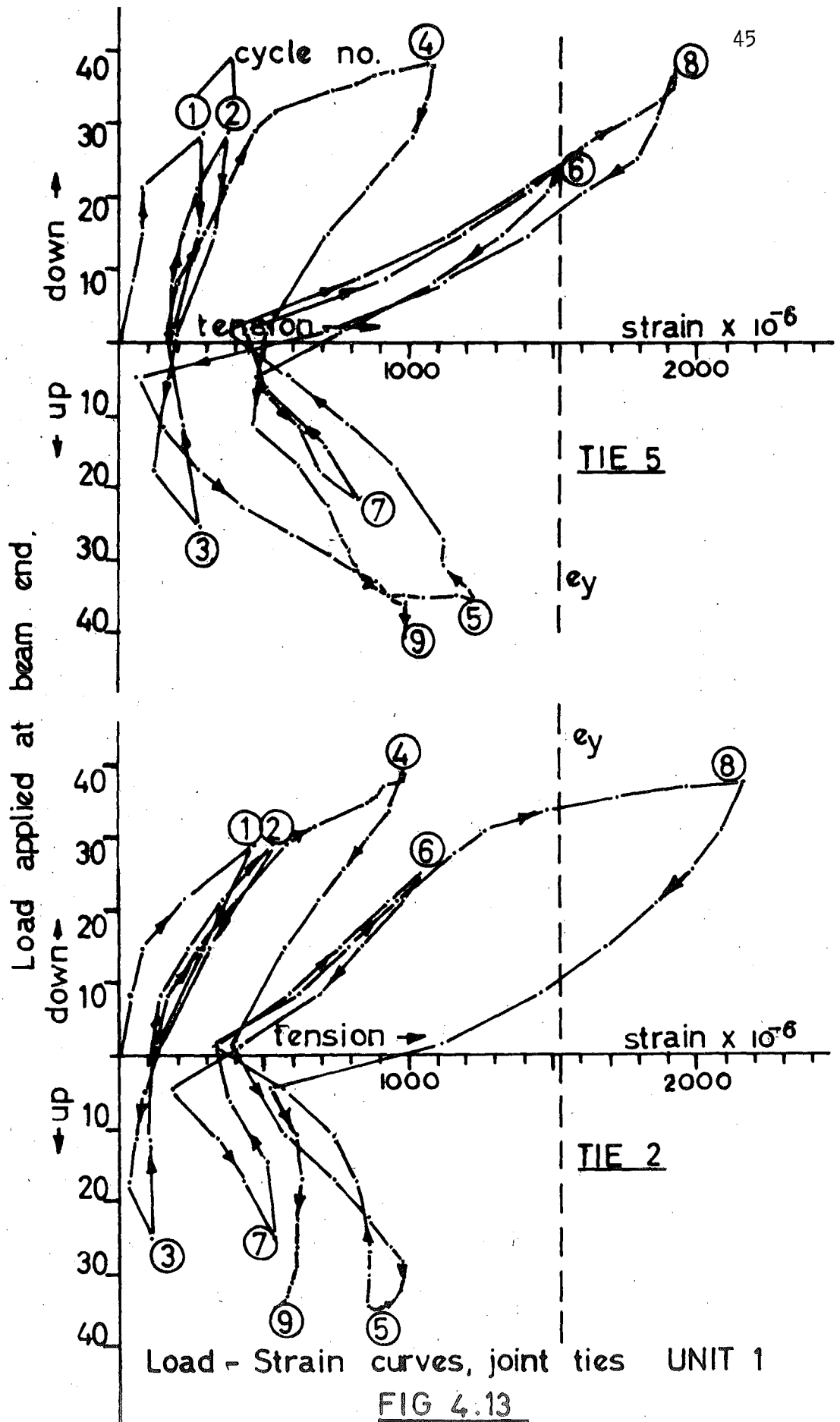


Strains in transverse ties thru' joint
at outer column level UNIT 1

FIG 4.12

are confined within the joint. The necessity of having metal to metal contact of these two sets of ties and the practical shortcomings involved with this, as mentioned before, **could** be the reason for the low steel stresses. It is evident that the lateral forces present in these ties are greater towards the top and bottom of the joint.

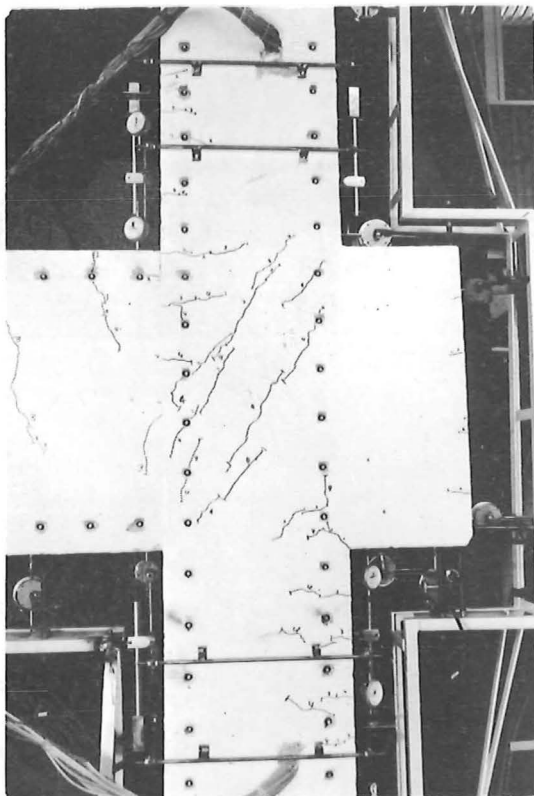
Fig. 4.13 is a plot of the strain history of two main ties within the joint. The ties are numbered from the top and hence tie 2 is an upper tie and tie 5 is the middle tie. The ties are in tension throughout the complete loading sequence. Tie 5 in earlier cycles shows strains which are approximately equal for load increments in each direction. As diagonal cracking occurred in a similar place in each direction this is to be expected. Tie 2 shows that the downward load cycles cause greater joint shears than do the upward load cycles. The reasons for this are explained earlier. Another feature is that the strains in the upper tie are of the same order of magnitude as the middle tie. There are two ties at the top and only one at the centre. This suggests that the joint forces are greater towards the top and bottom of the joint and hence a greater confining force is required in this region. In the plastic cycles it is observed that once the maximum load is reached there appears to be little increase in joint tie strains with a further increase in rotation of the beam and column, and in fact in some ties there is even a decrease in the strain values. When the load was completely released it was observed that the main ties still have a residual tensile force in them even though they have not yielded. This was due to slip in the cracks and hence they were



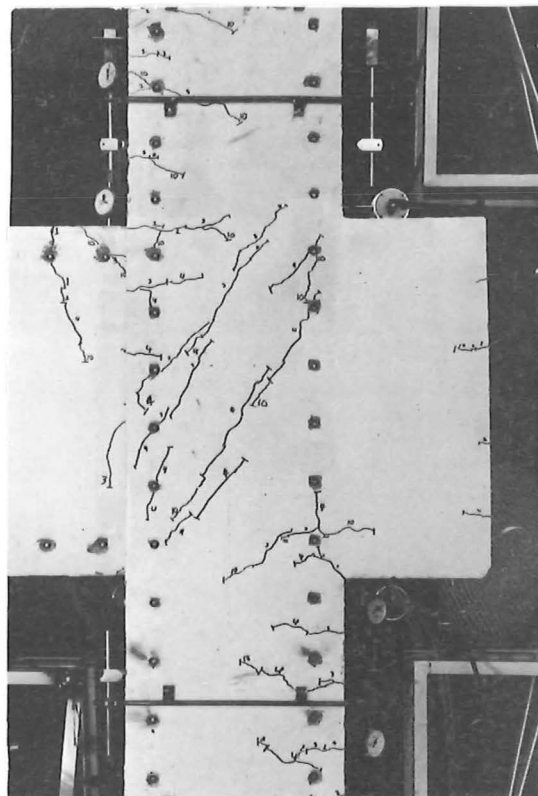
unable to close completely when the load was released.

4.3.6 Crack Development and Mode of Failure. Figs. 4.14.1 to 4.14.9 show the development of cracks in cycles 1,2,3,4,5,8,9,12,13. Fig. 4.14.10 show the extent to which plastic hinge had developed at the end of cycle 13.

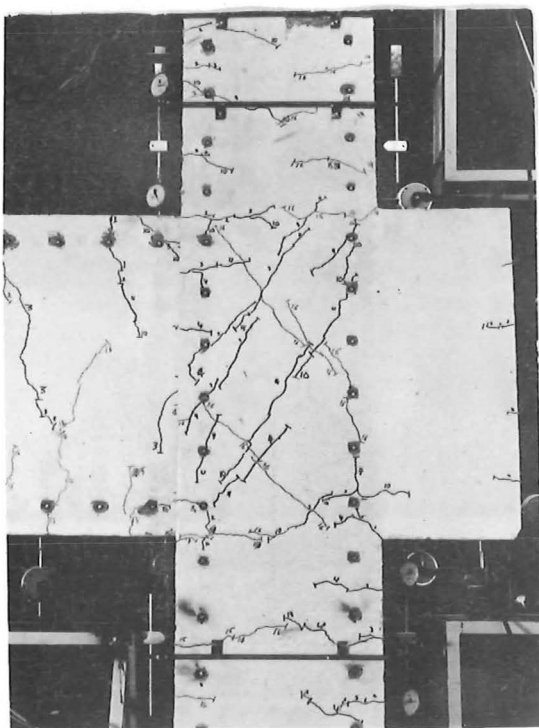
Flexural cracks occurred in the beam during the first load increment of cycle 1. The first diagonal tension cracks occurred in the joint in the third load increment of cycle one. Further diagonal cracks occurred in increment 10 of cycle 2 even though the specimen had been loaded to this extent in cycle 1. During cycle 4 a crack opened up down the level where the beam joined the column. Also there was the appearance of a few diagonal cracks in the upper part of the beam near the column face. The cracks at the extreme edge of the anchorage block were shrinkage cracks. Cycle 5 (Fig. 4.14.5) shows the onset of spalling in the upper column just above the anchorage block. Crushing of the cover concrete was observed in this area during the latter load increments of cycle 4. Evident in cycle 5 was the formation of cracks indicating the start of bond failure along the line of beam flexural reinforcement in the anchorage block. Cycle 8 (Fig. 4.14.6) shows the start of spalling on the column just above the beam and also the formation of a large tension crack in the corner between the anchorage block and the lower part of the column. The onset of spalling of the joint cover concrete was observed in cycle 9 (Fig. 4.14.7). Cycle 12 (Fig. 4.14.8) shows a further loss in the joint cover concrete and also a loss in some of the anchorage block



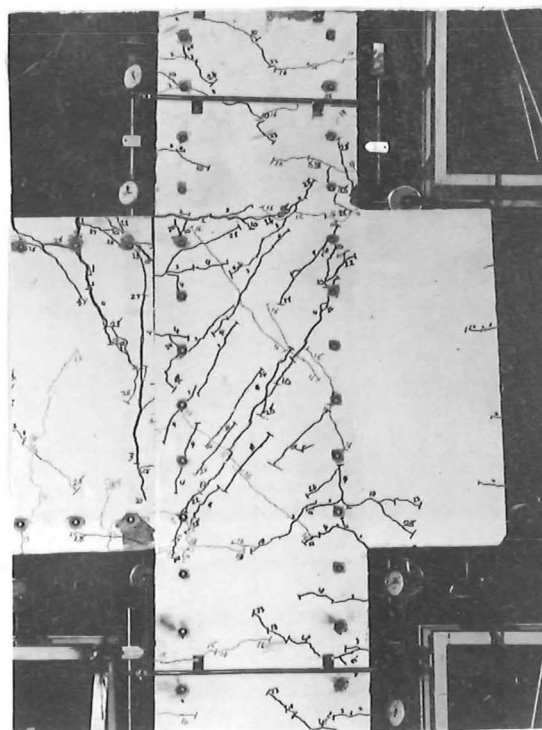
CYCLE 1.
Fig. 4.14.1.



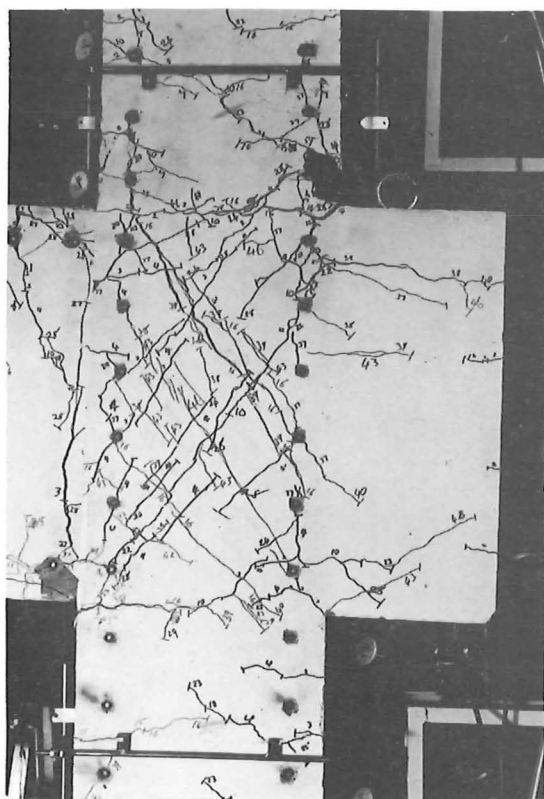
CYCLE 2.
Fig. 4.14.1.



CYCLE 3.
Fig. 4.14.3.

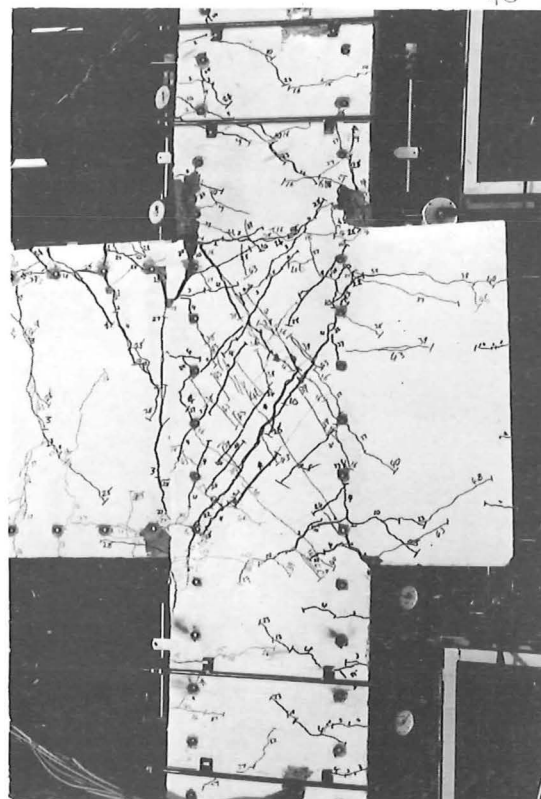


CYCLE 4.
Fig. 4.14.4.



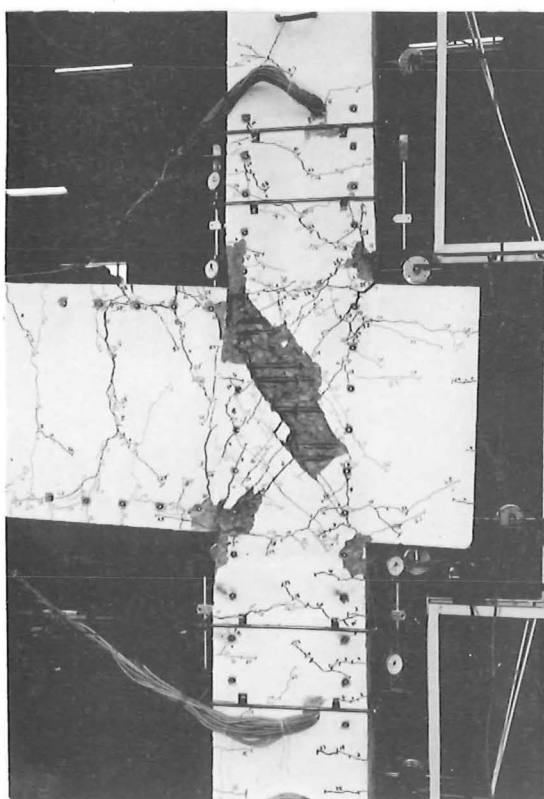
CYCLE 5.

Fig. 4.14.5.



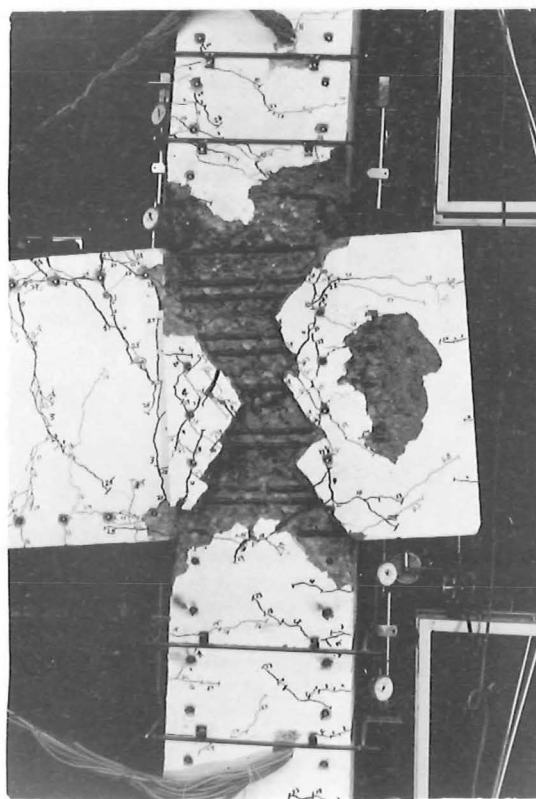
CYCLE 8.

Fig. 4.14.6.



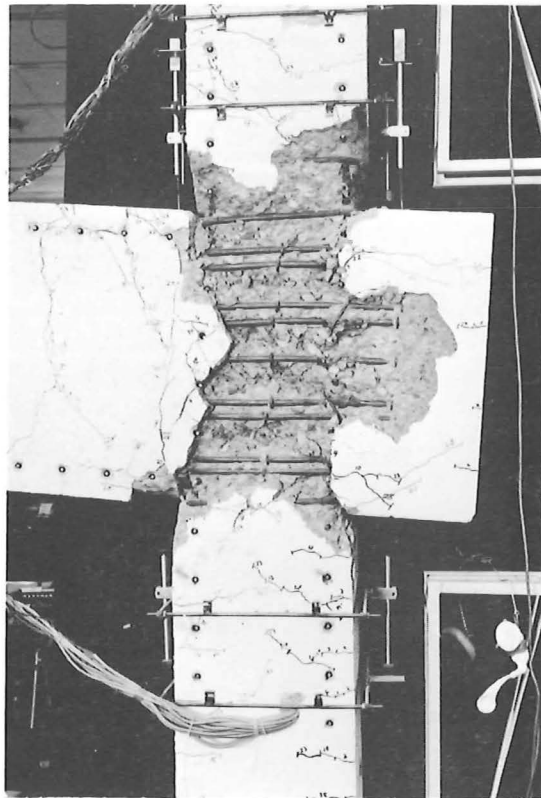
CYCLE 9.

Fig. 4.14.7.



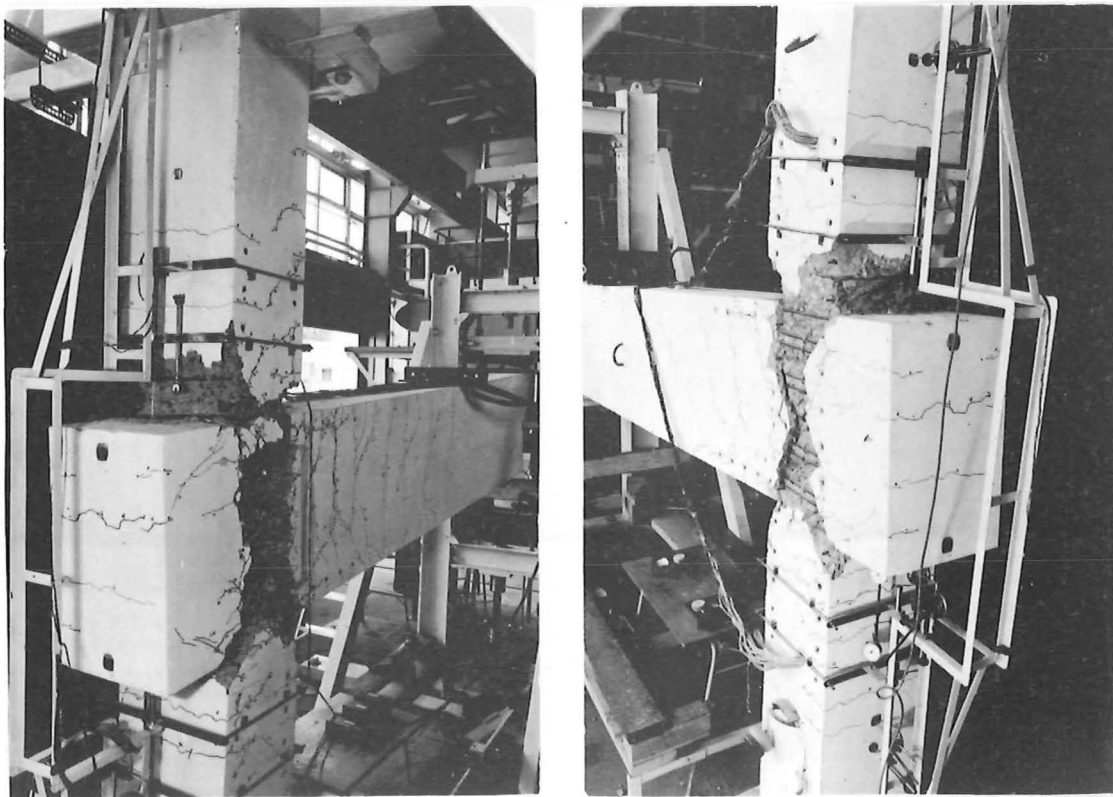
CYCLE 12.

Fig. 4.14.8.



CYCLE 13.

Fig. 4.14.9.



VIEW OF HINGE FORMATION IN TOP COLUMN.

Fig. 4.14.10.

cover. The formation of the upper column hinge was more developed and a displacement between the upper and lower part of the column, across the joint can be observed. Cycle 13 (Fig. 4.14.9) shows a further loss in cover concrete but there is little more development of the column hinge. In the latter cycles very little more cracking occurred in the beam. It should be noted here that the condition of the joint is only marginal but with better detailing this could be improved (see conclusions and discussion, Chapt. 5).

Fig. 4.14.10 gives an indication of the degree to which column hinging has occurred in the final plastic cycles. The spalling length on the back face of the column was about $d/2$. Rotation measurements on two seven inch gauge lengths on columns out from the beam showed that 75 per cent of the rotation occurred in the first gauge length for the upper column while 85 per cent rotation occurred in the first gauge length for the lower column.

The test specimen could not be considered to have failed as it was still carrying 84 per cent of its theoretical ultimate capacity at a combined section ductility of - 9 in the last cycle, although there was at this stage a substantial stiffness degradation. The unit was deflected to the physical limits of the test rig, but if further deflection had been possible, trends indicated that degradation of the joint would have occurred at the expense of further column hinge development.

4.4 UNIT 2.

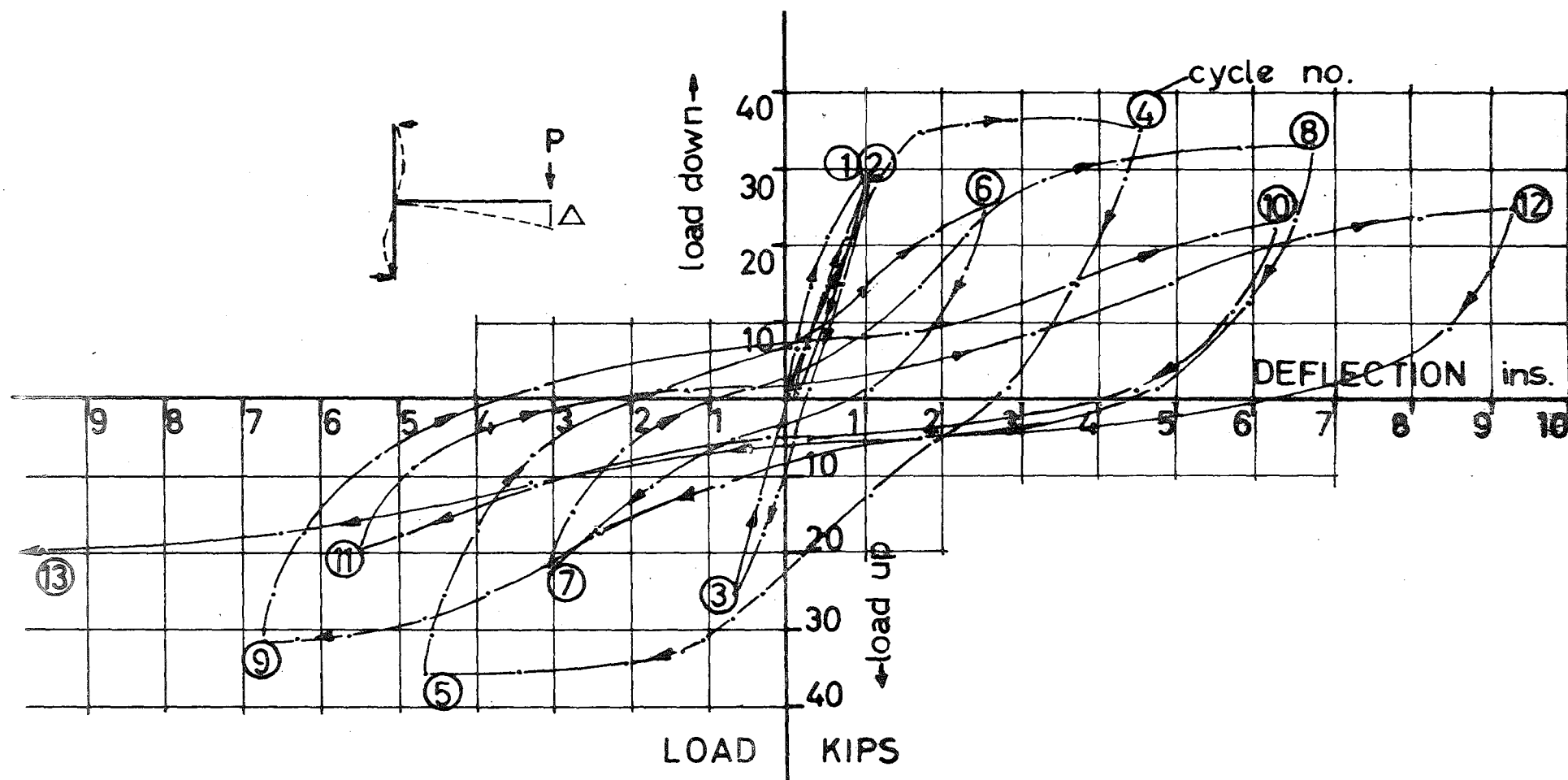
4.4.1 Load-Deflection. Although the only difference between

UNIT 1 and UNIT 2 was in the size and distribution of the lateral ties through the joint, the load deflection plot was inferior to that of UNIT 1 in the later cycles. Cycles 1 and 2, so called elastic cycles, show less stiffness than for UNIT 1. The slope of the line gives an indication of the stiffness of the overall unit. Hence on the plot (Fig. 4.15) the unit ductility factor $\left(\frac{\Delta}{\Delta_y}\right)$ corresponds to a deflection of about 1.25 inches ($\Delta = \Delta_y$ at this point).

The Bauschinger effect and the effect of the opening and closing of cracks are shown once again. Full theoretical ultimate moment was attained in the first two plastic cycles, 4 and 5. The slight increase in the theoretical ultimate moment of resistance was due to the strain hardening in the column bars.

Cycle 6, an elastic cycle, shows a stiffness of the same order as UNIT 1, as did cycles 4 and 5. The last load increment of cycle 6 and all of cycle 7 shows a decline in stiffness compared with UNIT 1. This becomes even more noticeable in the later plastic cycles, especially cycles 12 and 13. This reinforces a very important point, that although two different types of joint detailing can have the same initial qualities as far as stiffness is concerned one can be superior to another after several plastic cycles have occurred.

The falloff in moment resistance in UNIT 2 in the latter cycles indicates that the joint tie arrangement is unsatisfactory. Comparison with UNIT 1 shows that the $\frac{1}{4}$ inch ties through the middle of the joint greatly assisted in keeping it together. In cycle 12 only



UNIT 2 - LOAD DEFLECTION CURVE

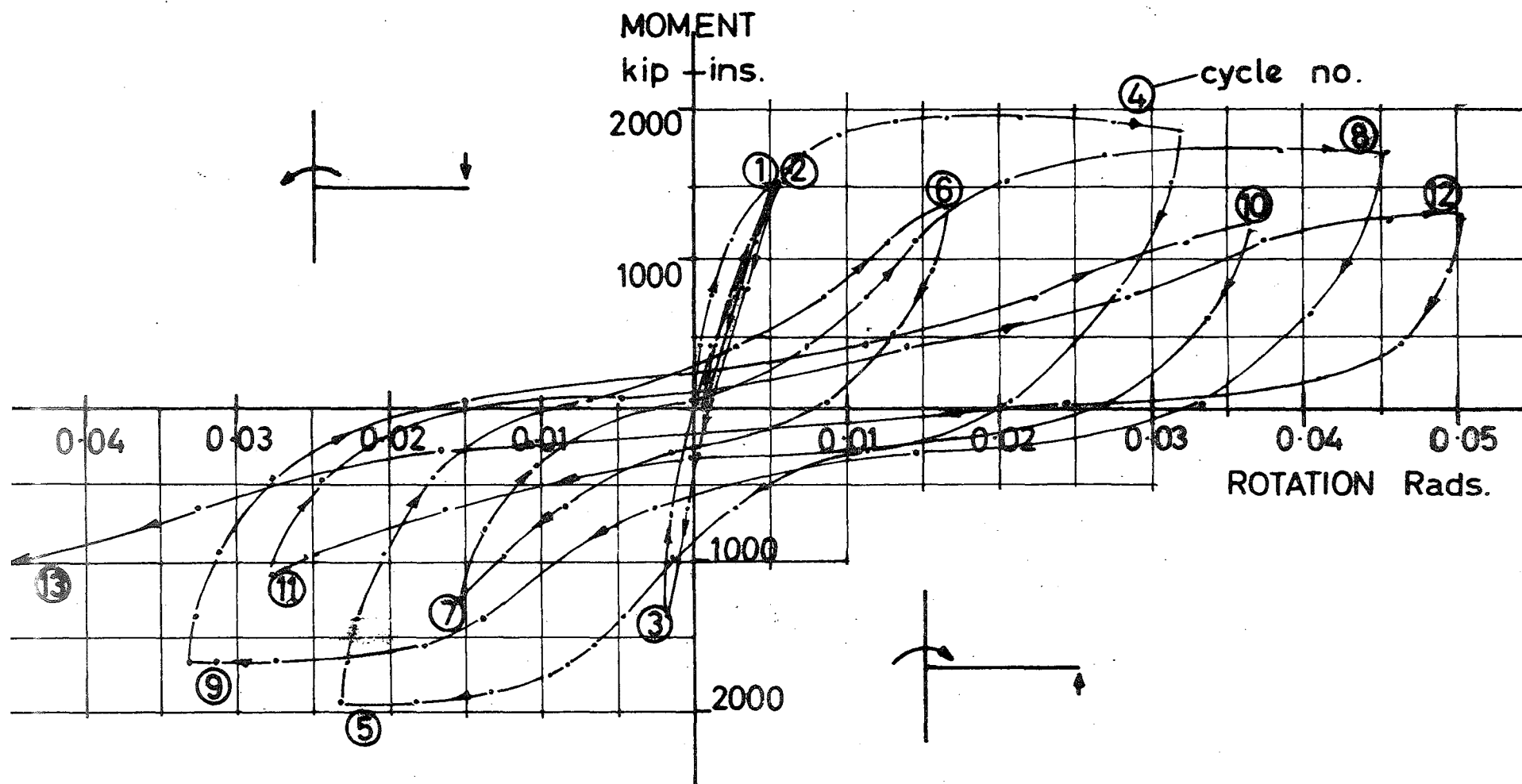
FIG 4 15

70 per cent of the theoretical ultimate moment was attained and in cycle 13 this value reduced to only 57 per cent. This reduction is due to the break down of the joint concrete.

In UNIT 2 the overall ductilities attained were less than those in UNIT 1. For example in UNIT 1 an overall ductility factor of about +11 was attained in cycle 12 while in UNIT 2 the value was only about +7.

4.4.2 Moment Rotation for Columns. Because of the degradation of the joint in UNIT 2 the values in the moment-rotation curves for the column regions are not indicative of the values that would have been obtained had the joint remained intact. The values up to cycle 6 are reasonable as it was at this stage that the joint started to deteriorate. As in UNIT 1 yielding in the beam steel was again recorded, and this in itself did not greatly affect the rotation values obtained. The rotation values obtained in the later cycles are less reliable as with the breakdown of the joint, bending of the column bars occurred largely within the joint. Also the value of load applied was not the maximum possible for the section because the load carrying capacity was determined by joint behaviour and it appeared that the column itself was capable of carrying a greater load.

Fig. 4.16 shows the moment-rotation plot for the upper column of UNIT 2. Cycles 1 and 2 are the so called linear-elastic cycles. Cycle 1 is much more curved than the second cycle due to the effect of cracking. The slope is less than for UNIT 1 indicating again that



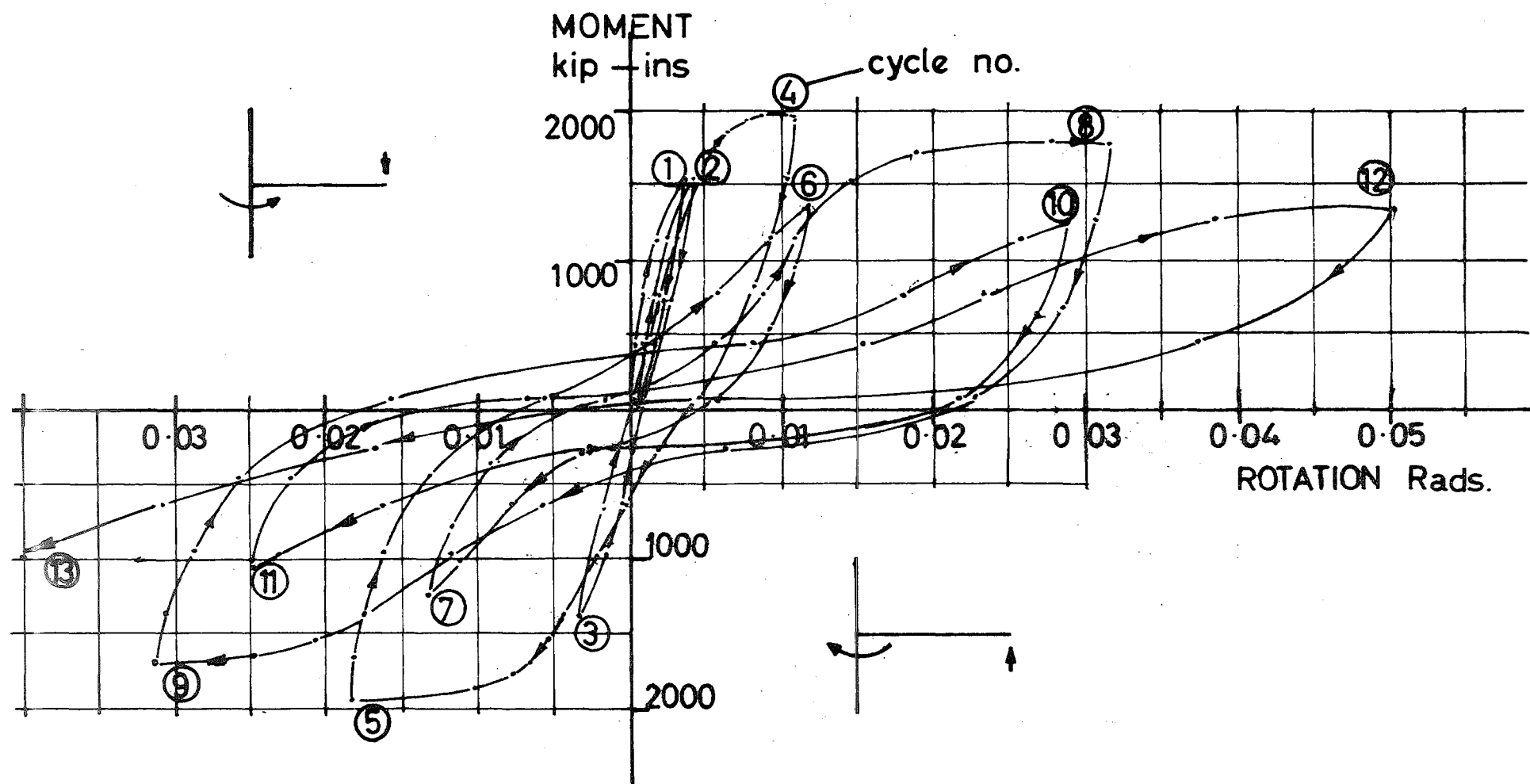
MOMENT — ROTATION CURVE
UPPER COLUMN — UNIT 2

FIG 4.16

the stiffness is slightly less. The non-linearity of cycle 3 indicates the start of crack formation for loading in this direction. Cycle 4, the first plastic cycle, had a maximum moment of resistance which was 6 per cent greater than the theoretical value. A rotational ductility factor of about +6 is obtained at full moment of resistance. The path from cycle 4 to cycle 5 shows increasing stiffness upon closing of cracks and the Bauschinger effect in the steel. Cycle 5 shows a decrease in ductility i.e. - 4.5. The reason for this is explained in chapter 4.3.2 where there is a different axial load present on the column for the load applied in each direction. Elastic cycles 6 and 7 give an indication of the progressive loss of stiffness in the whole unit rather than in the column section itself due to the excessive cracking within the joint region.

Plastic cycles 8 and 9 show reasonable rotation values but with a reduction in the maximum moments. The rotation in cycle 8 is greater than in cycle 9 (i.e. +9 as compared to -6.5) and this is again due to the different axial loads present with the reversed load cycles. The elastic cycles 10 and 11 show the further reduction in stiffness due to the degradation of the joint. Cycles 12 and 13 show the full effect of joint deterioration. In these cycles rotation occurred within the joint, leading to smaller rotations in the column. This is shown in cycle 12 where the ductility factor is only +10 compared to +9 in cycle 8.

Because of the joint deterioration it is impossible to say whether the column was adequate or not, but as the reinforcement



MOMENT - ROTATION CURVE
LOWER COLUMN - UNIT 2

FIG 4.17

was the same as in UNIT 1 the results obtained for that Unit gives a fair indication of the column's behaviour. Never-the-less the moment-rotation plot does give an indication of the behaviour of the column of UNIT 2 in plastic cycles 4 and 5.

The lower column rotations for UNIT 2 (Fig. 4.17) show the same effects of joint degradation as the upper column. Elastic cycles 1 and 2 show a greater stiffness than for the upper column. Cycle 4 shows little rotation (i.e. rotational ductility factor of +2) which is due to the effect of the increased column axial load leading to greater moment of resistance and hence the rotation in this cycle was confined mainly to the upper column. The lack of rotation occurring in the odd cycles i.e. 5,9,13 and loss of stiffness in the even cycles is due again to the breakdown of the joint. The same conclusions apply here as for the upper column.

4.4.3 Strains Within the Joint. The main ties in the joint were the same as in UNIT 1. The $\frac{5}{8}$ inch diameter lateral ties through the joint at the outer column bars were strain gauged. This gave an indication, of how the ties behaved unsupported over the length of the joint, and whether ties placed across the outer column bars greatly assisted the performance of the joint.

Fig. 4.18 shows the distribution of strains, for the peaks of various load cycles, in the main joint ties at a position in the middle of the joint. The ties were placed in a similar manner to UNIT 1 for the same reasons. As in UNIT 1 the strain plot shows that all ties do not take equal amounts of the joint shear. When the load is acting down on the beam the top five ties take

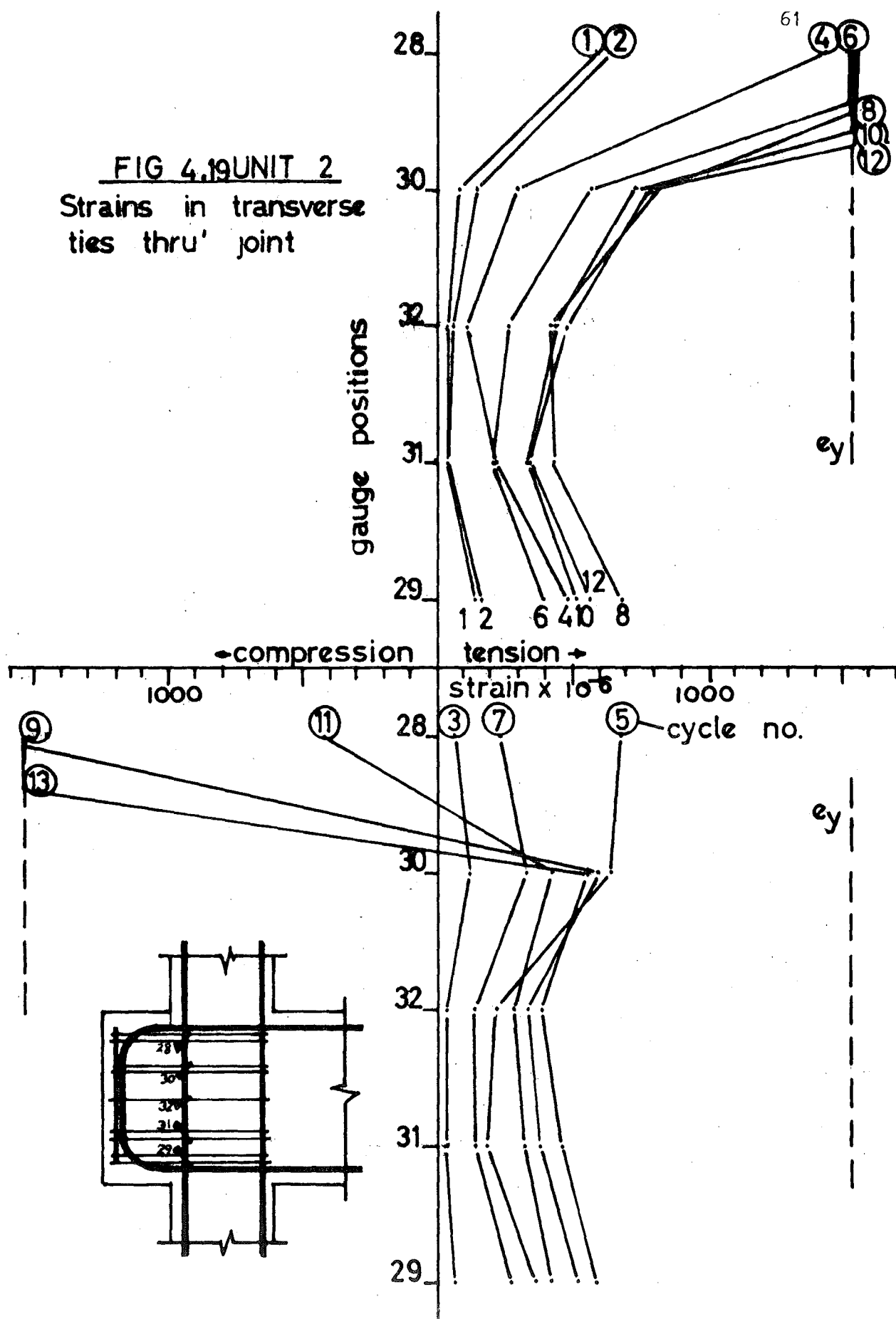
greater strains and when the load is acting up the bottom four take greater strains. The strain pattern for the joint ties in UNIT 2 (Fig. 4.18) are similar, though higher, than those in UNIT 1, up to and including cycle 5. The bottom ties yielded in cycle 5 in a similar manner to those in UNIT 1. This was the first yield of any ties.

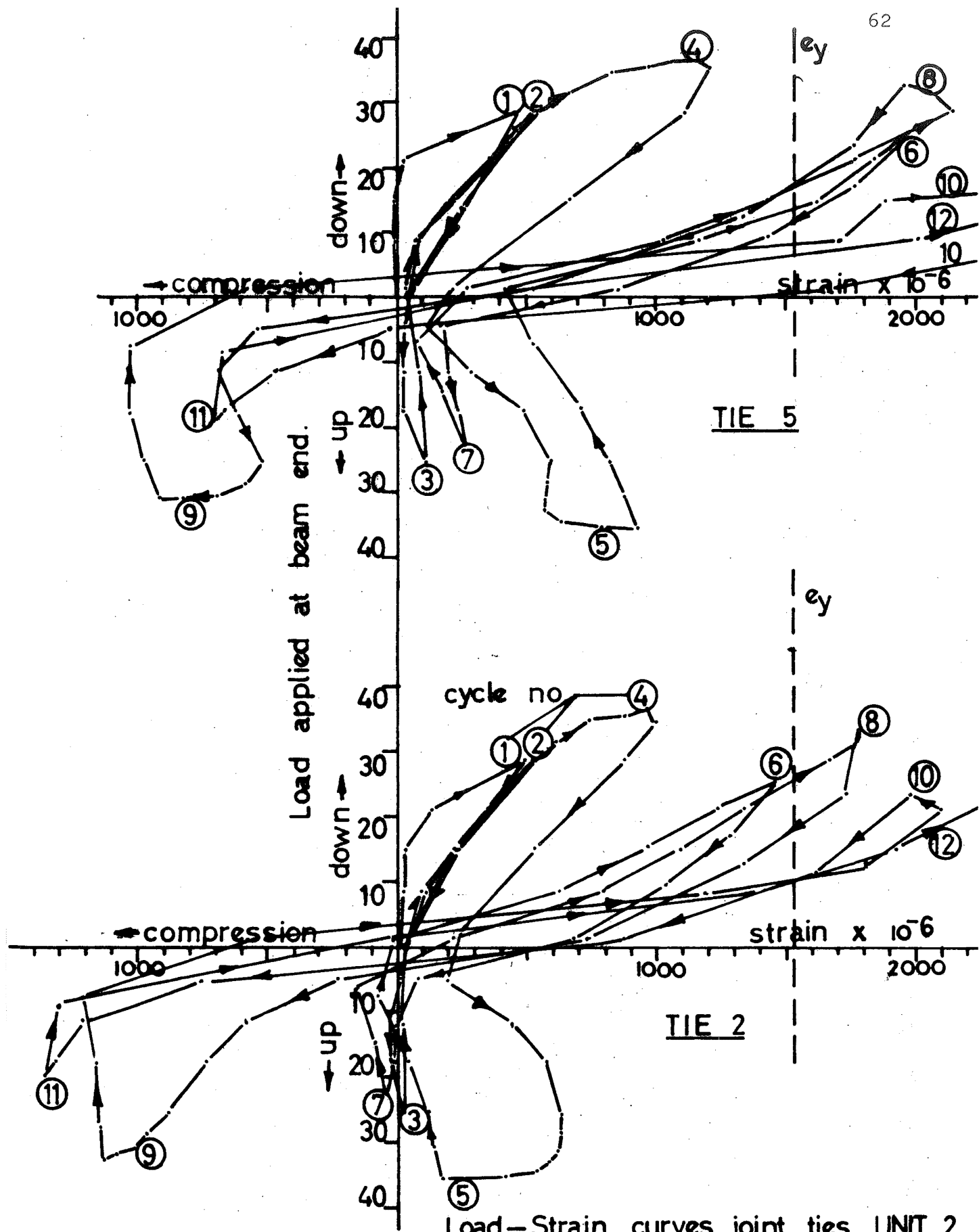
Yielding occurred in the upper ties during elastic cycle 6. Strains were higher than in UNIT 1 where only the middle tie had yielded at this point. Cycle 6 also showed the start of an interesting phenomenon which became more noticeable with successive cycles. While half the ties were yielding in tension, compression strains were becoming increasingly larger in the remainder. This process was reversible with each cycle so that the tie was generally, alternately in tension and compression. The first explanation for this is that the compressive force in the beam exerts compression on the joint ties. But because the compressive strains become large to the point of yielding in cycles 10 and 12 another explanation is called for. The joint started spalling from cycle 6 onwards and the bond around the inner column bars began to break down. This meant that with each cycle the column bars were less effectively held by the concrete and so were able to be bowed inwards by the compressive forces from the beam. This in turn led to bowing of the joint ties and hence erroneously high compressive strain readings. When the load was reversed the tensile forces present then straightened the ties out again. This emphasizes the extent to

which the joint has broken down.

Fig. 4.19 shows the distribution of strains in the lateral ties at the outer column level. When compared with the corresponding measurements taken in UNIT 1 the strains present are generally lower, except for the centre tie in which the strains are of equal magnitude. Because the lateral tie area in UNIT 2 is six times that of UNIT 1 the forces carried here are much larger. This suggests that because there is no restraining force at the centre of the joint in UNIT 2 the ties at the column level in fact do carry greater forces, but not as efficiently. The strain plot in Fig. 4.15 shows that at this level normal forces increase towards the top and bottom of the joint. The only anomaly that is apparent in this figure is the strain plot in tie 28. Cycles 1 and 2 appear normal but from this point on the strains do not follow the same pattern as the corresponding bottom tie and the strains quickly become high, alternating between yielding in tension and yielding in compression from cycle 8 onwards. As it would be most unlikely that compressive strains of this magnitude could develop and by inspection it appears the buckling of the tie in this position is impossible, the most likely explanation would be a faulty strain gauge. Because of the generally, relatively low strains present in the ties it is obvious that they are inefficient. One of the reasons for this is the same as the one for the lateral ties in UNIT 1. Unless the ties are bent such that a metal contact is achieved then it is possible for large strains to develop in the main ties before the lateral ties become effective. Clearly the practical difficulties, in bending a $\frac{5}{8}$ inch diameter tie in such

FIG 4.19UNIT 2
Strains in transverse
ties thru' joint



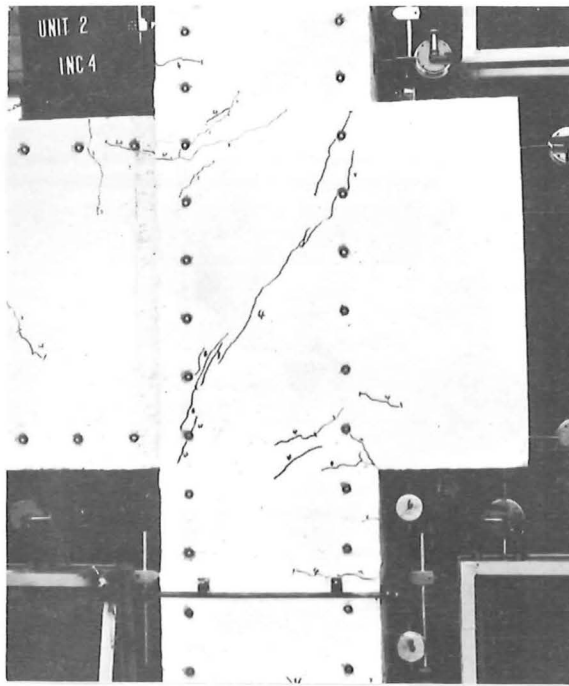


Load-Strain curves, joint ties UNIT 2
FIG 4.20

a manner, are much greater than for a $\frac{1}{4}$ inch tie. Hence this detail is practically, unfeasible.

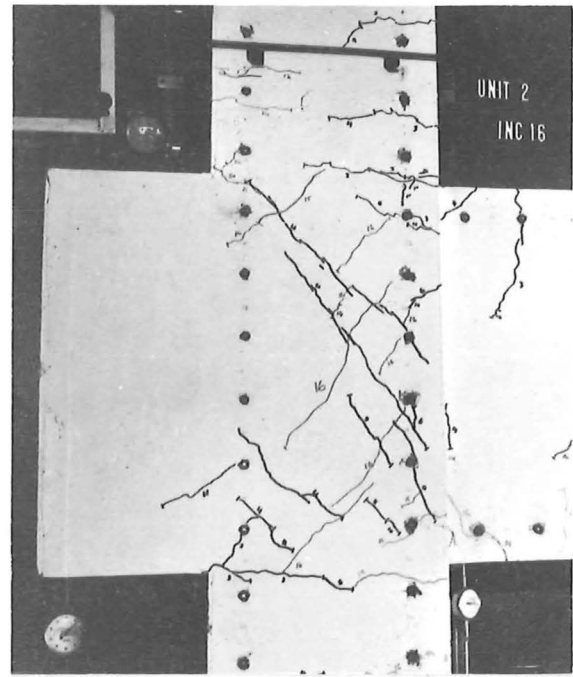
Fig. 4.20 shows a plot of the strain history of two main ties within the joint. The nine ties are numbered from the top of the joint to the bottom. Tie 5 shows approximately equal tensile strains for each load cycle up to and including cycle 5. Cycle 6 shows a dramatic increase in tie tensile strains at very low loads which is continued for the remaining even numbered load cycles. On the other hand the odd numbered cycles show increasing compression strains with each successive load cycle. This shows that with each load cycle, as the joint fails, the bowing of the ties increases. Tie 2 shows larger strains in cycles 1, 2, and 4 than in cycle 3 and part of cycle 4. This is conducive with the upper tie taking larger tensile strains in one direction compared with the other, as mentioned before. The strain plot for cycle 5 is interesting as after an initial increase in tensile strain a further load increase leads to lower strain values. This can be explained by the onset of bowing of the tie, as in this cycle this region of the joint is experiencing a compressive force from the beam. From this stage on tie 2 shows the same general trends as tie 5 although in general the strain values are less than for tie 5. This is because there are two ties in the region of tie 2 to take the forces and only one tie in the region of tie 5.

4.4.4 Crack Development and Mode of Failure. Figs. 4.21.1 to 4.21.10 shows the development of cracks in cycles 1, 3, 4, 5, 6, 8, 9, 11,



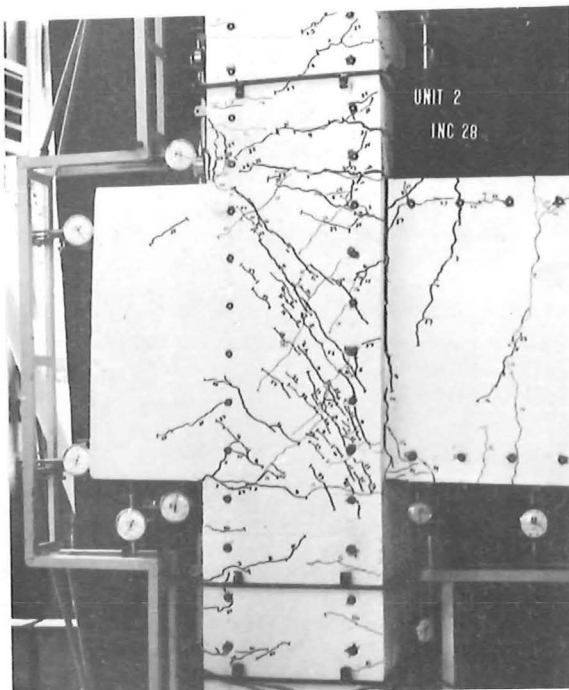
CYCLE 1.

Fig. 4.21.1.



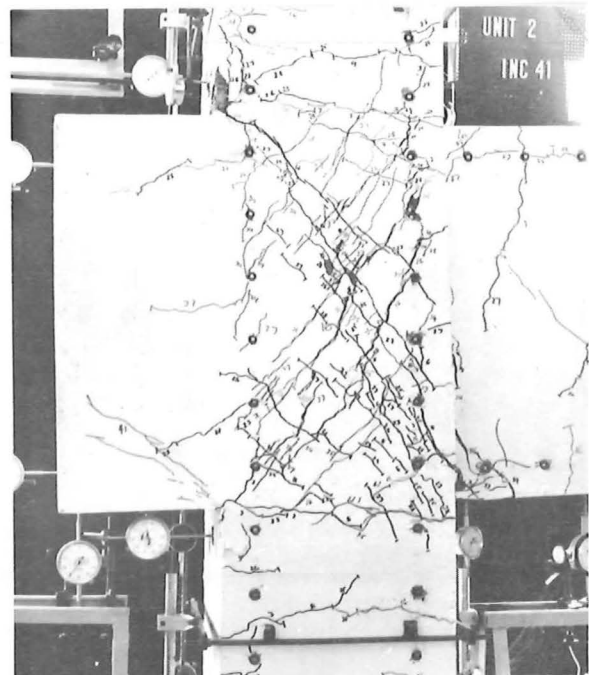
CYCLE 3.

Fig. 4.21.2.



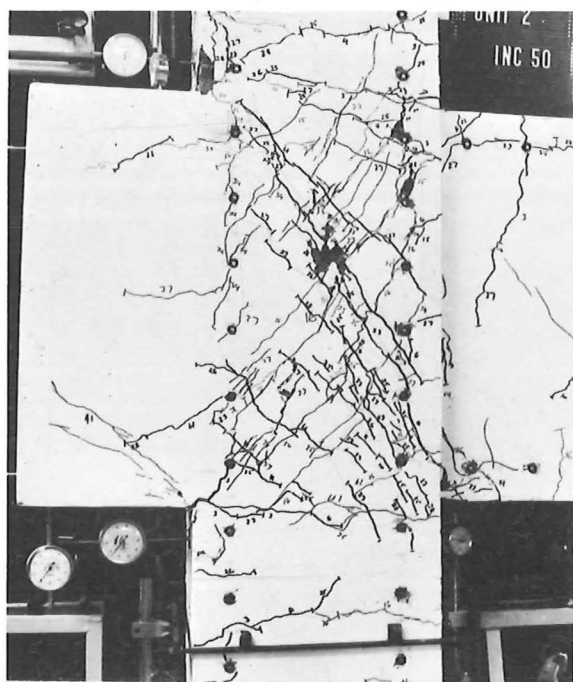
CYCLE 4.

Fig. 4.21.3.

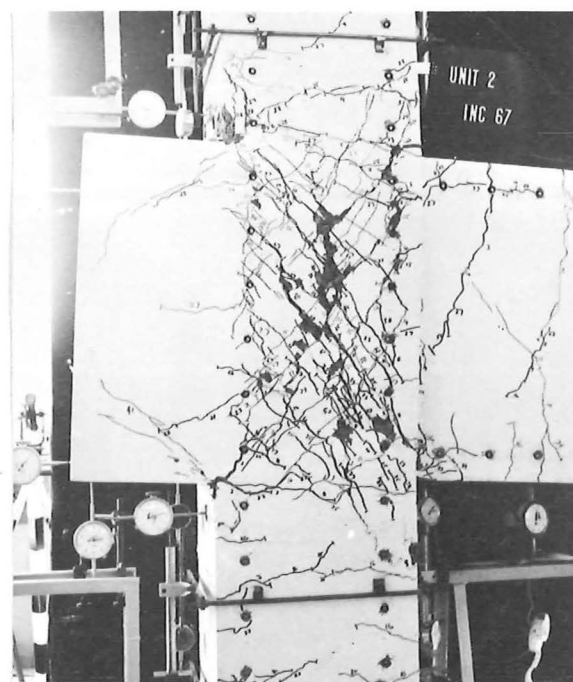


CYCLE 5.

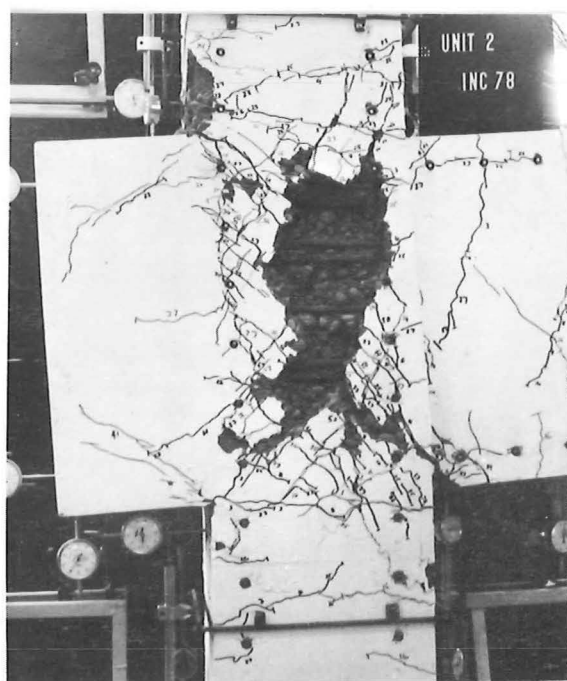
Fig. 4.21.4.



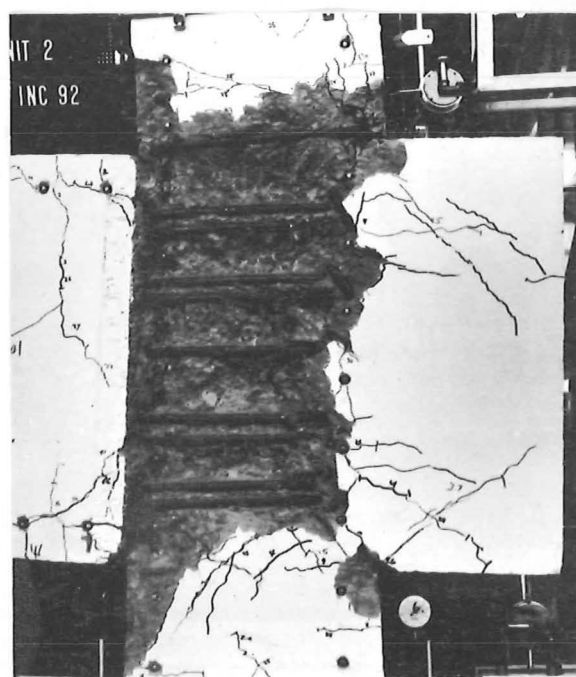
CYCLE 6.
Fig. 4.21.5.



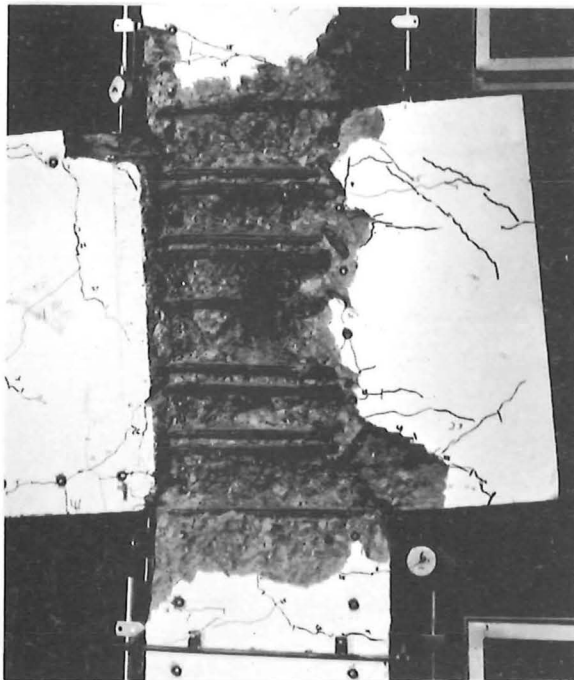
CYCLE 8.
Fig. 4.21.6.



CYCLE 9.
Fig. 4.21.7.

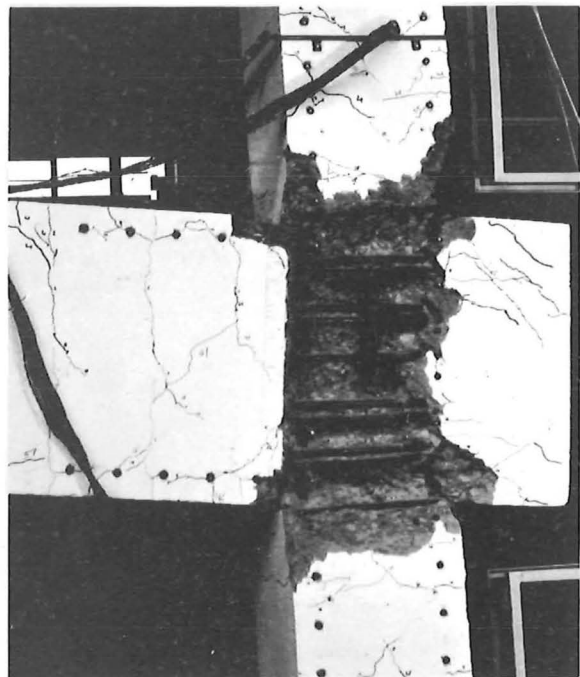


CYCLE 11.
Fig. 4.12.8.



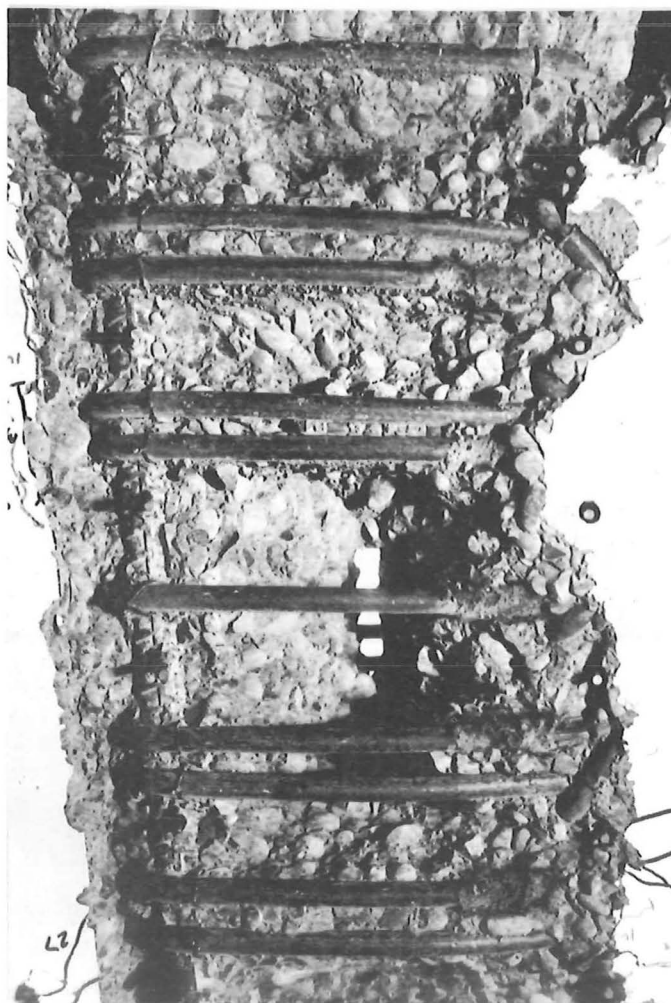
CYCLE 12.

Fig. 4.21.9.



CYCLE 13.

Fig. 4.21.10.



Joint Deterioration
at end of Load Cycles.

Fig. 4.21.11.

12,13. Fig. 4.21.11 shows the degree to which the joint has failed. Flexural cracks appeared in the first load increment of cycle 1 and joint diagonal tension cracks occurred in the last load increment of cycle 1. Fig. 4.21.2 shows the opening of the diagonal tension cracks for the load applied in the upward direction i.e. cycle 3. Cycle 4 (Fig. 4.21.3) shows the opening of a vertical crack at the beam-column junction. Cycle 5 (Fig. 4.21.4) shows the start of bond failure cracks along the line of the beam flexural reinforcement in the anchorage block. The first spalling of the joint cover concrete occurred in cycle 6, (Fig. 4.21.5) although the joint showed extensive cracking in earlier cycles. Further spalling is observed in the joint in cycle 8 (Fig. 4.21.6) and the back of the upper column shows signs of spalling. Also a large diagonal tension crack opened up from the corner where the anchorage block joined the lower column.

Fig. 4.21.7 shows extensive spalling in the joint region. The bond cracks in the anchorage block have increased slightly but there did not appear to be much crack development in the column regions above or below the joint. Cycle 11 (Fig. 4.21.8) is an elastic cycle and indicates a further degradation of the joint. It should be noted here that the load applied at this stage was only about 89 per cent of the maximum load applied in the first elastic load cycle. At this stage the inner column bars are well exposed and it can be seen that the bending in them occurred almost entirely within the confines of the joint. The bar is supposedly

in compression at the top of the column and the bending was most likely accentuated by the start of bowing due to the inability of the joint concrete to adequately restrain the bar. Cycle 12 (Fig. 4.21.9) shows a rapid breakdown of the joint by this stage. There was only slightly more spalling of the column but this was due to the effects of the joint breakdown rather than hinging occurring in the column. Also the crack at the beam-column junction had become somewhat larger. Even at this stage the anchorage block appeared to be fully intact. Cycle 13 (Fig. 4.21.10) shows the specimen at the end of the test. The joint has completely failed and the joint ties are fully exposed. Fig. 4.21.11 shows more closely the failure of the joint. The forces in the joint centre reduced the concrete to a powdered rubble. The buckling of the column bar is quite noticeable and the ties at the top bowed out to be easily observable on inspection.

The specimen was considered to have failed due to the complete breakdown of the joint. Not only had the cover concrete spalled but the interior of the joint had degenerated so much that buckling of the column bars was possible. With the degree of joint degradation it was quite remarkable that the specimen was still carrying 57 per cent of its theoretical ultimate moment of resistance. It was the anchorage block which ensured that some load was still being carried in the column at this stage due to a steel couple. Without the adjacent beam and anchorage block it is quite feasible that collapse of the structure would have occurred by this stage. This demonstrates the usefulness of the anchorage block even if poor

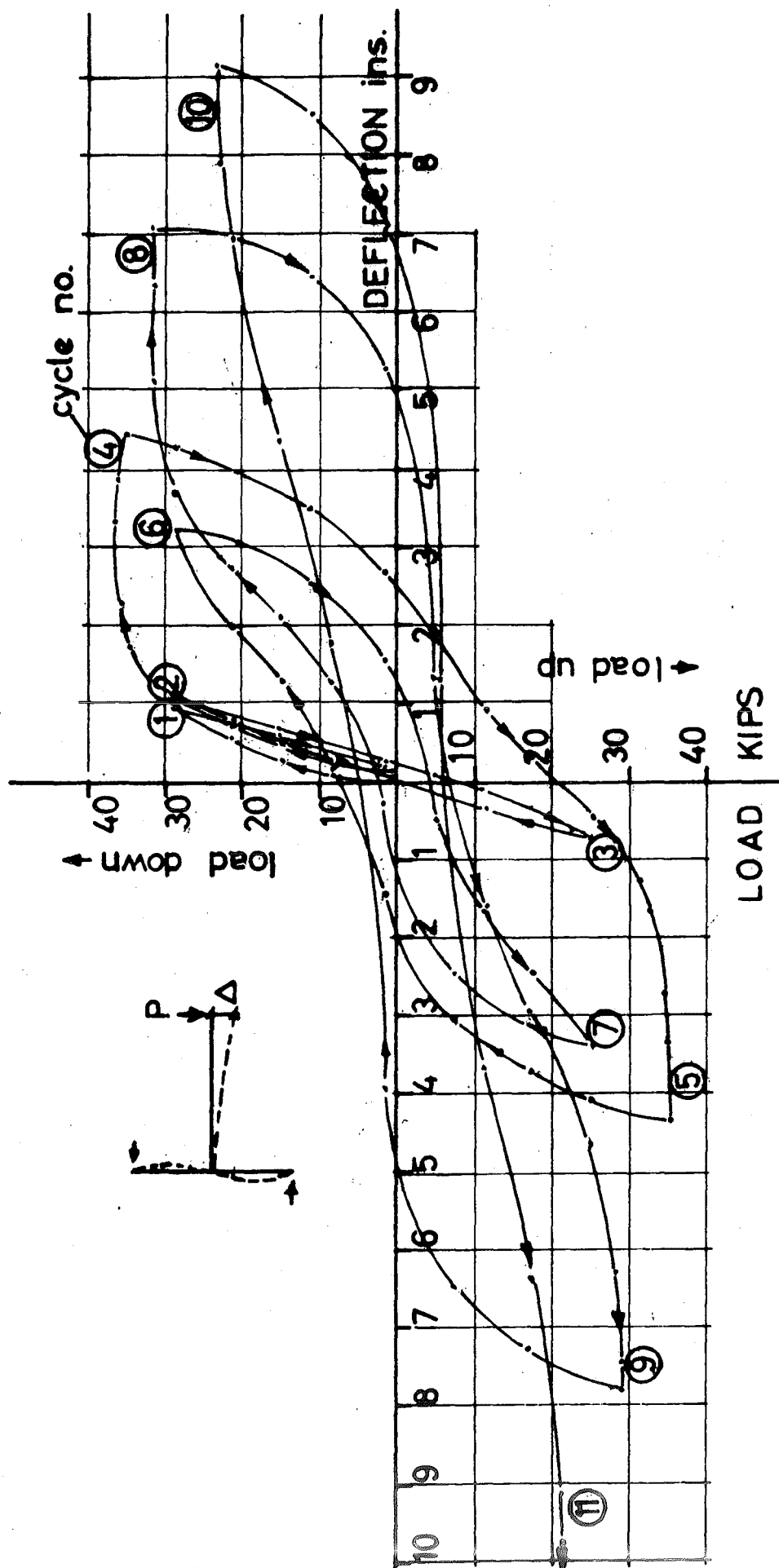
detailing leads to a joint failure.

4.5 UNIT 3.

4.5.1 Load-Deflection. There was a substantial difference in the joint steel detailing for UNIT 3 compared with UNITS 1 and 2. The first two units had nine main ties and the last one had five main ties. Once again the load-deflection plot is inferior to that of UNIT 1, but comparison with UNIT 2 reveals a close correlation. The slope of the graph, giving an indication of the stiffness, can be obtained from the elastic cycles. The point of yielding can be observed and the unit ductility factor $\left(\frac{\Delta}{\Delta_y}\right)$ corresponds to a deflection of about 1.25 inches. ($\Delta = \Delta_y$ at this point) (See Fig. 4.22).

The effect of closing of the cracks and the Bauschinger phenomenon are again apparent from cycle 4 onwards. The full theoretical ultimate moment was attained in cycles 4 and 5 and the extra strength was due to strain hardening in the column bars. As with UNIT 2, UNIT 3 showed a decline in stiffness after cycle 6. Up to this stage the stiffness is comparable with UNIT 1. Plastic cycles 8 and 9 are similar to UNIT 2 but inferior to UNIT 1.

Cycles 10 and 11 are also plastic cycles. For UNITS 1 and 2 they are elastic. Because of the rapid deterioration in the joint of UNIT 3 during cycle 10 nothing would have been gained by putting the specimen through another two cycles as the moment of resistance would have been very low by this stage. Only 67 per cent of the theoretical ultimate load was attained in cycle 10 and 62 per cent



UNIT 3 — LOAD DEFLECTION CURVE

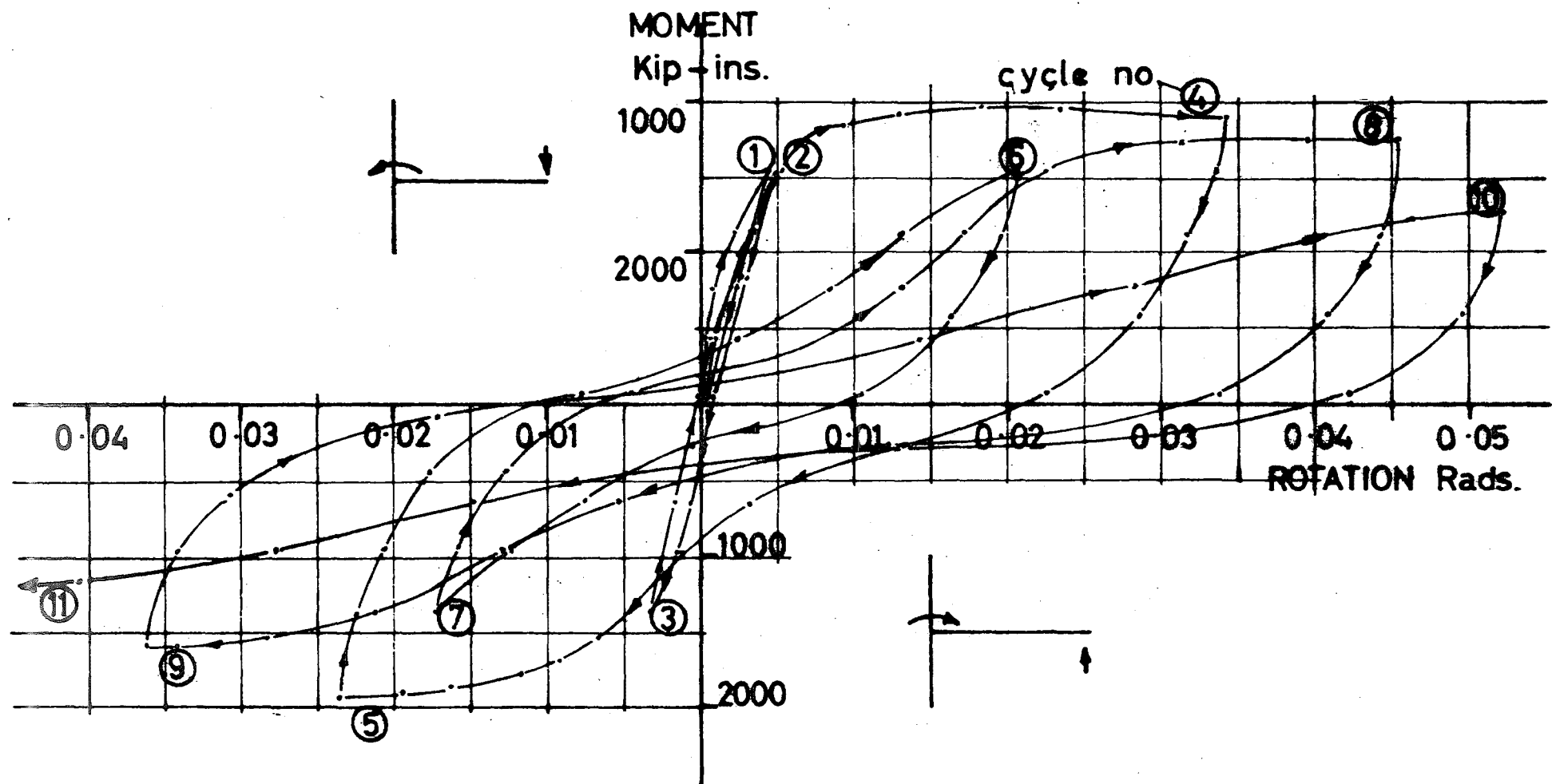
FIG 4-22

in cycle 11. This is much less than UNIT 1 and slightly less than UNIT 2 in the 12th and 13th cycles.

Overall deflections attained in UNIT 3 were slightly larger than UNIT 2 at a similar ultimate moment of resistance, but compared with UNIT 1 they were less, at a smaller ultimate moment of resistance, in the latter cycles. Deflections were comparable in the earlier cycles. This falloff in the ultimate moment of resistance was due to the deterioration of the joint rather than of the individual members.

4.5.2 Moment-Rotation for Columns. As with UNIT 2 because of the degradation of the joint the values in the moment-rotation curves are not indicative of the values that would have been obtained had the joint remained intact. Never-the-less up to cycle 6 when the joint began to rapidly deteriorate, the values are reasonable. The beam steel in UNIT 3 also yielded but as before this in itself did not greatly influence the rotation values obtained. Rotation values obtained in the later cycles included some rotation from the joint region due to the breakdown of the concrete. Also the value of the maximum load applied was reduced due to the inability of the deteriorated joint take its full design load, although the column appeared capable of taking the full load.

Fig. 4.23 shows the moment rotation plot for the upper column of UNIT 3. Again the plot is very similar to UNIT 2 but generally inferior to UNIT 1. The comments made for UNIT 2 apply generally for UNIT 3 and the values of moment and ductility are very similar. The only difference between these graphs is that whereas with UNIT



MOMENT - ROTATION CURVE
UPPER COLUMN - UNIT 3

FIG 4.23

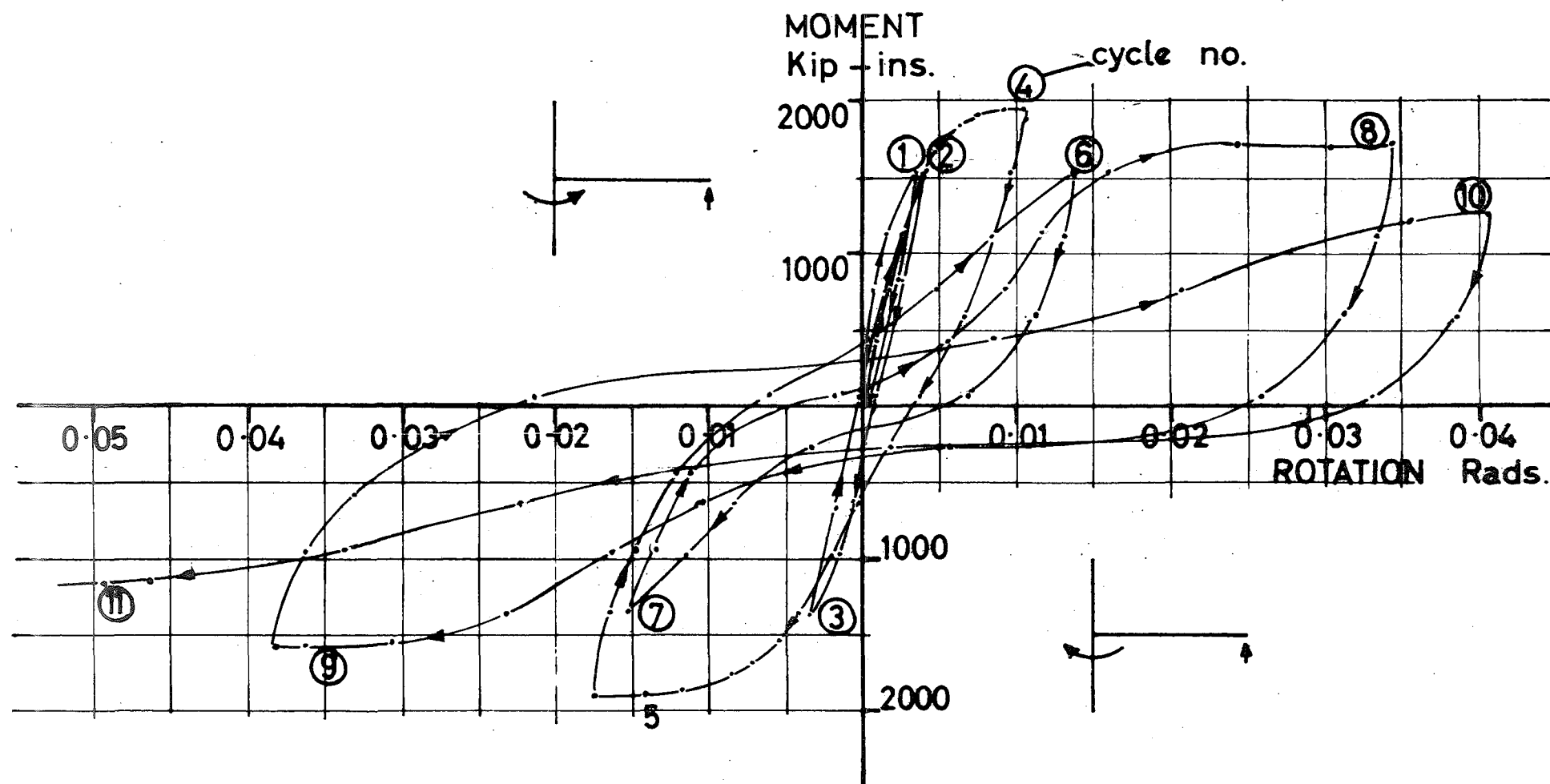


FIG 4.24

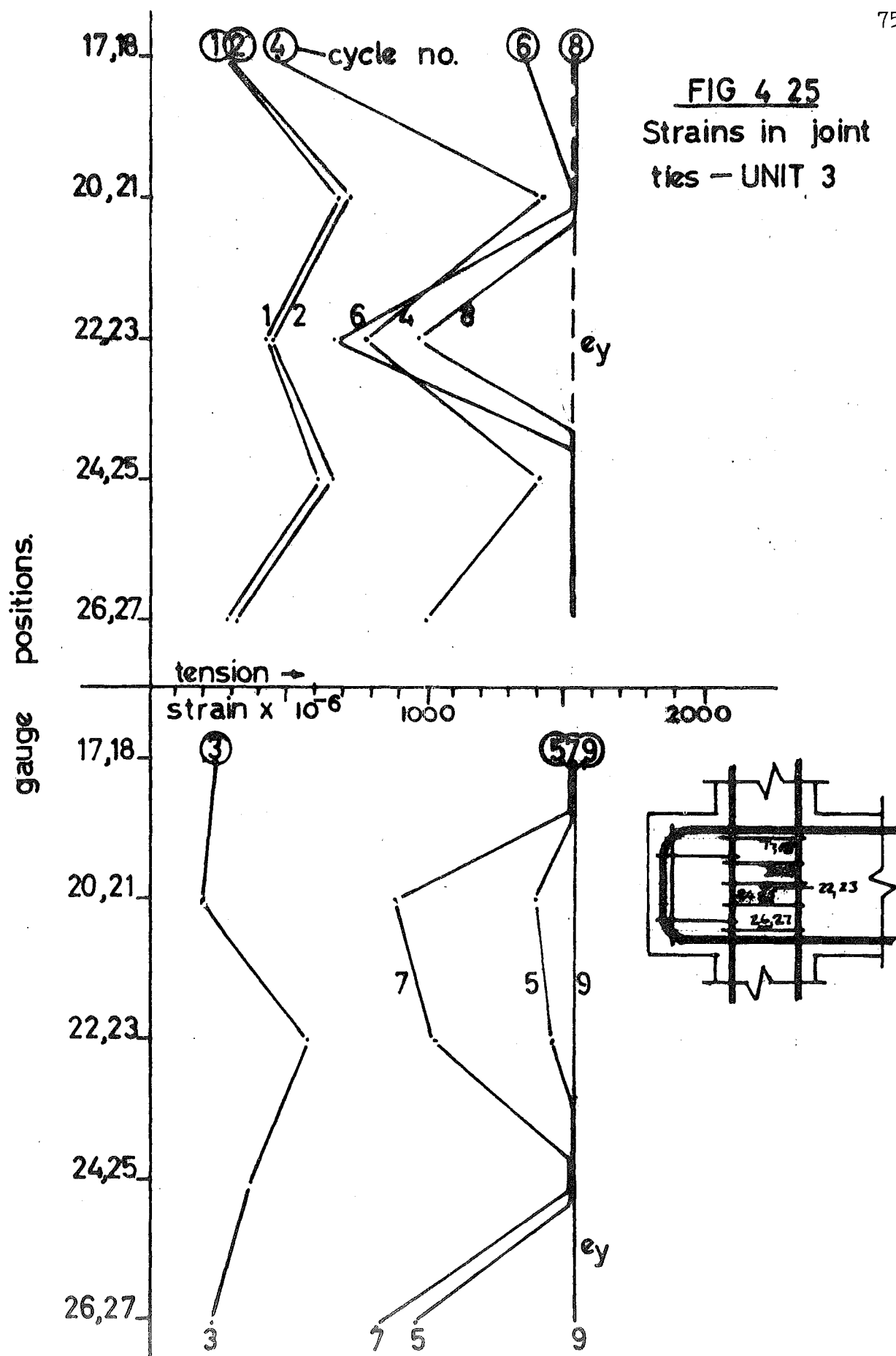
2 cycles 10 and 11 are so called elastic cycles, in UNIT 3 they are plastic ones. Cycles 12 and 13 were not applied to UNIT 3 for reasons mentioned earlier. Hence cycles 12 and 13 for UNIT 2 should be compared with cycles 10 and 11 for UNITS 3, and cycles 10 and 11 in UNIT 2 have no comparison in UNIT 3. Because of the failure of the joint the conclusions drawn as to the adequacy of the column are the same as for UNIT 2.

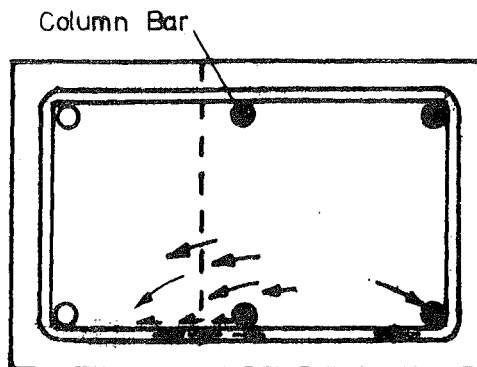
Fig. 4.24 showing a plot of the lower column rotations indicates the same effects of joint degradation as the upper column. Up to cycle 8 the plot is very similar to that of UNIT 2. The lack of rotation in the column in the later plastic cycles is due once again to the degradation of the joint. Hence the same conclusions can be drawn as for UNIT 2.

4.5.3 Strains Within the Joint. The steel arrangement within the joint of UNIT 3 was substantially different from that of UNITS 1 and 2. There were only 5 ties in the joint and these were around the column bars only. Two nominal ties in a horizontal position and a vertical tie were situated around the 'U' - bars in the anchorage block.

Fig. 4.25 shows the distribution of strains, for the peaks of various load cycles, in the joint ties at a position in the middle of the joint. The plot here reveals a different strain distribution than either UNIT 1 or UNIT 2. When the load is acting down the distribution of strains is very symmetrical about the centre line of the joint. The tie second from top and the tie second up from

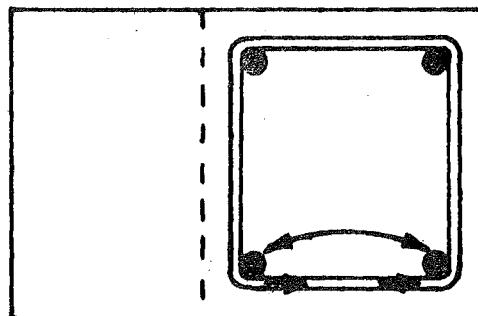
FIG 4 25
Strains in joint
ties — UNIT 3





Because the joint forces are confined to an area within the column bars the effect of the ties is reduced. There is not the effect of a positive force at the column bar level and the tensile force in the tie must be attained by the development of bond stresses in the anchorage block.

Units 1 & 2



- Development of strong compression strut mechanism in joint region to resist tie forces. The positive action of the 90° bend of the tie on the column bar ensures this.
- Also the tie leg is shorter than above which is significant when the tie yields.

Unit 3

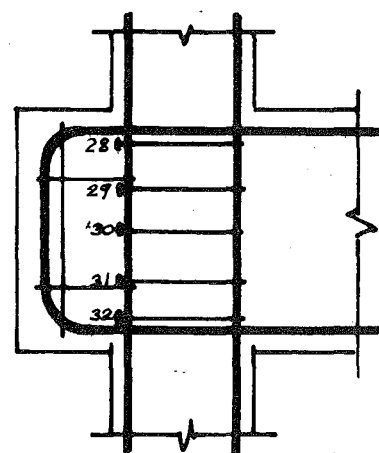
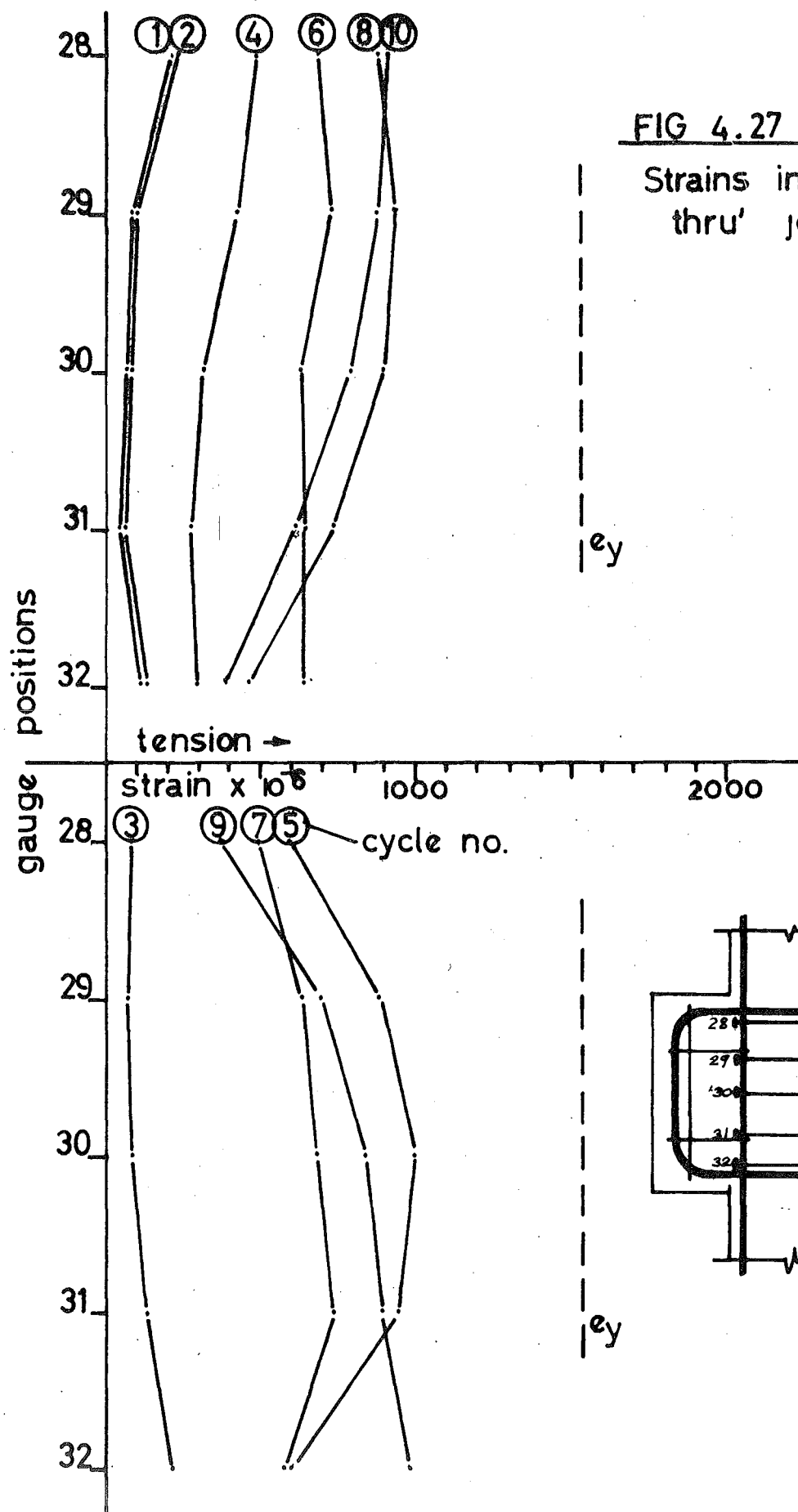
Comparison of Formation of Compression Strut Mechanisms.

FIG 4.26

bottom are both equally stressed and show the highest strains in the joint. The significant feature is the symmetry of all the plots for each load cycle. The ties mentioned above are the first to yield for load cycles in the downward direction and these are followed by the two outer ties in the joint. The forces in the middle of the joint appear to be less than for the outer areas.

The reason for the difference in strain variation when compared with UNITS 1 and 2 can be explained by looking at the tie shape. In the first two units because the tie takes in the anchorage block as well the confinement of the outer column bars is not so effective. This means that no efficient compression strut mechanism can be developed. Hence when the crack gets close to the end of the tie there is no effective way for the tie to develop an effective force so that it can yield. On the other hand UNIT 3, because the tie is located around the column bars, produces a very effective compression strut mechanism. Hence it is much easier for the joint ties, when held effectively at the 90 degree bend by this compressive force, to produce a force such that can yield. (see Fig. 4.26). Also a tie with a long leg will elongate more upon yielding and hence is unable to produce an effective confining force.

The strains in the ties for the cycles in which upward load was applied do not show the same symmetry when plotted. Nevertheless some symmetry is shown about a centre line higher than the centre of the joint. This is because there are no main diagonal cracks in this direction passing through the bottom tie. This is

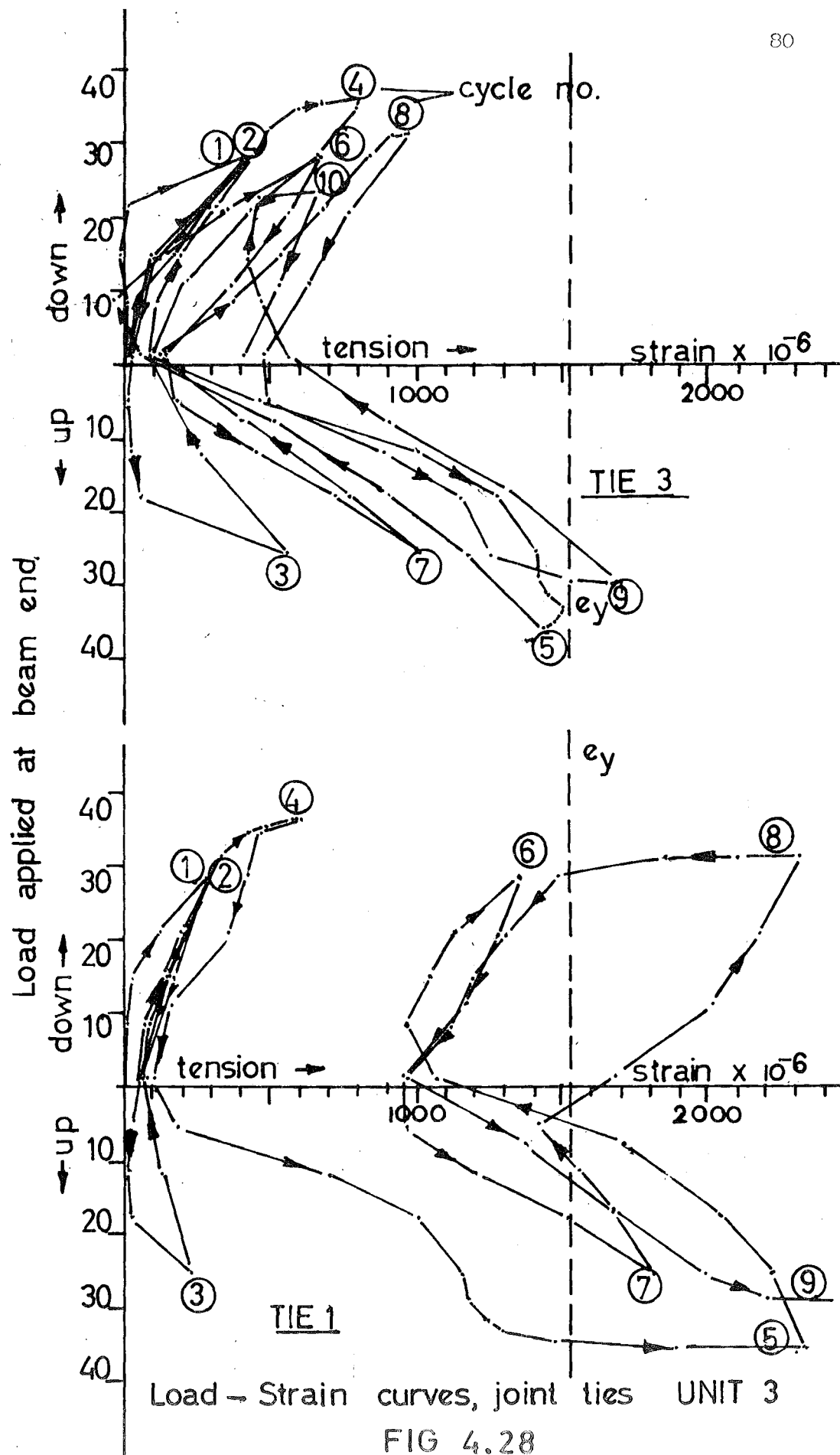


shown by the fact that the strains measured here are lower than in the top tie which did not pass across a crack.

The strains in the ties of UNIT 3 are generally higher than for the corresponding load cycles in UNITS 1 and 2. This is to be expected.

Fig. 4.27 shows the distribution of strains on the back leg of the tie running through the joint at the outer column bar levels. The strains generally are higher than for UNIT 2 showing that although the ties are of equal diameter and number those for UNIT 3 are being utilized much more efficiently. The variation of strains throughout the cycles does not coincide with the variation of the strains in the legs of the ties. But as the strains are generally low $\approx 6 \text{ } \mu\text{y}$ this is not very significant. In the elastic cycles the strains in the upper and lower ties are the larger whilst in the initial plastic cycles the strains in the middle ties are the larger. Plastic cycles 8,9,10 show a different strain distribution again. Cycles 8,10 exhibit a plot with highest strains in the top ties progressing to lowest strains in the bottom ties and vice versa for cycle 9. This means that after a few cycles the normal forces in the joint are larger closer to the beam tension reinforcement.

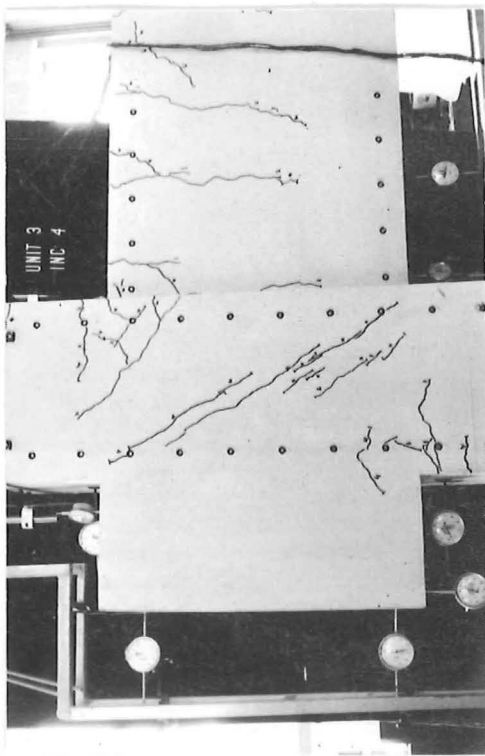
Fig. 4.28 is a plot of the strain history of two ties within the joint. Tie 3 is the middle tie and tie 1 the top tie. Tie 3 shows slightly larger strains for the upward load cycle than the downward load cycle. Only in cycle 9 is yield reached in the tie and as the tie is generally in the elastic range the cycle plots are fairly close together. At zero load there were some residual



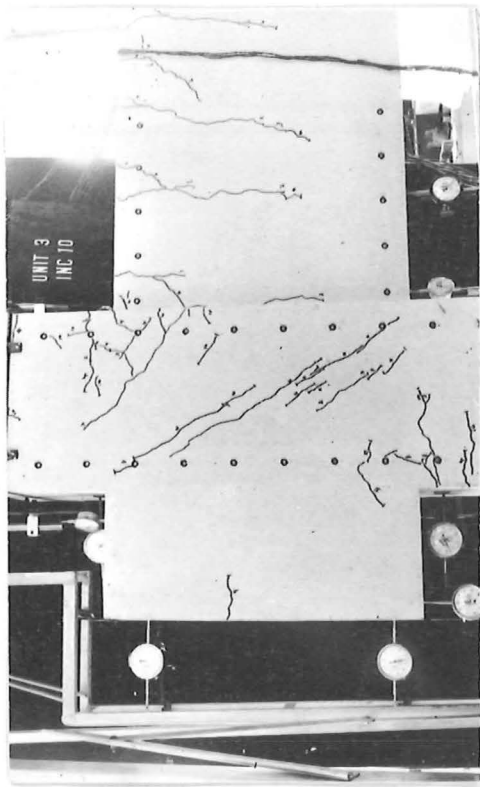
strains in the ties indicating that the cracks did not close properly.

Tie 1 shows strains generally larger than tie 3. The strains were approximately equal in each direction for the elastic cycles 1,2,3. Cycle 5 shows a dramatic increase in the strains and yielding of the tie was observed. From this stage on the strains remain consistently high. Much higher strains are observed at zero load and this was due not only to cracks not closing but mainly to the Bauschinger effect in the steel. For the joint, the ties can be considered useless when they have yielded as they can no longer effectively confine the joint region. The strain plots for UNIT 3 showed tensile strain values which were generally higher than either UNITS 1 and 2. This would be consistent with the fact that there are fewer ties in the joint and that these ties are used more efficiently.

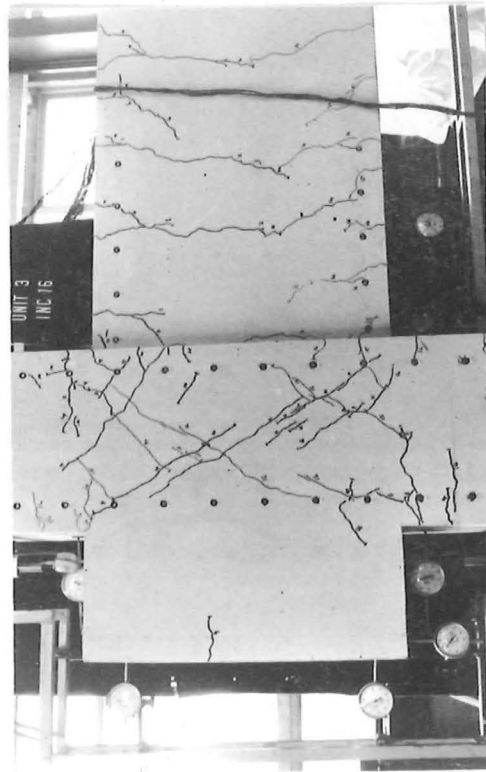
4.5.4 Crack Development and Mode of Failure. Figs. 4.29.1 to 4.29.11 shows the development of cracks in cycles 1 to 11. Fig. 4.29.12 shows the condition to which the joint has deteriorated by the end of the test. Flexural cracks appeared in the first load increment of cycle 1 and joint diagonal tension cracks occurred in the third load increment of this cycle. (see Fig. 4.29.1). The main diagonal cracks can be observed to extend virtually from corner to corner. Fig. 4.29.2, the second plastic cycle, shows only slightly more cracking in the upper column region. Fig. 4.29.3 shows the start of diagonal cracking in the 3rd load cycle. Tension cracks appeared on the outer face of the column. Cycle 4 (Fig.



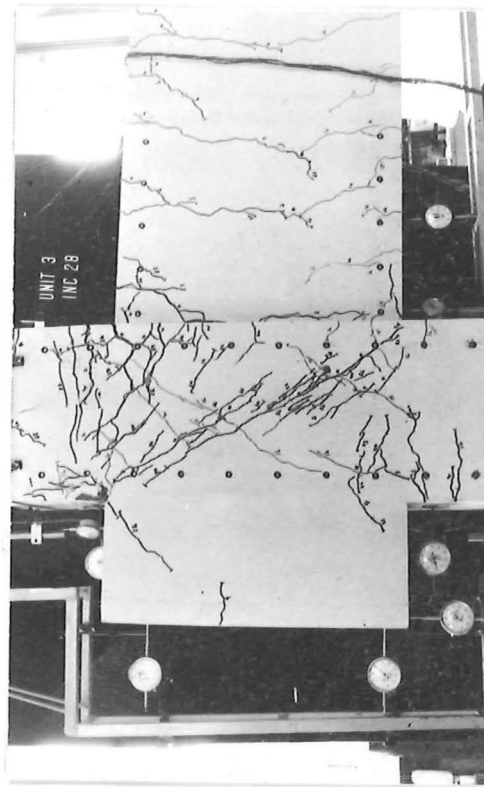
CYCLE 1.
Fig. 4.29.1.



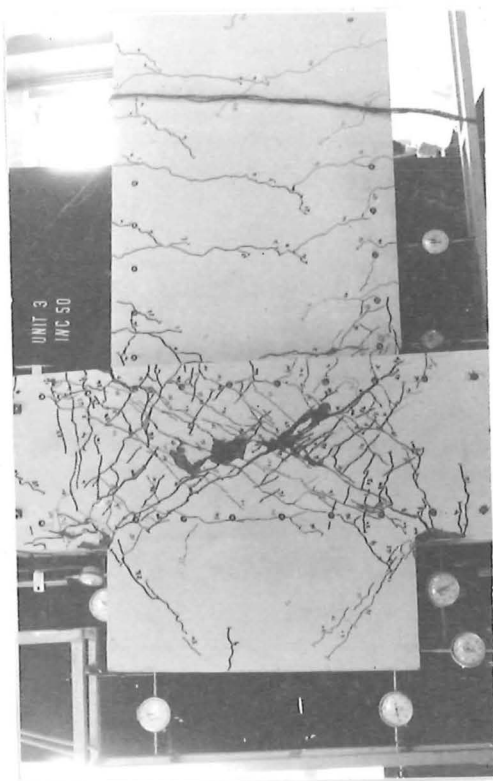
CYCLE 2.
Fig. 4.29.2.



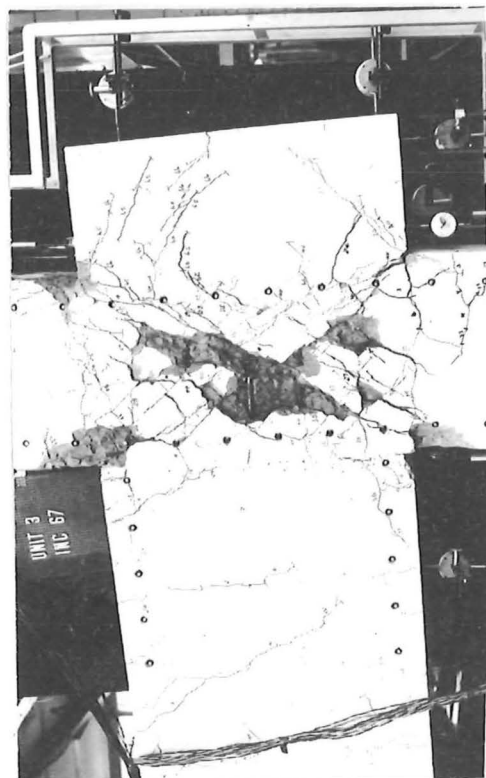
CYCLE 3.
Fig. 4.29.3



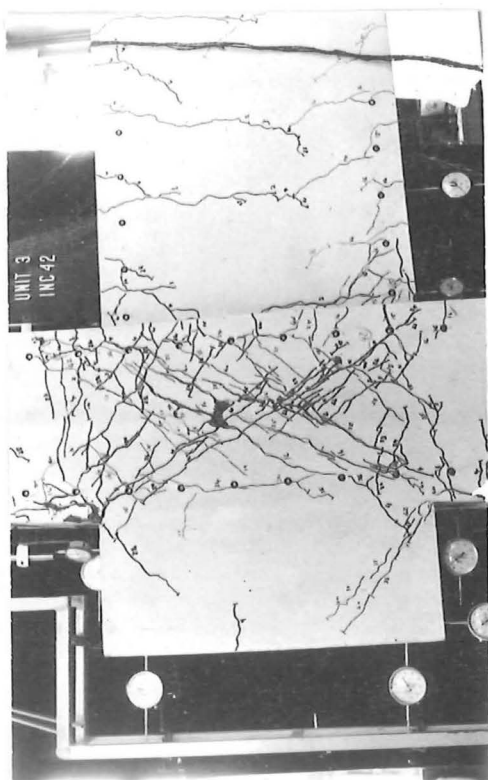
CYCLE 4.
Fig. 4.29.4.



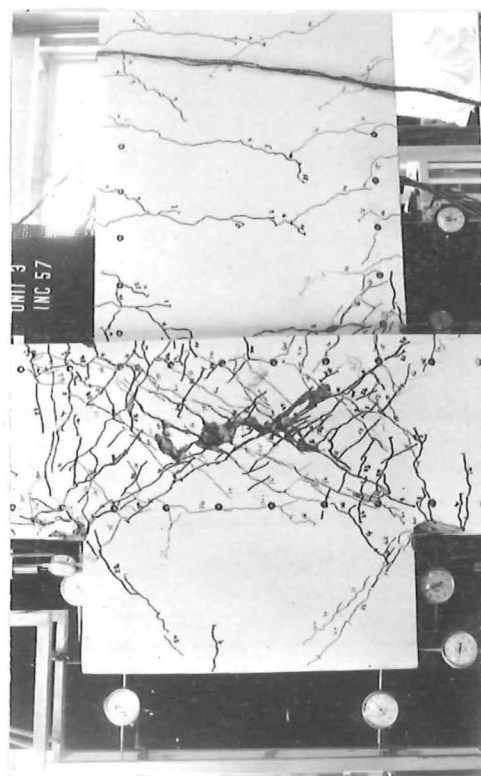
CYCLE 6.
Fig. 4.29.6.



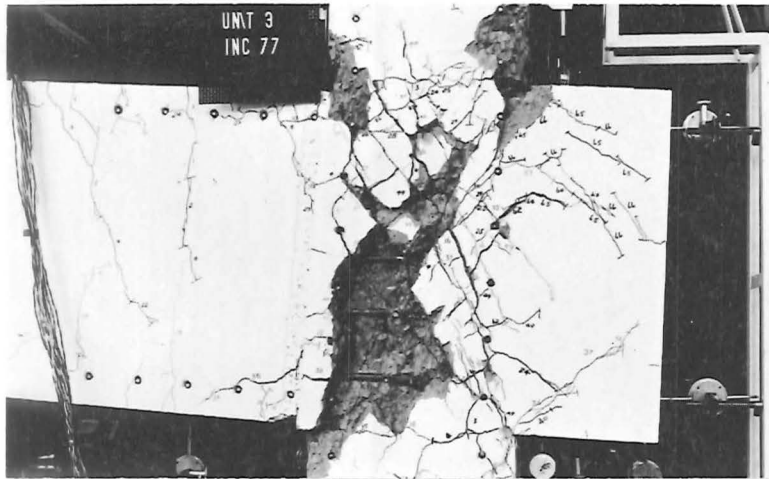
CYCLE 8.
Fig. 4.29.8.



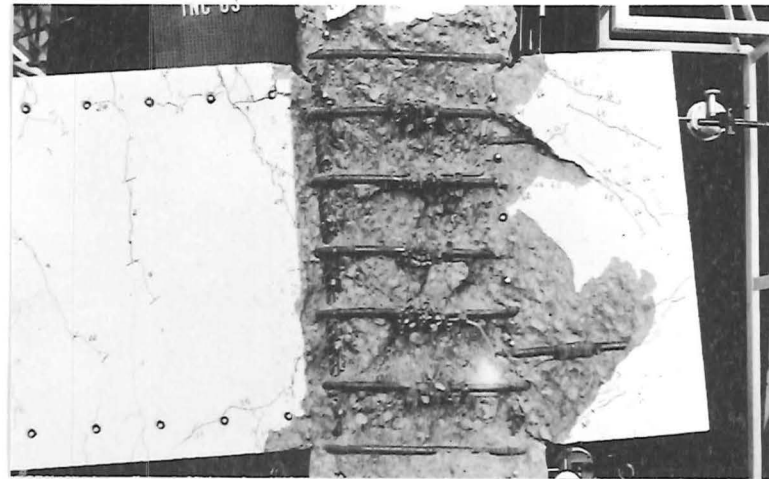
CYCLE 5.
Fig. 4.29.5.



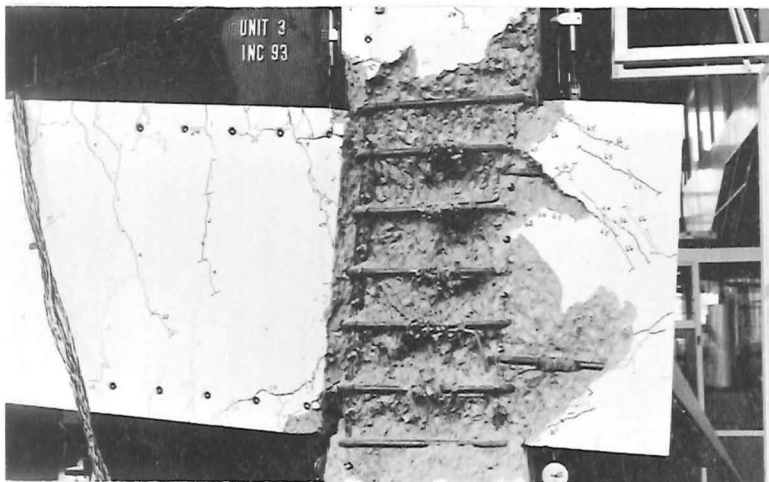
CYCLE 7.
Fig. 4.29.7.



CYCLE 9.
Fig. 4.29.9.



CYCLE 10.
Fig. 4.29.10.



CYCLE 11.
Fig. 4.29.11.

Joint Deterioration
at end of load cycles.

Fig. 4.29.12.



4.29.4) showed substantial joint diagonal cracking and on increase in the tension cracks in the column. These extend down the column to below the level of the beam flexural reinforcement. The start of a bond failure crack in the anchorage block was also noticed. Cycle 5 (Fig. 4.29.5) showed the start of spalling of the joint cover. Further bond failure cracking was observed in anchorage block and a vertical bond failure crack appeared at the level of the outer column bars. There was not much increase in cracking in the column or beam which indicated that failure was concentrated primarily in the joint region. Cycle 6 and 7 (Figs. 4.29.6 and 4.29.7 respectively) which were elastic cycles to the same value as the first elastic cycles show further spalling of the concrete cover in the joint region.

Plastic cycle 8 (Fig. 4.29.8) shows an increase in the cracking of the anchorage block and also further spalling of the joint cover concrete. A small amount of spalling was also observed on the outer face of the upper column. Cycles 9, 10, and 11 (Figs. 4.29.9, 4.29.10 and 4.29.11) showed progressive deterioration of the joint with a further small amount of spalling in the column areas above and below the joint. Some spalling of cover concrete in the anchorage block region was also observed. By the end of the test the inner column bars were almost fully exposed as seen in Fig. 4.29.12.

The specimen was considered to have failed due to breakdown of the joint. Once the joint ties yielded they were unable to provide sufficient confinement pressure to the core of the joint. The joint

deteriorated very quickly towards the end of the test and the last two elastic cycles were omitted.

CHAPTER V.

CONCLUSIONS AND SUGGESTED FUTURE RESEARCH.

5.1 CONCLUSIONS. Although none of the specimens can be considered to have solved the problem of joint reinforcement detailing, the information obtained should enable a satisfactory joint to be designed. Several important features were observed and these are listed below with appropriate discussion.

i) Beam Bar Anchorage. Previous tests conducted by Renton² indicated that the placing of the beam bar 'radius' within the joint seriously affected its (the joint's) performance. The provision of an anchorage block overcame this problem successfully. The length of the anchorage block was determined by the anchorage requirements of the beam tension bars. The anchorage length was calculated according to ACI 318 - 71 and the length of 'U'- bar from the near face of the column to the centre of the far end of the block was made equal to it. On the basis of the tests conducted, it would appear that making the top and bottom bars separate (instead of U - bars) and ensuring that the 'radius' of the bar is outside the line of the outer column bars would also provide a satisfactory solution to the anchorage problem. This alternative solution would ensure that the anchorage block dimensions are kept to a minimum since the anchorage length could be considered to extend down the full depth of the anchorage block if necessary.

ii) Crack Formation. The specimens were designed assuming a 45 degree crack pattern and using the classical shear formulae. The

assumption regarding the angle of cracking proved erroneous and the cracks generally formed on a corner to corner basis. The diagonal cracking was confined to the joint bounded by the column bars. Also the contribution of the concrete other than from the diagonal compression mechanism is doubtful. This means that a method of designing the joint ties based on a more realistic crack orientation and placing less emphasis on the shear carried by the concrete is necessary.

iii) Joint Ties. Because the forces were confined to the joint, the ties which were placed only around the the column bars (UNIT 3) worked much more efficiently than ties which extended into the anchorage block (UNITS 1 and 2) UNIT 3 showed a much better distribution of strains in the ties throughout the joint than either of the first two specimens. This was due basicly to the formation of a compression strut mechanism and the fact the main tie legs were shorter in length. Ties around the column bars ensured that the confining pressure was exerted over the whole of the joint with each load cycle. The superior behaviour of UNIT 1 compared with UNIT 2, when the lateral ties at the centre of the joint were the only difference, indicates that some restriction should be placed on the maximum unsupported length a tie can have between the main bars. If this length is exceeded some additional lateral ties must be provided. Long unsupported lengths of tie sides lead to ineffective confinement due to lateral bowing of the tie side. Also it is essential to ensure that a confining force is maintained in the joint by the main ties, without them reaching the yield stress, otherwise disruption of the core concrete occurs due to wide cracking.

It appears that only nominal ties are required in the anchorage block.

iv) General. The sole object of joint design is to ensure that the joint remains intact throughout several post-elastic cycles, so that the individual members rather than the joint, limit the capacity of the structure. It is impossible to prevent, the cover concrete from spalling and the diagonal cracking occurring in the joint, but never-the-less it is essential that this be minimized so that there is no stiffness degradation of the overall structure because of joint deterioration. With a greater number of beams spanning into the joint the problem of confinement will be greatly improved, but it must be remembered that it was the beam bars that had the greatest effect on the joint. Hence these tests should give an indication of the behaviour when beams span into one, two or three faces of the column. For these cases the provision of an anchorage block is recommended. The following section gives a suggested method of design.

5.2 SUGGESTED FURTHER RESEARCH. As the use of an anchorage block has proved successful the following design procedure is suggested and should be checked by further tests.

Design of joint.

where

$$V_j = T - V'$$

$$V_j = \text{total force to be carried in joint.}$$

$$T = A_s f_y = \text{beam tensile force.}$$

$$V' = \text{horizontal shear on joint from column.}$$

$$A_v = \frac{V_j}{\phi f_y}$$

A_v = total area of joint ties.

ϕ = capacity reduction factor.

$$\text{no. of ties} = \frac{A_v}{n a_s}$$

a_s = area of individual bar.

n = no. of legs in tie.

= 2 for practical purposes.

Note. This design procedure assumes that the concrete takes no shear other than participating in the diagonal compression mechanism with the ties.

For the specimen tested this design requirement would be approximately $7 - \frac{5}{8}$ in. diameter ties in the joint. These should be spaced equally between the top and bottom beam bars within the joint. There are some limitations placed on the above design method. One of these is from the M.O.W. code. The content of ties in the joint should not be less than that required for ductility in the columns according to the appropriate design equations. In the case of the specimen tested the number of ties required for ductility was $6 - \frac{5}{8}$ inch diameter. A further limitation is that if the distance between two bends in the main tie, of 90 degrees or more, is greater than 10 bar diameters or 6 inches then special lateral ties should be placed. For the specimen tested $\frac{1}{4}$ - inch ties through the centre of each main tie as in UNIT 1 are recommended. Another alternative is to put a 'hairpin' tie in from each side of the joint so that it is anchored on the opposite side. This is an easier solution from a practical point of view but the anchorage doubtful. This requirement for supplementary lateral ties would only be necessary if there was no beam

framing into the particular side of the column.

Design of anchorage block:

ACI 318 - 71 code requirements give the anchorage length for beam tension bars as;

$$L_d = 0.04 \frac{a_s f_y}{f_c}$$

For the specimen tested an anchorage length of 33 inches was required. The minimum inside radius for the bar was 5 inches. Hence to keep the radius outside the core of the joint the anchorage block could be made 6 inches long. There would be sufficient anchorage length for the beam bars if they are crossed over rather than formed into a 'hairpin'.

The above proposed design procedure is based solely on the results of the three specimens tested. Besides the testing of these proposals, further work needs to be done in several other areas.

Firstly the effect of more than one beam framing into the column should be investigated; especially a corner column where the effect of beam anchorage could be more critical.

Secondly the use of some form of mechanical anchorage in lieu of the anchorage block, on the exterior face of the column could be investigated. This could take the form of a steel plate to which the beam bars are welded. Special attention would need to be paid here to the anchorage of the beam compression steel.

Thirdly the effect of the level of axial load on the joint needs investigating. This should be considered from the point of

view of the effect of little or no axial load applied, rather than the beneficial effect gained from having a constant axial load. The reason for this is that in many multi-storey buildings the axial load on a column varies with the structures oscillation through a seismic loading cycle. In fact it may even be possible for the column axial load to be a tensile rather than a compressive force at some stage in the cycle.

Fourthly beams entering columns eccentrically is a popular architectural feature and the additional shears induced by torsion should be studied.

APPENDIX A.REFERENCES.

1. Park, R., and Paulay, T., "Ultimate Strength Design of Reinforced Concrete Structures" Printed for a Seminar Arranged by Departments of Civil Engineering and Extension Studies, University of Canterbury.
2. Renton, G., "Effect of Reverse Loading on Reinforced Concrete Joints" M.E. Thesis Presented at University of Canterbury, 1972.
3. ACI "Building Code Requirements for Reinforced Concrete".
ACI 318 - 71.
4. Ministry of Works, Office of the Chief Structural Engineer, "Design of Public Buildings", Code of Practice, PW81/10/1, May, 1970.
5. Blume, J.A., Newmark, N.M., and Corning, L.H., "Design of Multi-Storey Reinforced Concrete Building for Earthquake Motions". Portland Cement Association, Stokie, Ill., 1961.
6. Hanson, N.W., "Seismic Resistance of Concrete Frames With Grade 60 Reinforcement". Tentative P.C.A. Stokie, Ill., Oct., 1970.
7. Meggett, L.M., "Anchorage of Beam Reinforcement in Seismic Resistant Reinforced Concrete Frames" M.E. Report, University of Canterbury, 1971.

8. Corley, G., and Hanson, N.W., "Design of Beam-Column Joints for Seismic Resistant Reinforced Concrete Frames". Proceedings 4th World Earthquake Conference on Earthquake Engineering, Santiago, 1969.